Characterising Termite Mound Spatial Patterns in the Eastern Cape Karoo: Applying Drone Remote Sensing, GIS and Spatial Statistics

L.S.N MNGCELE

2022

Characterising Termite Mound Spatial Patterns in the Eastern Cape Karoo: Applying Drone Remote Sensing, GIS and Spatial Statistics

Lizalise Mngcele

Submitted in fulfillment of the requirements for the degree of

MSc (Geosciences)

in the *Faculty of Science*

at the

Nelson Mandela University

Date: 05 August 2022

Supervisors : Profs M. Doucouré ; C. Thiart ; M. de Wit

Declaration

Name: Lizalise Sive Nqaba Mngcele

Student Number: 210050128

Title: Characterising Termite Mound Spatial Patterns in the Eastern Cape Karoo : applying Drone Remote Sensing,GIS and Spatial Statistics

I, Lizalise Sive Nqaba Mngcele (210050128), hereby declare that this Masters dissertation is my own work and that it has not previously been submitted for assessment to another University or for another qualification.

Signature: ______________________________

Lizalise Sive Nqaba Mngcele

Date: 05 August 2022

Official Use:

In accordance with Rule G5.6.3,

5.6.3 A treatise/dissertation/thesis must be accompanied by a written declaration on the part of the candidate to the effect that it is his/her own work and that it has not previously been submitted for assessment to another University or for another qualification. However, material from publications by the candidate may be embodied in a treatise/dissertation/thesis.

NELSON MANDELA
UNIVERSITY

PERMISSION TO SUBMIT FINAL COPIES

OF TREATISE/DISSERTATION/THESIS TO THE EXAMINATION OFFICE

Please type or complete in black ink

FACULTY: SCIENCE

SCHOOL/DEPARTMENT: Life, Earth, Environmental and Agricultural Sciences / GEOSCIENCES

I, (surname and initials of supervisor) DOUCOURÉ, C.M.

and (surname and initials of co-supervisor) THIART, C.

the supervisor and co-supervisor respectively for (surname and initials of

candidate) Lizalise Sive Nqaba MNGCELE

(student number) 210050128 a candidate for the (full description of qualification)

Masters of Science (Geology)

with a treatise/dissertation/thesis entitled (full title of treatise/dissertation/thesis):

Characterising termite mound spatial patterns in the Eastern Cape Karoo: applying drone remote sensing, GIS and spatial statistics.

It is hereby certified that the proposed amendments to the treatise/dissertation/thesis have been effected and that **permission is granted to the candidate to submit** the final bound copies of his/her treatise/dissertation/thesis to the examination office.

11 Nov. 2022

SUPERVISOR **DATE**

And

On Behalf of Prof Thiart)

11 Nov. 2022

CO-SUPERVISOR **DATE**

Abstract

The Eastern Cape Karoo in South Africa, has been earmarked for potential Shale Gas development, which has necessitated the understanding of existing ecosystems to be quantified pre-development, in order to have a baseline against which the exploration can be monitored. Termite mounds as baseline mechanisms, are known to be sensitive to ecosystem disturbance and because of their abundance in the exploration zone, have been studied as indicator species. They are both a surface and subsurface phenomena which makes them an ideal baseline monitoring mechanism.

Termite mound height, basal circumference and geospatial data was collected against natural and anthropogenic factors: elevation, vegetation, water, soil, geology, human settlements and roads. Mound distributions were observed across four study sites, and seven plots, using a DJI Phantom 4 Pro drone, an aerial and ground survey. Observed mound data on the drone and aerial survey was compared to that of the ground survey.

Overall, the drone survey outperformed the aerial survey in recording accurate termite mound data. This was largely attributed to the scale of the study which gave the drone a competitive advantage. It allowed for drone data to be collected at 40 m altitude with an image resolution of 2-6 cm/pixel on each plot. In addition, drone detection accuracy was improved through the ability to generate digital surface models (DSMs) through point clouds and overlaying them with orthomosaics.

Considering observed mound spatial point patterns, both the drone and aerial survey were more than 50% percent consistent with the ground survey, although the drone survey detected 28.57% more accurate mound spatial point patterns than the aerial survey.

Recorded overall mound densities were 176.34 ma.ha^{-1} for the ground survey, 163.59 ma.ha^{-1} for the drone and 111.04 **ma.h**a^{-1} for the aerial survey. Mean nearest neighbour distances were 4.03 m, 4.50 m and 6.25 m for the ground, drone and aerial surveys.

On the ground survey, all mounds were separated according to age and categorised between young and old in order to uncover their underlying structure and spatial behaviour. Across the study sites, old mounds had higher densities than young mounds, suggesting that the termite mound population largely consisted of mature colonies. Old mounds recorded 20.08% more sightings than young mounds. Overall, old mound colonies had longer nearest neighbour distances (6.20 m) than young ones (5.28 m), alluding to the need for more resources by mature colonies. Old mounds had heights of 0.34 m and basal circumferences of 3.01 m, with young mounds having heights 0.07 m and basal circumferences of 1.76 m.

Prior to all mounds being divided between young and old, majority of their observed spatial point patterns were random. Post separation, 85.72% of old mound point patterns were evenly split between dispersion and clustering, with young mounds experiencing 71.43% clustered spatial patterns. Recorded overall mound densities were 105.51 ma.ha^{-1} for old mounds and 70.89 ma.ha^{-1} for young mounds. Old and young mounds maintained a positive correlation between basal circumference and height across all study sites.

Old mounds in the study proved more resilient to anthropogenic disturbance and also seemed to favour regions of higher elevation than young mounds. High abundance of old and young mounds had a good relationship with water presence in the form of rivers and dolerite dykes. The Elandsberg Member, Amathole Montane Grassland and Lithic Leptosols, were the geology, vegetation and soil layers with the highest abundance of young and old mounds, an indication of high resource availability. Both young and old mounds had longer foraging networks on the Middleton Formation, Great Fish Thicket and Leptic Regosols, indicating high intraspecific competition and scarce resources. There were varying degrees of termite mound spatial patterns recorded across the anthropogenic and natural features, with the dominant being dispersion for old mounds and clustering for young mounds.

KEYWORDS: Drone, GIS, Termite Mounds, Spatial Patterns

Acknowledgments

I would sincerely like to thank:

- My Supervisors: Prof Moctar Doucour*é*, Prof Christien Thiart and the late Prof Maarten de Wit for all the guidance, support and encouragement
- A special thanks to Prof Christien Thiart for her patience and helping me with the statistical components of the study and so much more
- My mother Pumla Mngcele for affording me the opportunity to study and her love, prayers and support on this journey
- My fellow researchers at the Africa Earth Observatory Network Commons
- Aviwe Gqwaka for helping me navigate my writing software and friendship
- Dr Bastien Linol, Dr Lucian Bezuidenhout, Martin Bentley and Okuhle Poto for assisting me in carry out field work
- Dr Wilma Britz for allowing me to attend her GIS classes and always proving valuable input into my GIS journey
- Keegan Jeppesen and Vhuhwavhohau Nengovhela for assisting me with my maps and figures work
- My good friends, Sanele Msibi, Yonela Mashalaba and Dr Siyabulela Mandela for the constant support and words of encouragement

- The National Research Foundation, African Earth Observatory Network and the Nelson Mandela University Postgraduate Scholarship for the scholarship awards to carry out this study

- The International Statistical Institute and Esri for awarding me 2nd Place Prize at the 62 World Statistics Congress 2019 (Malaysia) for presenting a part of my study

- The International Biometric Society for featuring my work on their news bulletin 2018/2019

- The South African Statistical Association for featuring my work on their 2019 news letter

- The Journal of Remote Sensing for publishing part of my work in an article titled "Earth Stewardship Science Transdisciplinary- Contributions to Quantifying Natural and Cultural Heritage of Southernmost Africa"

- The Department of Science and Technology for allowing me to present my work at the 4th National Global Change Conference

Contents

List of Figures

List of Tables

Chapter 1

Introduction

Problem Statement

In light of the interest expressed by numerous companies to explore for shale gas in the Eastern Cape Karoo Basin, the South African government led by the Academy of Science of South Africa (ASSAF) has released recommendations that need to be met before any exploration may take place (Academy of Science of South Africa (ASSAF), 2016). These recommendations took cognisance of the baseline research programme initiated in 2014 by the Africa Earth Observatory Network (AEON) to establish what the natural environment of the Karoo looks like prior to any exploration of shale gas. This is because it is expected that exploration of any kind of natural resource may lead to the disturbance of the natural environment, therefore making it important for this information to be quantified (AEON, 2018; Academy of Science of South Africa (ASSAF), 2016). An aspect of AEON's baseline research is the distribution of termite mound populations aggregated across large tracks of both natural regions and farmlands of the Karoo, acting as Indicator Species (IS) of change in their ecosystem.

Rational

Since not everything of potential interest in an ecosystem can be measured to assess its health, it is crucial that a specie or group of species that interact at different scales within that ecosystem be identified and monitored (Cairns and Pratt, 1993).

This is because their state reflects or predicts the conditions of the environment in which they are found (Siddig *et al.*, 2016). The idea behind IS is informed by understanding that ecosystem change is reflected through trends in density, diversity and patterns of occurring species.

Understanding that termites as indicator species are highly responsive to changes in their environment, they are expected to respond to ecosystem mechanisms that are exogenous to the ecosystem, such as shale gas leakage into the environment (Siddig *et al.*, 2016; Vlieghe, 2016). Since termite mounds are both a surface and subsurface phenomena, this allows them to interact at different scales within an ecosystem (Constantino, 1998). Pribadi *et al.* (2011) agree that the way in which termites behave ecologically is affected by land use and that variation in their diversity as a consequence, may signal compromised ecosystem integrity. Conducting ecosystem monitoring using termite mound populations, allows for easy measurement of demographic parameters such as age, density and spatial structure (Siddig *et al.*, 2016).

Brief Background

Termite mound abundance, and spatial distribution patterns are primarily influenced by intraspecific competition and environmental heterogeneity. Intraspecific competition acts at local scales and environmental heterogeneity at larger scales (Tarnita *et al.*, 2017; Jean-Pierre *et al.*, 2015). However these parameters may also be influenced by anthropogenic disturbance such as deforestation and urbanisation.

Korb and Linsenmair (2001) suggest that spatial point patterns preferred by old termite mounds are due to intraspecific competition which is informed by the availability of resources, like water and food among others. Juergens *et al.* (2015) observed this behaviour in their study of Namibian desert Fairy Circles as a hypothesis on sand termites creating regular bare patches of soil on the ground as as result of resource competition.

In the case of environmental heterogeneity, termite mounds tend to prefer undulating topography over floodplains. They avoid areas that are sandy or have high clay concentrations, preferring regions that have a well balanced soil mixture (Korb and Linsenmair, 2001). The exploration zone in the Karoo closely resembles some of these preferences, with inconsistent topography largely made of plains and mountains (Linol and De Wit, 2016; Catuneanu and Elango, 2001).

Termite mound structural attributes and spatial point patterns do vary greatly across environmental gradients. Muvengwi *et al.* (2018) and Korb and Linsenmair (2001) conducted a study of their behaviour on geology and vegetation. On geology, Muvengwi *et al.* (2018) found that old mounds forming on granite exhibit dispersion, while random spatial patterning on basalt. They also observed mounds to be significantly bigger on granite than on basalt.

On vegetation, Korb and Linsenmair (2001) noticed that between savanna and forest populations when viewed collectively (young and old), termite mounds formed random spatial patterns in both habitats. Spatial point patterns of termite mounds can be an indicator for underlying mechanisms that regulate their population dynamics, with dispersion indicating healthy intraspecific competition and clustering density dependent thinning, signaling poor resource availability.

The occurrence of mounds on different vegetation, geology and soils suggests that termite mounds are not a unique outcome of a particular flora and that at larger scales environmental heterogeneity plays a role in the spatial point patterns they form.

Significance

Since the Karoo has been earmarked for potential shale gas development, termite mound data needs to be collected and analysed against their environment pre-exploration, in order for it to serve as a baseline mechanism against which to assess the impact of exploration on the existing ecosystems. It is well documented that during hydraulic fracturing, interaction between fracking fluids and the natural environment may lead to habitat loss and decline in biodiversity (Todd *et al.*, 2016; Kiviat, 2013).

In this study termite mounds as IS are used as a cost effective proxy that is applied in early detection of natural and anthropogenic disturbance. Ground and remote sensing surveys are conducted for termite mound data collection. They are premised on previous works such as those of Mujinya *et al.* (2014); Vranken *et al.* (2014) on applying remote sensing as a method of termite mound identification and data acquisition in South America and in Africa. They made use of satellite imagery and airborne surveys to identify termite mounds. This study expands on this and explores the usage of drone surveys in termite mound data acquisition.

Collected termite mound spatial data and geometric attributes are then analysed using geographic information systems (GIS) and spatial statistics. These tools are used to characterise the existing termite mound densities, correlations and spatial point patterns in the Karoo to explore the feasibility of termite mounds being used as baseline IS to track potential environmental disturbance post shale gas development.

In this study, in order to understand the effects of environmental dynamics on termite mound compositions, environmental heterogeneity is introduced. It is in the form of natural and anthropogenic factors and termite mound characteristics are investigated against these. Intraspecific competition is explored through analysing both young and old mound spatial patterns separately, as well as a collective to understand existing ecosystem dynamics.

Research Aim:

The aim of this study is to compare the accuracy in termite mound data collection using aerial vs drone surveys, compared to conventional ground surveys. Secondly, to characterise the trends in density, correlation and spatial patterns of termite mounds to understand the existing ecosystem conditions in the Eastern Cape Karoo (Raymond Mhlaba Municipality).

The research aim has been divided into three objectives:

- To investigate which, between the aerial and drone survey, is the most consistent with the ground survey.
- To characterise termite mound spatial point patterns from the ground survey.
- To establish the influence of natural (elevation, vegetation, water, soil, geology) and anthropogenic (roads, human settlements) factors on termite mound spatial point patterns.

Overview and Structure

This thesis is structured into eight chapters. Chapter 1 provides the overview, problem statement, rational, brief background, importance, research aim and objectives of the study. Chapter 2 gives background of the relevant topics to be covered. Shale gas exploration and the process involved with its implications are highlighted. The importance of baseline research is presented, together with the earmarked exploration zones in the the Karoo. Termite mounds as indicator species and ecosystem engineers are introduced. Chapter 3 presents the study area and auxiliary data of where the study takes place. This includes the study sites where sampling was conducted with site descriptions, sampling plots and maps. Auxiliary data in the form of anthropogenic and natural factors that may influence termite mound distributions are discussed. Chapter 4 introduces the data summary and data acquisition methods. This includes data processing of the different surveying techniques. The application of remote sensing (drone images and aerial images) in data acquisition is discussed. Chapter 5 presents the statistical methods of analysis for the termite mound data. It starts off by giving an introduction to Poisson point processes. The first section deals with the Poisson point processes and complete spatial randomness, the null hypothesis against which the spatial point patterns of the termite mounds will be tested against. The Clark and Evans Aggregation Index R and the G-Function are the second order distance based methods of analysis used to evaluate the observed termite mound spatial patterns. Chapter 6, 7 and 8 are the results, discussion and conclusion sections respectively.

Chapter 2

Background

2.1 Hydraulic Fracturing and Baseline Research

Hydraulic fracturing is a natural gas extracting process where a fluid cocktail containing water, sand, chemicals and proppant is pumped at high pressures into tight shale rock formations. The formations then fracture under the pressure, allowing for the trapped shale gas to escape and be extracted to be used as a fossil fuel (Meng, 2016).

Hydraulic fracturing is commonly known by its household name "fracking". The initial process of fracking begins with the drilling of a well (Figure 2.1) and lining it with a casing, usually made of steel. The casing is secured in place by cement, creating a barrier between the inside of the well and ground water to prevent contamination (Rehu, 2012).

Globally, fracking activity has been responsible for economic boom, a rise in jobs, coupled with lower energy and electricity prices (Jackson *et al.*, 2014). Economic growth and low electricity prices are sought after by countries. This is relevant to South Africa, a developing country that has a stagnant gross domestic product (GDP) and a struggling national electricity supplier (Mngcele, 2017).

However, concerns have been raised about well casings getting compromised and flow back fluids during fracking.

Leaking well casings and flow back fluids lead to ground water contamination and ecosystem disturbance. Howarth *et al.* (2011); Vengosh *et al.* (2013); Clancy *et al.* (2018); Kiran *et al.* (2017); Krupp (2014) are some of the authors who have written substantially on the details surrounding hydraulic fracturing and well casing leaks. They argue that it is often difficult to track the contamination and disturbance of ecosystems due to prior baseline research not being available to compare with post well leakage conditions. This often leads to conflict between government, communities and companies, as no party can be held accountable due to the unavailability of baseline data, against which to contrast the damage (AEON, 2018).

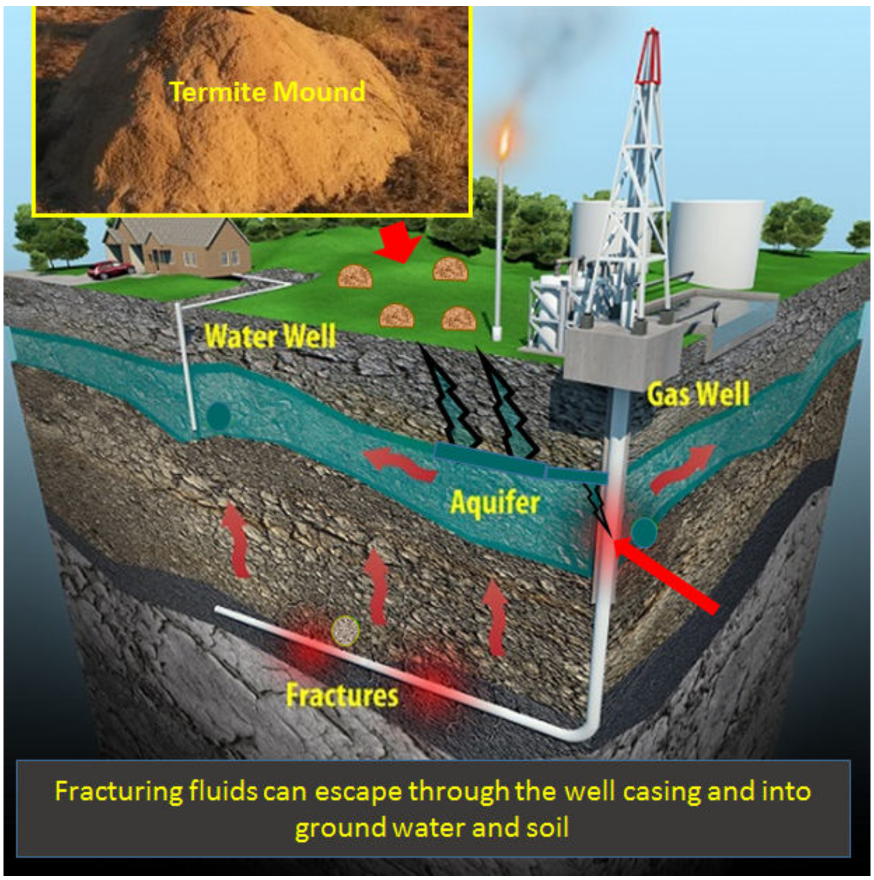

Figure 2.1: Typical hydraulic fracturing site in operation within an ecosystem (modified from aiche.org). On the right side of the figure is a gas well responsible for transporting the shale gas and fracking fluids, next to it is a field with termite mounds. The layer below, has an aquifer which the gas well cuts through. A leak in the gas well will allow fracking fluids to mix with the aquifer and seep to the surface through the aquifer fractures. Once at the surface the contaminated water will interact with the ecosystem and its organisms such as termites.

Baseline research regarding natural resource extraction allows for the quantification of the value of land, its resources and the well being of people dwelling in it.

It enables the creation of knowledge and the collection of data on important environmental parameters that may be disturbed during the course of present or future exploration (Ssekamatte and Okello, 2016; Burns, 1984).

This experimental data then allows for a precise characterisation of the region or area that has been earmarked for exploration. Baseline research enables policy makers to introduce rigorous regulations that can be implemented and tested to ensure safe and reliable extraction practice (AEON, 2018). Data on environmental parameters at different spatial and temporal scales are collected in order to form a baseline surface over the whole region of interest.

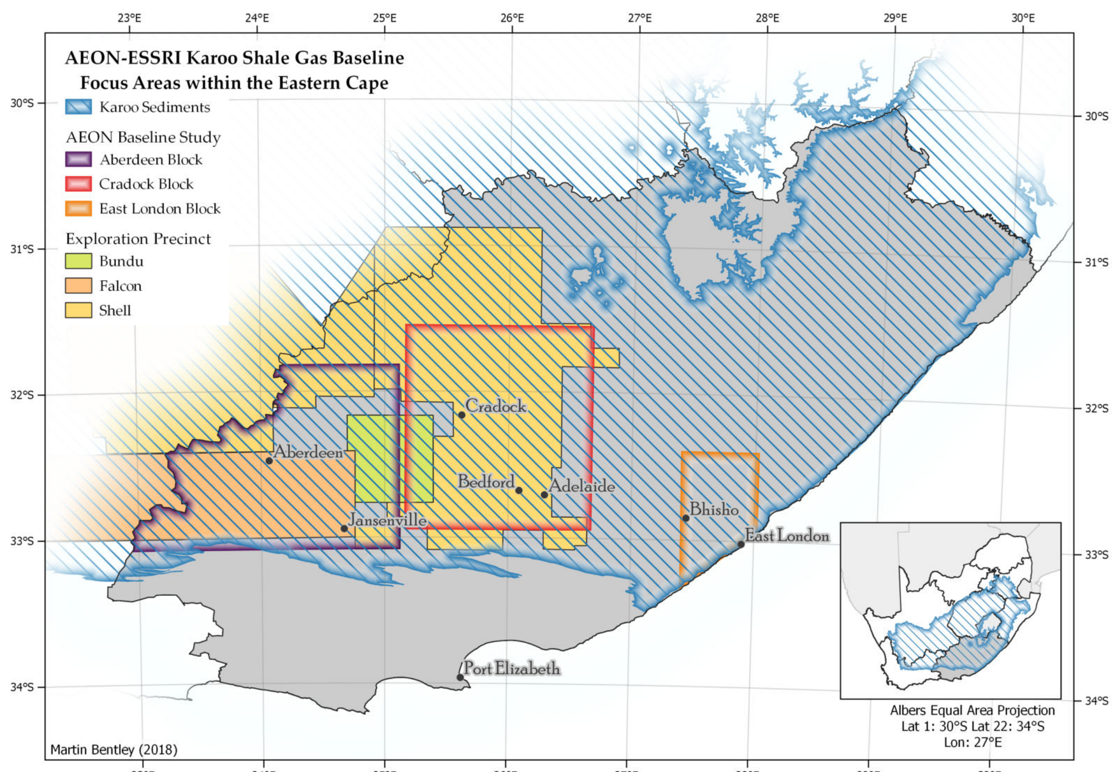

Figure 2.2: Map showing the potential hydraulic fracking zones in the Eastern Cape Karoo Basin ((AEON, 2018))

In this study, termite mounds have been selected as baseline mechanisms against which to detect ecosystem disturbance. This study is conducted within the region zoned by the energy companies interested in exploration (Figure 2.2) in the Eastern Cape Karoo.

2.2 Termites as Ecosystem Engineers and Indicator Species

Mound building termites are known to build a variety of mounds in different environmental conditions (Figure 2.3), to construct their mounds they use saliva, clay and sandy soils. The structure of the termite mound (Figure 2.4) is made up of many complex galleries that are responsible for air circulation and transportation of food around the mound (Mujinya *et al.*, 2014). If the surrounding soil is too sandy, the termites will bring up clay from the subsurface to keep the mound soils together. During this process, fine ecosystem life sustaining minerals are brought up to the surface.

In semi-arid and subtropics, termites drill through to the shallow water table in order to access water needed to maintain humidity in the nest (Constantino, 1998). The humid conditions inside the mound are necessary for the fungi that is cultivated and to maintain the moisture on their bodies.

Figure 2.3: Heaps of soil above the grass line, showing termite constructed mounds, distributed across the Karoo.

Termites are of vital importance in an ecosystem as they increase plant diversity, improve soil pedogenesis and decompose dead matter through their foraging activities. While decomposition is taking place, rich nutrients are released to the surrounding soils and elements like nitrogen and phosphorous are released.

They increase the spatial heterogeneity of the ecosystem by providing hot spots for plant growth and stimulating foraging activity for other organisms.

This allows for an increased number of organisms in an ecosystem compared to areas where the soils are less fertile (Davies *et al.*, 2014).

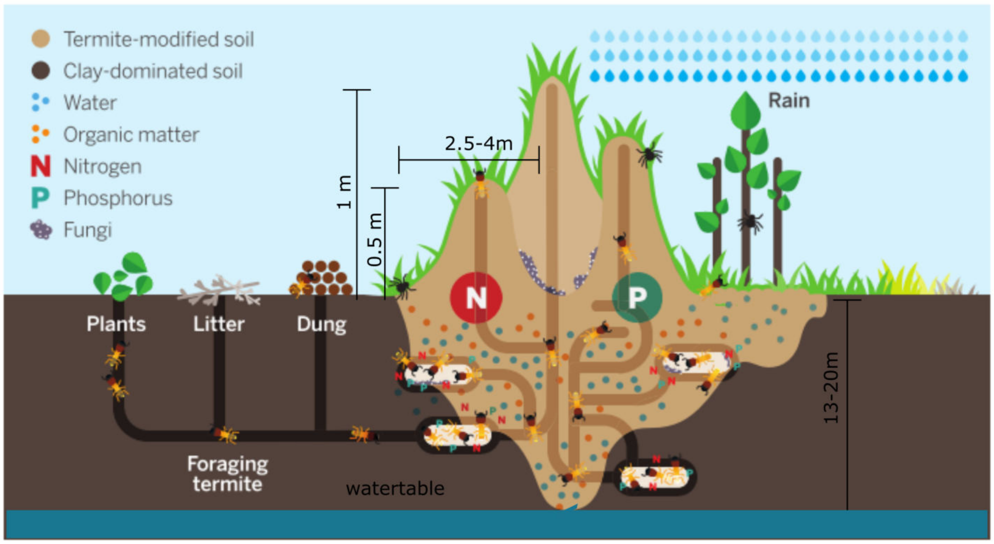

Figure 2.4: Termite mound cross section (modified after (Pennisi, 2015)). While foraging, termites will bring dead plant matter and other organic waste materials into the mound. The fungi contained inside the mound will break it down to soil enriching nutrients, like nitrogen and phosphorous allowing for plant growth and animals around to flourish. During foraging, termites make the soil more porous increasing filtration rates of the surrounding soils. They modify the soil content to a desirable cast for constructing their mounds.

When a termite mound erodes overtime it's soil material is added to the surrounding top soil, which can alter significantly the physical properties and geochemistry of the topsoil (Pomeroy, 1977). In semi-arid regions due to plant competition for water, bare patches develop on the ground but there is always a high concentration of plants around termite mounds due to their fertility and water retaining ability (Juergens *et al.*, 2015).

All these abilities of termites being able to interact at diverse spatial scales within their environment make them ideal indicator species for ecosystem change. Termite mounds have been used in the identification of natural resources and change in composition of or anthropogenic disturbance of an ecosystem. Brown (1997); Constantino (1998) suggest that the main attributes that justify the usage of termite mounds as indicator species are :

- Widespread geographic distribution
- High abundance
- Low loco-motor capacity
- Ease of sampling
- Short response time to anthropogenic disturbances

In termite mound populations, similar size colonies tend to coexist with an emergent common radial foraging boundary. Mounds sharing a common foraging boundary are refereed to as nearest neighbours. Among old mounds, short nearest neighbour distances are associated with resource abundance, while long nearest neighbour distances with heightened competition for resources (Muvengwi *et al.*, 2018). In young termite mounds, the common clustering spatial patterns are associated with a patchily distributed micro climate.

As the young termite colonies grow overtime, so does the demand for resources, resulting in colony clashes and some being destroyed. With the destruction of some colonies, foraging distances increase for the now remaining older colonies. This leads to random colony spatial patterns and increase in size of each of the remaining colonies. Increase in colony size in turn leads to greater demand for resources, resulting in more colony clashes and destruction (Davies *et al.*, 2014).

Post colony clashes, foraging territories are then re-established between the remaining colonies resulting in dispersed spatial patterns and resource abundance. Resource abundance results in a high number of colonies and a decrease in nearest neighbour distances. The degree of termite mound colony spatial patterns vary over different environmental gradients whereby both dispersed and clustered patterns can emerge at short-scales (Juergens *et al.*, 2015).

It is important to note that there is limited available research on the characterisation of termite mounds in the Karoo that could be accessed during this study outside that of mima mounds or heuwetjies which are deemed to be ancient relic mounds. These mounds are not built by termites and a common theory of their origin is that they are an accumulation of wind-blown sediments around vegetation to form coppice dunes (Cramer and Midgley, 2015). Since these mounds are relic mounds, they are larger and almost form part of the surrounding area camouflaging as small hills.

Chapter 3

Study Area and Auxiliary Data

3.1 Study Area

The study was conducted around the neighbouring towns Adelaide, Bedford and Fort Beaufort, falling within the Raymond Mhlaba Municipality in the Eastern Cape Karroo of South Africa. The selection of the study area was based on it forming part of the zone that has been earmarked for potential shale gas exploration (Figure 2.2).

Four study sites were selected based on the abundance of termite mounds (termite mounds per hectare ($\geq\sim$ 1 ma.ha^{-1}), see Davies *et al.* (2014)), topographic profile, visibility and accessibility of the area (Figure 3.1, Table 3.1). Google Earth Pro was used for the initial surveying of the sites where sampling plot polygons were delineated. The sampling plots were selected based on termite mound visibility of termite mounds and accessibility based on Google Earth Pro.

On each of the four study sites two plots were delineated with the exception of Site B, where only one plot could be sampled due to it falling into private property that researchers could not access.

The sampling included sampling along an elevation profile as part of understanding the influence of environmental heterogeneity on termite mounds. The elevation map (Figure 3.2) shows the altitudes and distances between the study sites.

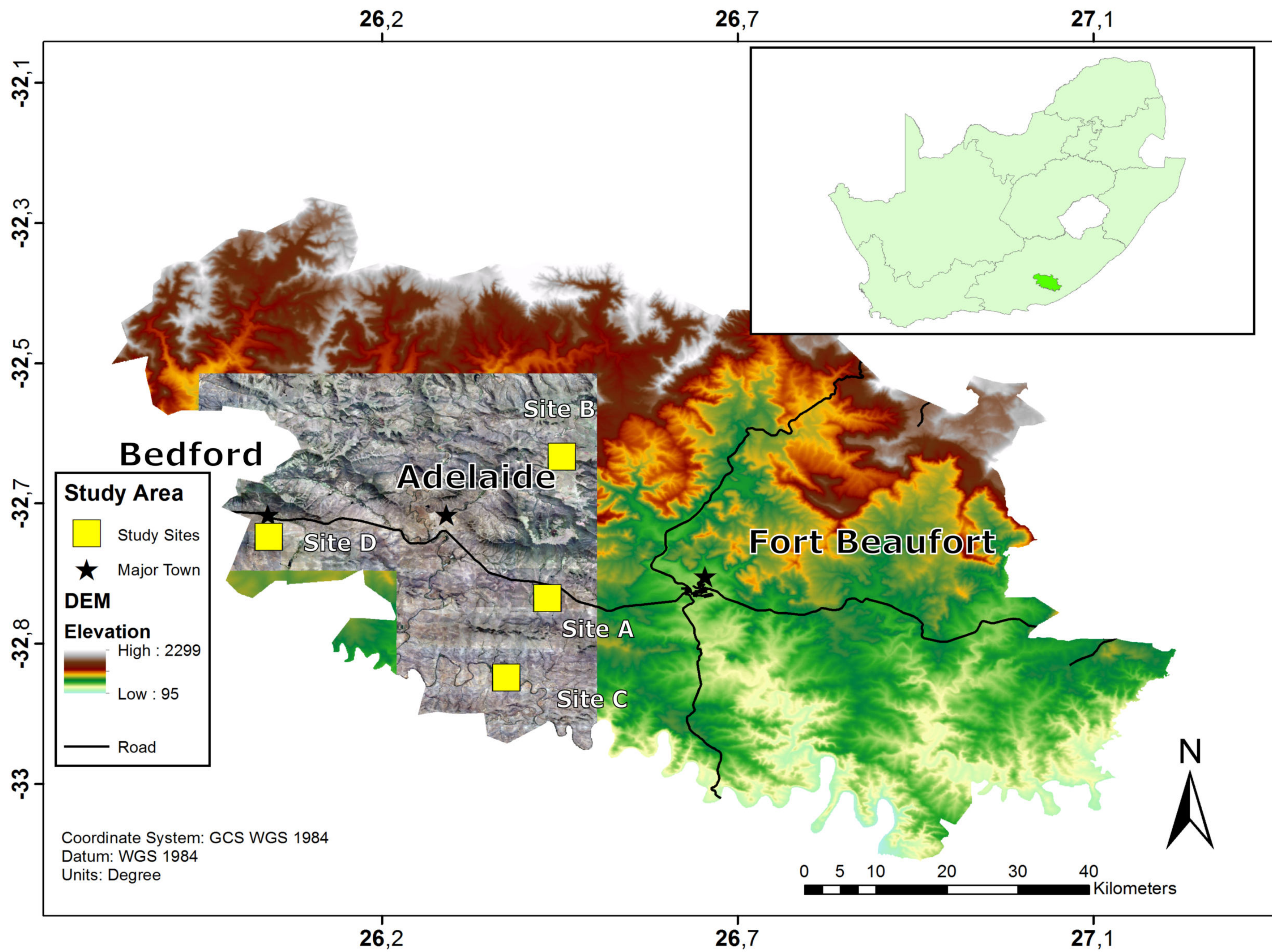

Figure 3.1: The Digital Elevation Model of Raymond Mhlaba Municipality in the Eastern Cape Karoo, showing the different elevations and locations where termite mound sampling was conducted (Oghenekome, 2012).

Table 3.1: Location and names of sampled study sites.

Study Site	**Name**	**Location**	**Terrain Elevation (m)**	**Number of Plots**
Site A	Yellowwoods	26°26 'E 32°46 'S	671	2
Site B	Thorn Hill	26°27 'E 32°35 'S	1048	1
Site C	Groot Draai	26°23 'E 32°52 'S	435	2
Site D	BedFord	26°50 'E 32°41 'S	755	2

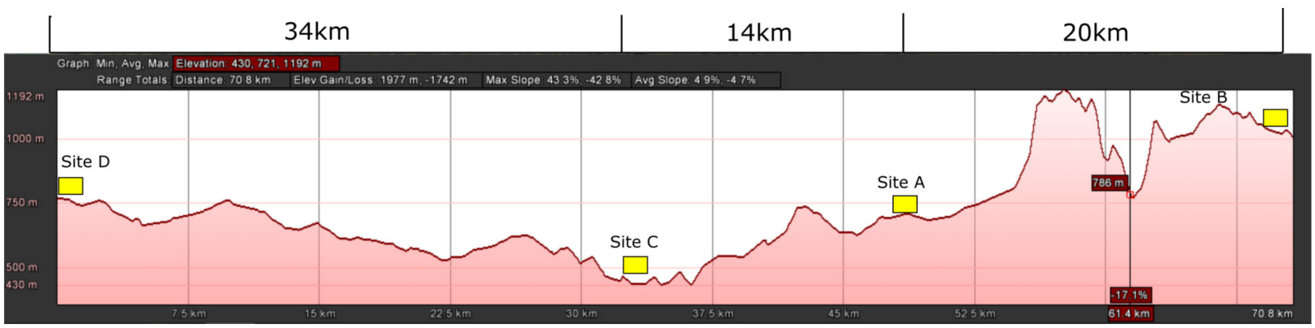

Figure 3.2: Terrain elevation profile of the study sites.

3.1.1 Site A (Yellowwoods)

Site A (Figure 3.3) falls within a game farm next to a school with a grassy and dry savannah looking landscape. It is close to a main road with a few trees surrounding it. Termite mounds and grassy vegetation cover were present, with one plot having a handful of tree cover and another being void.

The are numerous small ponds on site, indicating good water source presence. Eutric Regosols are the dominant soil type, with abundant small stones and pebbles. Bedford Dry Grassland is the vegetation cover that is present. The site sits on the Daggaboersnek Member of the Balfour geological formation.

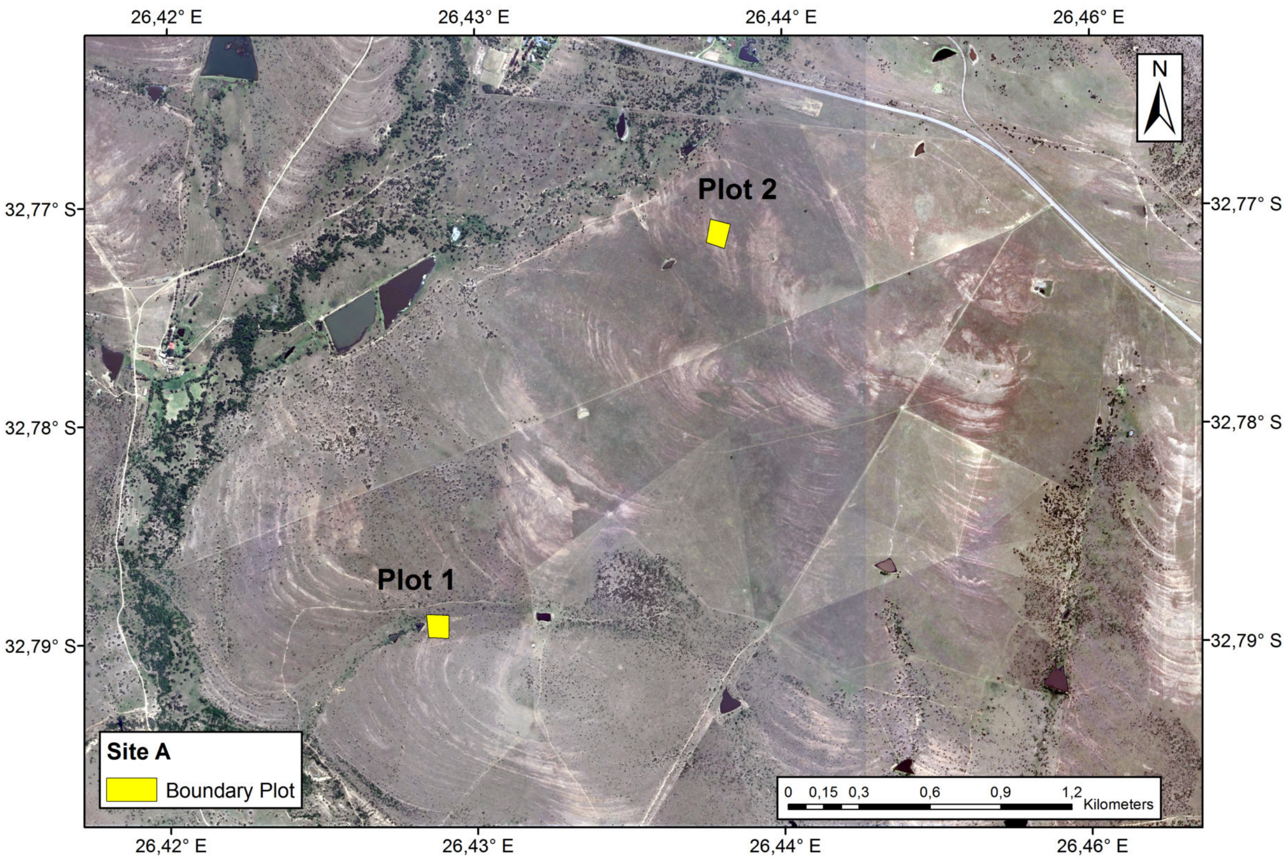

Figure 3.3: Aerial photograph of the Yellowwoods site. Elevation: 671 m, Coordinates: 26°26 'E 32°46 'S. The size of plot 1 is 8773.81 m^2 and the size of plot 2 is 8699.84 m^2.

3.1.2 Site B (Thorn Hill)

Site B (Figure 3.4) falls within a remote farm away from main roads with dense grassy vegetation. Lithic Leptosols are the dominant soils in the area, sandy and porous alluvial in make up. There is a nearby grazing field. Here termite mounds appeared to be larger than in other sites. Some mounds are red in colour like the soil cover of the area and others are sandy looking reflecting the contrast in soils.

The mounds here are more pronounced on Google Maps Pro due to the elevation of the region. Tree cover is prominent on the site, but there are no trees at the sampling plot. Amathole Montane Grassland is the dominant vegetation on the site. It sits on the Elandsberg Member of the Balfour Geological Formation.

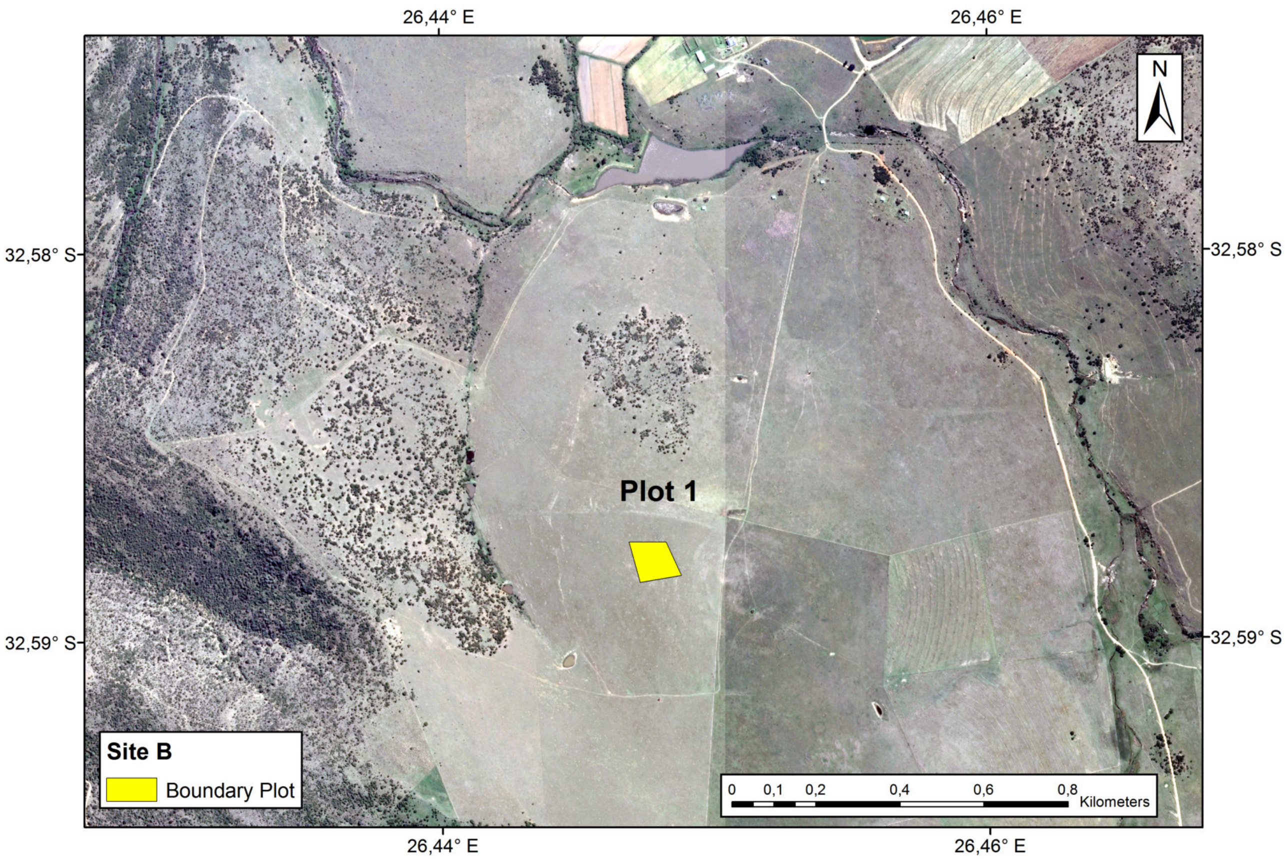

Figure 3.4: Aerial photograph of the ThornHill site. Elevation: 1048 m, Coordinates: 26°50 'E 32°41 'S. The size of plot 1 is 8436.66 m^2.

3.1.3 Site C (Groot Draai)

Site C (Figure 3.5) falls within a farm with a river running through it nearby to the sampling plots. On Google Earth Pro, it was difficult to identity termite mounds on this site. This is attributed to dense tree cover at the sampling plots in comparison to other sites. During ground surveying, it was confirmed that termite mounds were present here.

The dense tree cover on the site has formed a canopy over the termite mounds, preventing them from clear detection on Google Earth Pro. The site is rocky with hard dry ground and shrubby vegetation. Great Fish Thicket is the main vegetation here with Eutric Regosols as the dominant soils. The site sits on the Middleton Geological Formation.

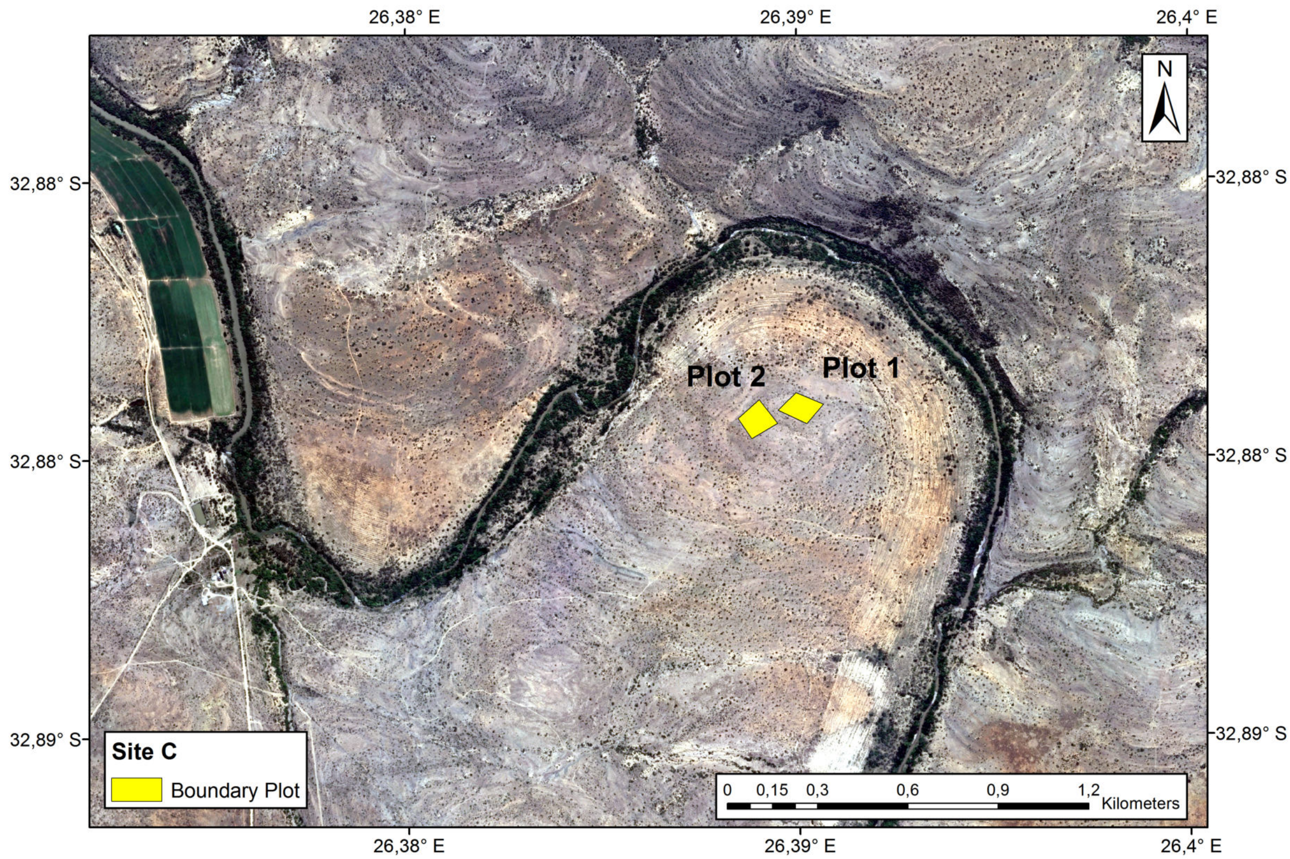

Figure 3.5: Aerial photograph of the Groot Draai site. Elevation: 435 m, Coordinates: 26°23 'E 32°52 'S. The size of plot 1 is 8777.92 m^2 and the size of plot 2 is 8870.14 m^2.

3.1.4 Site D (Bedford)

Site D (Figure 3.5) falls just outside of the Bedford town and close to human settlements with pronounced foot paths. It is near a main road and has numerous small ponds around it. There is good grassy vegetation cover present. Mounds here seemed to be densely populated in relation to other sites.

Bedford Dry Grassland is the main vegetation cover, it overlays Leptic Regosols which are the dominant soils. The site sits on the Daggaboersnek Member of the Balfour Geological Formation.

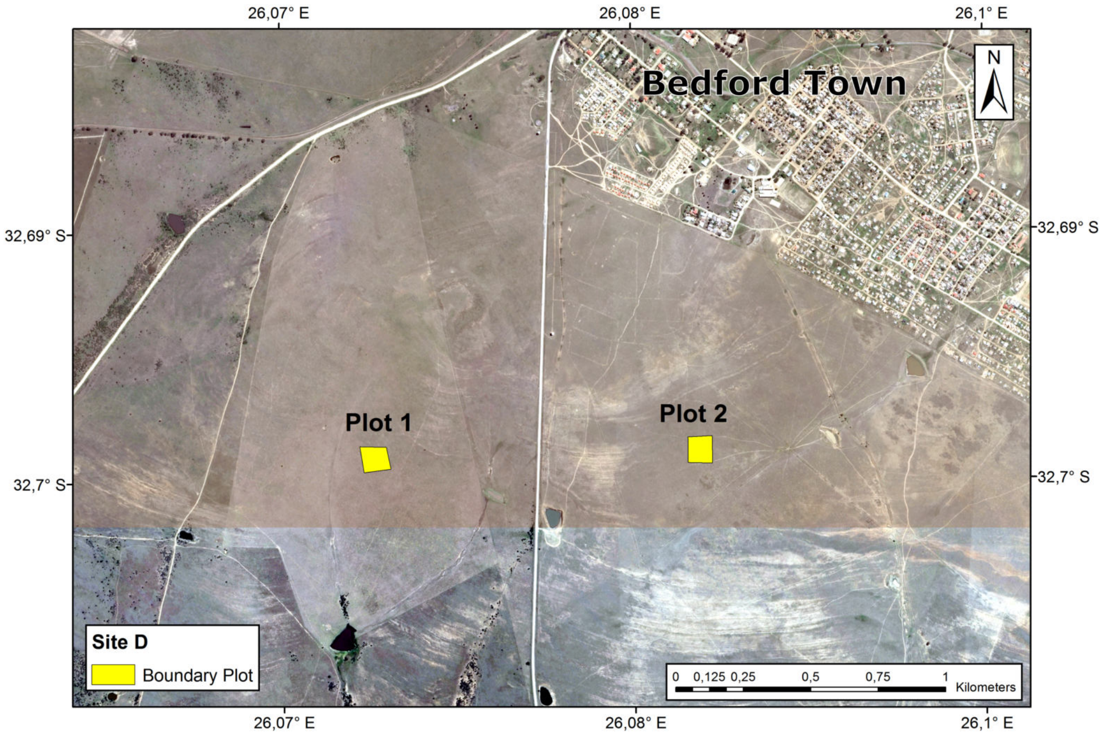

Figure 3.6: Aerial photograph of the Bedford site. Elevation: 671 m, Coordinates: 26°26 'E 32°46 'S. The size of plot 1 is 8870.14 m^2 and the size of plot 2 is 8870.14 m^2.

3.2 Auxiliary Data

This section presents the auxiliary data present at the study sites, in the form of anthropogenic and natural factors including vegetation, soil, geology, elevation & rivers, human settlements & roads.

3.2.1 Vegetation

There are three dominant vegetation types in the study (Figure 3.2) Bedford Dry Grassland, Great Fish Thicket and Amathole Montane Grassland (Figure 3.7). The variable vegetation provided for spatial heterogeneity characterisation of the termite mounds present at the sites.

Great Fish Thicket

Great Fish Thicket forms in the Eastern Cape river valleys of Keiskamma and Great Fish, extending from Adelaide towards Cradock and Cookhouse and beyond.

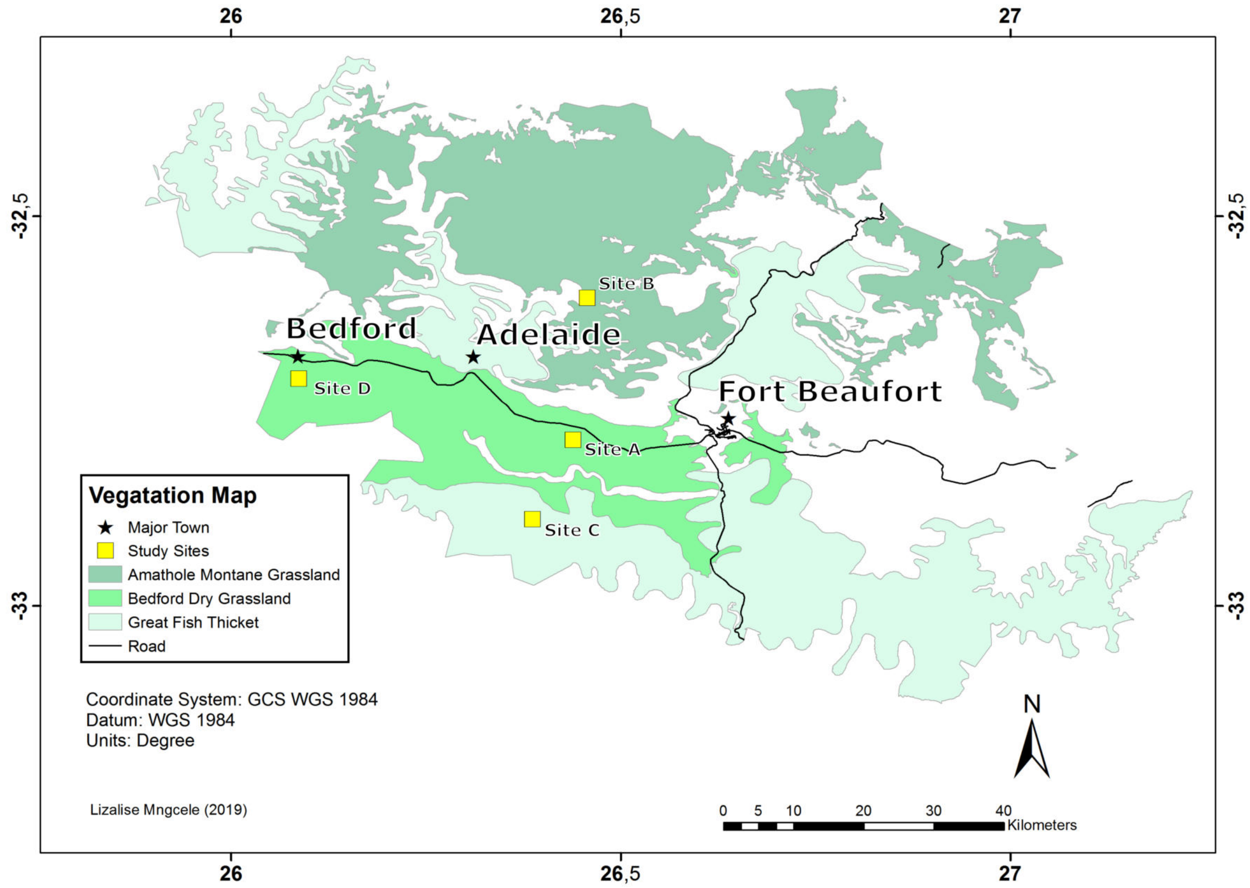

Figure 3.7: Vegetation map of Raymond Mhlaba Municipality showing the different vegetation types present at the study sites (Aucamp and Tainton, 1984; Vlok *et al.*, 2003).

It forms part of the Albany Thicket Biome (Vlok *et al.*, 2003). The thicket has not been significantly altered with the exception of cultivation and urbanisation (Vlok *et al.*, 2003). The vegetation is dense, woody and semi-succulent thorny scrubs, standing between 2-3 m tall. Northeasterly, there is prevailing grassland and thorn-tree savannah type vegetation due to increased seasonal rainfall.

Fynbos is more prevalent southwest due to increase in winter rainfalls (Aucamp and Tainton, 1984). It derives its name from the its impenetrable nature experienced by grazing livestock.

The soils are are majority clay soils with the presence of a few endemic species existing in succulent shrub, low shrub and succulent herb life forms. Great Fish Thickets vary between tall medium to short spinescent shrubs with succulents and woody trees (Aucamp and Tainton, 1984).

Mean annual precipitation is 449 mm with annual temperature of 17.1 Frosting in the vegetation is more regular in the upper parts of the valley. Great Fish Thicket usually lies at altitudes of up to 1000 m above sea level with higher coastal areas having a mean annual precipitation of 600 mm in contrast to 300 mm of inland regions (Martin, 2017). There are nutrient rich zoogenic mounds in the region occupied by endemic geophytes may induce thicket clumping, with a distinctive feature of a closed canopy vegetation type.

Bedford Dry Grassland

Bedford Dry Grassland is found in the Eastern Cape in regions were the soil conditions are mostly clay or loamy. It forms part of the Grassland Biome, which is divided into sourveld and sweetveld with the former found in high altitude and the latter in low altitude regions (Vlok *et al.*, 2003). Soils in the sourveld are leached and dystrophic with high plant production and canopy cover.

In sweetveld the soils are eutrophic. Bedford Dry Grassland has no endemic vegetation type although its falls within the Albany center of endemism (Vlok *et al.*, 2003). It has a relatively even mean annual precipitation of 423 mm across the region with a mean annual temperature of 16.5 °C.

Precipitation tends to be more in mountainous areas (Martin, 2017). Andropogonoid grasses are abundant in regions with a rainfall of above 600 mm and the sweet chloridoid abundant in regions with less rainfall (Huntley, 1984). Only a small fraction of Bedford Dry Grassland has been altered through cultivation. The grassland is found at altitudes of above 480 to 990 m and experiences both low and high erosion. The vegetation is dominated by grass with Kowie Thicket and Albany Broken Veld (Huntley, 1984).

Amathole Montane Grassland

Amathole Montane Grassland forms predominantly in the mountainous regions of the Eastern Cape where the soils are freely drained, deep and highly weathered.

Abundance of forbs characterise the short grassland, with the northern watershed region's vegetation forming a mosaic with Karoo Escapement Grassland (Vlok *et al.*, 2003). Amathole Montane Grassland erosion rate is low and has been by altered by livestock grazing, plantation and cultivation (Mucina and Rutherford, 2006). The latter is more pronounced in mountainous regions.

Dominant grasses include but not limited to: Eragrotis chloromelas, Sporobolus africanus, Elionurus muticus. The grassland forms at altitudes of between 150 m and 650 m above sea level. It is characterised by biomodal spring and late summer peaks of rainfall with mean annual precipitation at 672 mm and a mean annual temperature of 14.7 °C. (Mucina and Rutherford, 2006).

3.2.2 Soil

Leptic Regosols, Lithic Leptosols and Eutric Regosols are the dominant soils present throughout the study area (IUSS Working Group WRB, 2014) (Figure 3.8). The properties are summarised in Table 3.2.

Regosols

Regosols are referred to as weakly developed mineral soils in loosely arranged materials with no significant profile development (IUSS Working Group WRB, 2014). Their content is thin or moderately rich in coarse fragments, does not have a mollic or umbric horizon, void of sandy or fluvic materials. Parent material is generally fine-grained and unconsolidated material, eroding lands is where they are most prominent also at accumulation zones.

Regosols correlate with soil taxa that are marked by incipient soil formation (IUSS Working Group WRB, 2014). Environmentally they occur at all climate zones with the exception of permafrost and at all topographic profiles. They are consistent with mountain terrain, arid to semi arid regions.

Slow soil formation or the age influences the profile development. Irrigation is needed for crop production in Regosols forming in regions with rainfall between 500-1000 mm per year. This is due to them having a low water holding capacity. The prominent principal qualifiers of Regosols are Leptic, Folic, Greylic, Stagnic, Brunic, Dolomotic, Sodic and Eutric. (IUSS Working Group WRB, 2014).

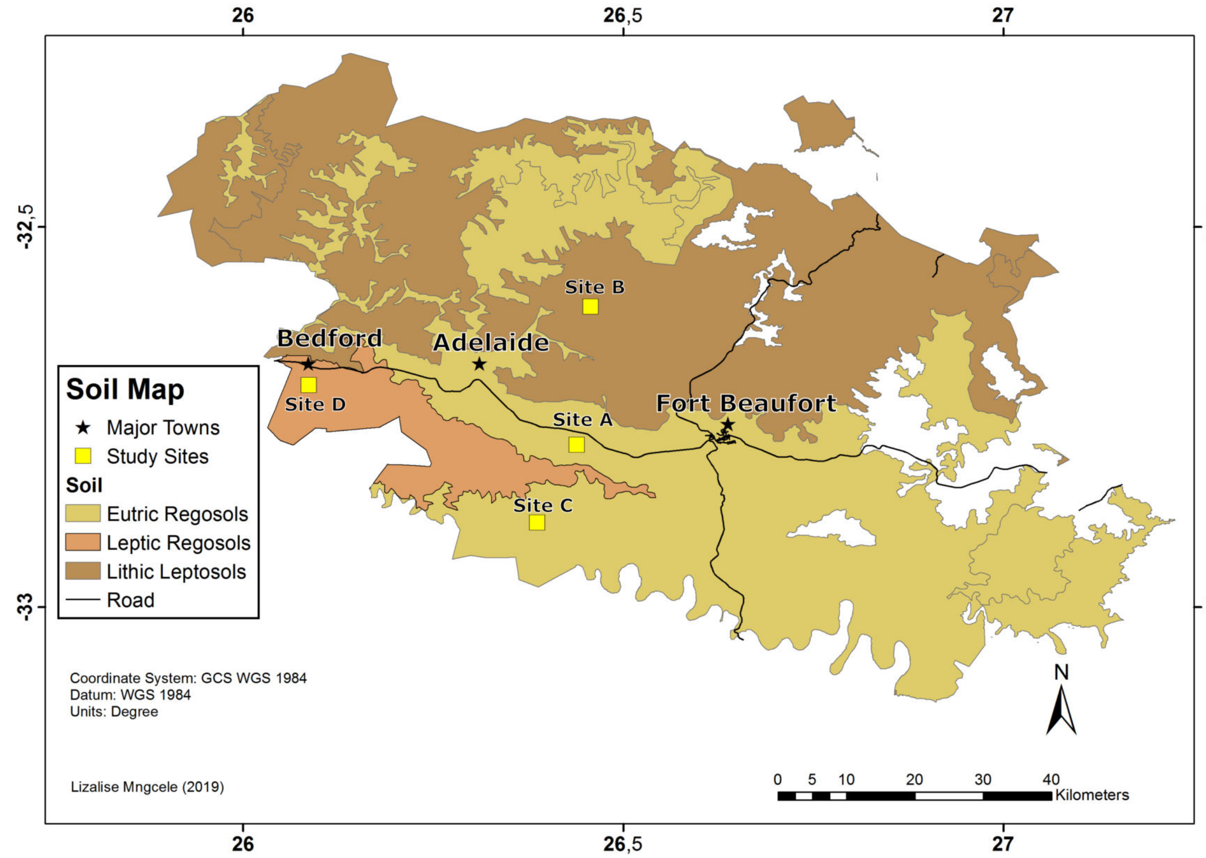

Figure 3.8: Soil map of Raymond Mhlaba Municipality showing the different types of soil found in the study region (IUSS Working Group WRB, 2014).

Leptosols

Leptosols are those thin soils over continuous rock and soils that are endowed in coarse fragments. Mountainous regions are ideal areas for Leptosols as they occur mostly at high or meduim altitude and with strongly dissected topography. Leptosols consist of less than 25% of fine earth averaged over a depth of 75 cm from the soil surface or to continuous rock or technical hard material (IUSS Working Group WRB, 2014). They are found on weathering resistant rocks or where erosion has removed the top of the soil profile or has kept up with soil formation.

Leptosols are also found in strongly eroding areas, regions of abundance in either hot or cold dry climatic conditions. They are extremely gravelly and have a mollic horizon in weathered calcareous material. The most extensive Leptosols are those with continuous rock at less than 10 cm depth in Montane regions. On hill slopes they are more fertile than on more level land with extensive internal drainage and shallow depth (IUSS Working Group WRB, 2014).

Leptosols are void of petroduric, petrogypsic, petroplinthic calcic, chernic, spodic horizon or duric. Principal qualifiers are Dolomitic Folic Subaquatic Cambic, Eutric and Lithic to mention a few (IUSS Working Group WRB, 2014).

Table 3.2: Properties of soil types.

Soil Type	**Properties**
Leptic Regosols	Leptic Regosols are defined as Regosols having continuous technic hard or continuous rock material starting at below 100 cm from the soil surface. They are soils with a texture of sand or loamy.
Eutric Regosols	Eutric Regosols posses a $\mathrm{pH}_{\mathrm{water}}$ level ≥ 5.5 in the major part with organic material within 100 cm of the soil surface.
Lithic Leptosols	Lithic Leptosols form in mountainous regions and are the most extensive Leptosols on earth. They have a technic hard or continuous rock material starting at less than 10 cm from the soil surface.

3.2.3 Geology

The Karoo Basin is a large southward deepening basin as the result of the Cape Fold Belt system formed inside the Gondwana continental interior and represents a large-scale episode of intermittent subsidence and sedimentation (Lindeque *et al.*, 2011; Tankard *et al.*, 2009). Unconformity-bounded mega-sequences make up the sedimentary fill and consist of a three stage evolution. A crustal uplift, fault-controlled subsidence and long periods of regional subsidence when faulting was subordinate.

The Karoo Basin was deposited on the rigid Natal, Namaqua and Kaapvaal crustal blocks, this is evident in its tabular and underformed stratigraphy (de Wit and Jeffery, 1988). The Main Karoo Basin contains the Karoo Supergroup which spans about 600 000 km^2 and has a maximum thickness of approximately 5500 m above the Namaqua basement block (Tankard *et al.*, 2009). The Karoo Supergroup consists of five groups: the Drankensberg, the partly marine Ecca and Dwyka groups to the fluvial and aeolian Beaufort and Stomberg Groups. Karoo sedimentation was halted by the large igneous province, characterised by the Drankensberg basaltic lava flows and dolerite lower Jurassic sill complexes and dyke intrusions (Linol and De Wit, 2016).

These groups are intruded by dolerite dykes present throughout the sedimentary sequences. The Adelaide Subgroup's geology in particular is of interest in this study.

It separates into the Beaufort Group that divides into the Balfour and Middleton Formation. Figure 3.9 shows the geological map of the study area that falls entirely within the Adelaide Subgroup and the different geological formations of the Beaufort Group and their members found on the study sites.

Beaufort Group

The Beaufort Group (3.9) marks a transition between the marine Ecca deposits to fluvial mudstones, siltstone and sandstone deposits (Tankard *et al.*, 2009). The sandstones of the Beaufort Group much like those of the Ecca contain a high rock fragment content dominated by felsitic grains (Johson, 1976). A useful lithostratigraphic marker are the thick persistent delta-front sheet sandstones at the top of the Ecca Group. The different margins of the Karoo Basin inform the Lower Beaufort sediments which lead to fine-grained sandstones and pebbly sandstones in the north (Johson, 1976).

Sedimentation of the Beaufort Group in the south western Karoo Basin was initiated in the middle Permain by uplift in the Gonwanide mountainlands. Permo-Triassic rocks of the Beaufort Group make up 20% of South Africa's total surface area, with the foredeep accounting an approximate maximum cumulative thickness of 7000 m decreasing in the northerly direction (Catuneanu and Elango, 2001). In the foredeep there is a thick deposition of a succession of sandstones and mudstones containing rich tetrapod faunas. The lithology and variation in the depositional environment of the Beaufort Group separates into two groups: Adelaide Subgroup and the Tarkastad Subgroup (Nengovhela, 2018).

Adelaide Subgroup

The Adelaide Subgroup (3.9) is a basin-filling unit with upward-fining where deposition took place in the floodplain, fluvial and lacustrine environments (Chere, 2015). It is a late Permian sequence with a lower southward-thickening wedge of up to 700 m and reaching 100 m - 200 m in the north with alternating sandstone and mudstone lithologies (Tankard *et al.*, 2009). A south and southeast principal provenance in the Adelaide Subgroup is indicated by Palaeo-current data, with secondary source areas from the northeast, west-northwest, and southwest (Nengovhela, 2018).

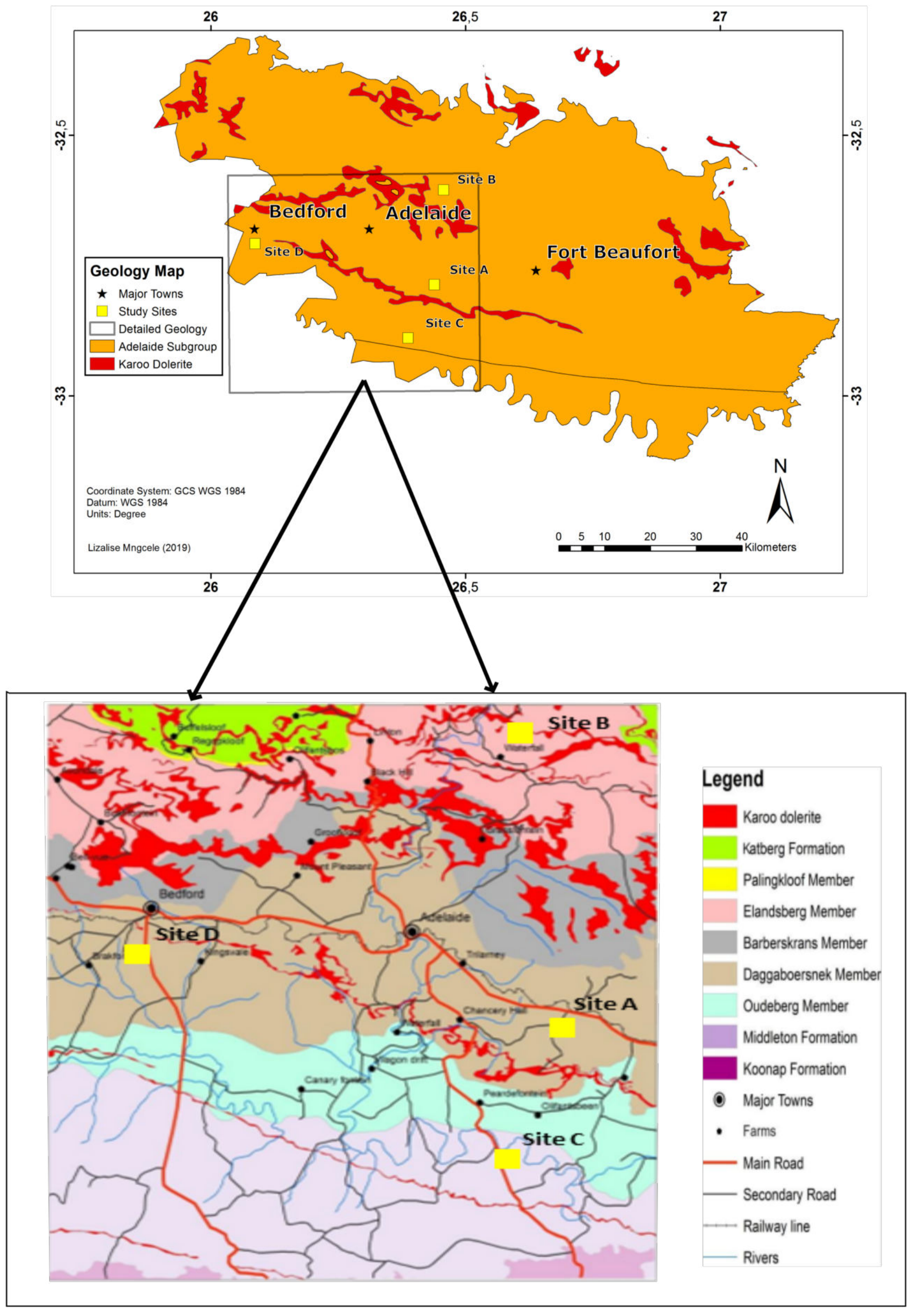

Figure 3.9: Geological map of Raymond Mhlaba Municipality showing homogeneous geology of the Adelaide Subgroup and Karoo Dolerite. Below is a detailed map of the geological formation and members present at the different study sites (Oghenekome, 2012).

The high mud and sand ratio sediments coupled with the fine grained nature of the overlaying sandstones are indicative of deposition and meandearing rivers. The subaerial delta plain setting is where the lowermost sediments are deposited. The Adelaide subgroup divides into the Koonap, Middleton, Abrahamskraal, Teekloof, Middleton and Balfour Formations (Chere, 2015).

Balfour Formation

The Balfour Formation (3.9) is the upper unit of the Adelaide Subgroup and consists of a fluvial succession that accumulated in the foredeep of the Karoo Basin (Tankard *et al.*, 2009). It consists of prominent sandstone units and fining upward sandstones dominated sequence. There is unconformity at the base caused by the lithospheric uplift after the seduction event. It corresponds to one second order depositional sequence with braided river sequences grading upwards into meandering stream systems (Linol and De Wit, 2016).

Fining upward sandstone dominate the sequence and are interbedded with shale and mudstone. Persistent sandstone lithosomes occur in the middle and upper parts. Sandstone lithosomes are subtabular to moderately lenticular in shape excluding the middle to upper members, with light grey to medium grey appearance. Mudstone varies from slightly greenish to medium grey (Catuneanu and Elango, 2001). The Balfour Formation divides into five units according to lithostratigraphy: the Daggaboersnek, Elandsberg, Palingkloof, Oudeberg, and the Barberskrans Members, but only three are discussed for purposes of this study.

- Daggaboersnek Member

Lower sandstone percentage than the underlying and overlying strata of the Balfour Formation characterises the Daggaboersnek Member with rhythmitite of poorly to moderately well-developed mudrocks that constitute between 5-10% of the total Balfour thickness (Johson, 1976). Regular, generally non-lenticular, overall stratification with lithosomes subtabular to moderately tabular, characterise the member. Cross-bedding and flat-bedding are a rare occurrence with mostly regular bedding, abundance of tin, tabular sandstones, presence of wave ripple marked surfaces displaying east north-east to west south-west orientation. This is coupled by a presence of dark shales (Johson, 1976).

The mudstone appearance ranges from medium to dark grey beds. Sandstone contains amounts of moderately to poorly sorted grains. Low rock fragment content characterise the sandstone that contains heavy minerals with more monocrystalline than polycrystalline quartz grains (Oghenekome, 2012).

- Elandsberg Member

The Elandsberg Member is a predominantly argillaceous unit, that comprises alternating sequences of mudrock and subordinate fine to medium-grained sandstones. It has a thickness of approximately 700 m and is overlain by red mudstones and shales of the Palingkloof Member (Oghenekome, 2012). Trough cross bedding at the base characterise the lenticular sandstone units with thick flat bedded units of mudstone that sometimes alternate with siltstone. It has a high content of mudstone and abundance of near planar erosion surfaces.

The mudstone is predominantly greenish to gray (Linol and De Wit, 2016). Subordinate sandstone occurs as well developed massive to ripple laminated or trough cross bedded units. The minerals consist of quartz, feldspar and mica with a few lithic fragments (Oghenekome, 2012).

- Middleton Formation

The Middleton formation has vertically stacked fining upward sequences that overly mudrock dominated succession consisting of a shallow lacustrine facies at the base. It represents deposition associated with inactive tectonic loading. A mudstone dominated unit with conformable lower and upper boundaries (Bordy *et al.*, 2011).

Majority of the formation comprises of fine grained rock types composed of thick monotonous successions. Comprising the sequences are erosively based sandstone, siltstone and mudstones deposited by delta distributary and meandering river channels. Small oscillation ripple marks are occasionally present with roughly symmetrical crests (Bordy *et al.*, 2011; Johson, 1976).

Flanking these meandering rivers are extensive areas of mud dominated floodplain and crevasse splays (Catuneanu and Elango, 2001). Sandstone beds here typically form weakly fining successions.

The sandstone is grey to medium grey in colour particularly when fresh although whitish speckling is common. The mudstone varies from meduim grey to greenish meduim grey. Red mudstone can be observable here in contrast to the Balfour Formation (Johson, 1976).

Karoo Dolerite

Dolerite are andesites and tholeiitic basalts that are subalkaline and heavily constituted by trace elements and are intrusive in nature (Neumann *et al.*, 2011). Intrusion into the Karoo Supergroup sediments by these dolerite dykes and sills transpired in the Jurassic during the Gondwanaland breakup. They form as sills and dykes that intrusively penetrate geological strata. Sills constitute horizontal penetration and dykes vertical penetration of strata. In Figure 3.9 the abundance of Karoo Dolerite in the study area is represented by the red features.

Karoo Dolerite are responsible for the drainage systems of the Basin and influence majority of the second order geomorphological features (Woodford and Chevallier, 2002).

While performing a hydro-census in the Karoo Basin, Woodford and Chevallier (2002) noted that boreholes drilled alongside dolerite dykes appeared to be more productive. As a result intrusion of dolerites has come to be associated with potential zones for open fracturing in aquifers. For this reason dolerites dykes in particular are known for their water yielding capacity.

3.2.4 Elevation and Rivers

Subsidence in Southern Africa is prevalent towards the southern tip and spreading northwards to the equator (Cole, 1994). This is attributed to the Karoo terrain being warped into basins and intervening swells. Present day topography between the coast and escarpments preserve a number of erosion surfaces. The terrain is rugged with a varying elevation profile home to diverse ecosystems.

Mountainous terrain are common in the region often as a result of intruding dolerite sills. The topography is inconsistent, largely made of plains and mountains with high relief and lowlands (Linol and De Wit, 2016). The sills act as both sources and local barriers of rivers.

The Great Fish and Orange River form as the main rivers meandering along the floor of big sill complexes with tributaries.

In the Balfour Formation there are numerous braided river sequences forming. The Karoo is prevalent in seasonal and ephemeral rivers that are dependent on ground water due to the dry climate conditions.

Majority of the rivers in the region seem to disappear underground during extended drought periods, hence the interaction of ground and surface water is important in the region for sustaining the existing ecosystems (Botha *et al.*, 2002; Woodford and Chevallier, 2002). Ground water recharge allows for the water table to intersect with the river channel.

3.2.5 Human Settlements and Main Roads

Earth systems have started to experience the elongated complex systemic relationships between human and nature interactions in the Anthropocene (Henschel *et al.*, 2018). Given this relationships between nature and humans, it is difficult to ascertain the cause and effects of its impact on nature. The impact of human actions over time in the Karoo has grown since pre-historic times.

The erection of human settlements and construction of roads has lead to negative impacts on ecosystems (Henschel *et al.*, 2018). Drainage patterns are often altered during these processes. Invasive alien species gain opportunities to flourish during the periods of distabilisation.

Chapter 4

Data Acquisition and Pre-Processing

Data was collected using a combination of two data sources, mainly primary and secondary data. The ground and drone surveys were performed during the month of August in 2018. Images for the aerial survey were extracted from the National Geo-spatial Information (NGI), dated 2015 (National Geo-Spatial Information, 2013). Although there is a three year difference, the aerial images were still relevant for use as the average mound colony takes about 5 years to grow Korb and Linsenmair (2001). Details on the drone and aerial survey are covered in their subsections later in the chapter.

Auxiliary data (Table 4.1) was acquired in the form of shapefiles from the AEON database and was discussed previously in Chapter 3. Rivers, roads, human settlements and Karoo dolerite were digitised and their Euclidean distances from the termite mound plots recorded for the ground survey. Geology, soil and vegetation were overlayed over the termite mound plots in the study.

Table 4.1: Auxiliary data containing natural and anthropogenic features.

Natural	**Anthropogenic**
Rivers	Main Roads
Karoo dolerite	Human Settlements
Geology	
Soil	
Vegetation	
Terrain Elevation	

These features were then used to create a Spatial Join with the termite mounds, allowing each termite mound at the plot to have the data of each feature associated with it.

ArcGIS version 10.6 was the GIS software used for data pre-processing. Drone flight planning, mapping, data acquisition, photogrammetry and image processing was done using DroneDeploy and Pix4D. The R statistical programming language, “spatstat” CRAN package, was used for performing spatial statistical analysis (Baddeley *et al.*, 2015).

In remote sensing, ground data is collected as a means to interpret, validate and relate to acquired satellite or aerial data. Remote and ground surveyed data can both be stored and matched in a GIS to assess the accuracy of the remotely sensed data. Remote sensing avoids the impracticality of comprehensive field surveys. However, depending on the type of remote sensing, it can limit the detection of certain natural features that are not commonly discernible due to size (Ruwaimana *et al.*, 2018).

To combat this problem, unmanned aerial vehicles (UAVs) commonly known as “drones” have been introduced. It is expected that application of this technological advancement can contribute greatly to termite mound data acquisition (Table 4.2) and will allow for a more flexible resolution adjustment in order to detect and acquire spatial data of these small natural features (Noor *et al.*, 2018). The introduction of consumer drones has made remote sensing more affordable in contrast to conventional aerial and satellite surveys.

Table 4.2: Advantages and disadvantages of the different data collection techniques in the study.

	Advantages	**Disadvantages**
Ground	insitu, less error prone, more detailed resolution	time consuming, high costs, not easy to scale
Aerial	time saving, easy to scale	high costs, less detailed resolution
Drone	less costly, more detailed resolution, time saving, generate more detailed 3D models, realtime data streaming, data is cloud backed up	not easy to scale

4.1 Data Survey

4.1.1 Ground Survey

Ground surveying (Figure 4.1) was conducted using a hand held Garmin GPS with a 3 m positional accuracy to record the locations of each termite mound found inside the sampling plots. Measurements of termite mound height and basal circumference were taken using a measuring tape. For measuring basal circumference, the measuring tape was wrapped around the base of the mound where it touched the ground. The height was measured from the base of the mound where it touched the ground to the highest point on the mound.

Figure 4.1: Termite mound field mapping, using a measuring tape and GPS to collect data on mound geometric attributes.

In order to maintain consistency in mound detection, the following protocol was applied:

- Termite mounds with height less than 0.20 m were classified as having zero height, this was to eliminate destroyed abandoned mounds or mole hills which were prevalent at the sites

- To be recorded, termite mounds needed to be bigger or equal to1m in basal circumference, this was to eliminate destroyed abandoned mounds or mole hills which were prevalent at the sites

- All sampled mounds had active termites about them (Vranken *et al.*, 2014; Davies *et al.*, 2014)

The collected termite mound location data from the GPS and the recorded attributes of height and basal circumference for each mound, were matched and then exported into ArcGIS and R for processing and analysis.

Ground surveyed termite mound basal circumferences were aggregated for all the plots (globally) and also at local scale for each individual plot. The straight-line crossing the scatter plot (Figure 4.2), shows that the mean global basal circumference was around 2 m. The histogram (Figure 4.2) is tailed towards the right, showing data skewness and that a low number of the global basal circumferences were larger than 3 m.

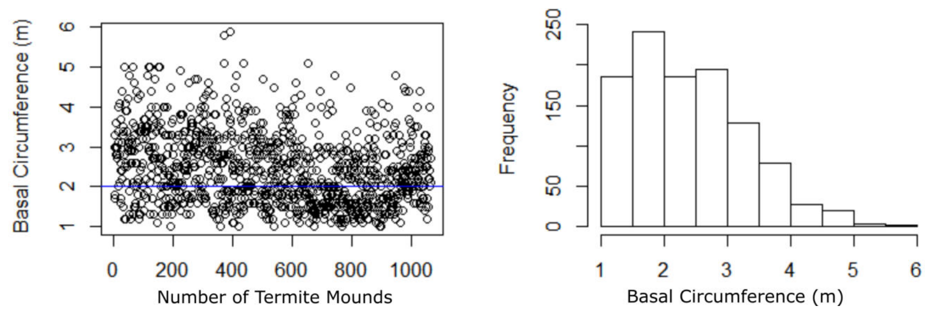

Figure 4.2: The scatter plot and histogram show the global distribution of ground surveyed termite mound basal circumferences across all plots.

Pre-Processing A data summary (Table 4.3) at global and local scale was performed for the study sites in order to understand the distribution of termite mound height and basal circumference. Using basal circumference as a proxy for age (Table 4.3), all mounds were divided and categorised according to age, young and old.

The rational in separating mounds by age is premised on the notion that young and old mounds behave differently when viewed in isolation and their structure provides underlying information on the ecosystem's health and resource availability (Davies *et al.*, 2014).

In each plot, mounds less than or eqaul to the median were categorised as young, while those bigger than median were categorised as old. Globally, young mounds were classified (Table 4.3) as those with a basal circumference less than or equal to 2.35m and old were those with a basal circumference bigger than 2.35 m.

Their density, correlation and spatial patterns (Figure 4.3) were used to infer the ecosystem conditions present, whether favourable or not (Davies *et al.*, 2014).

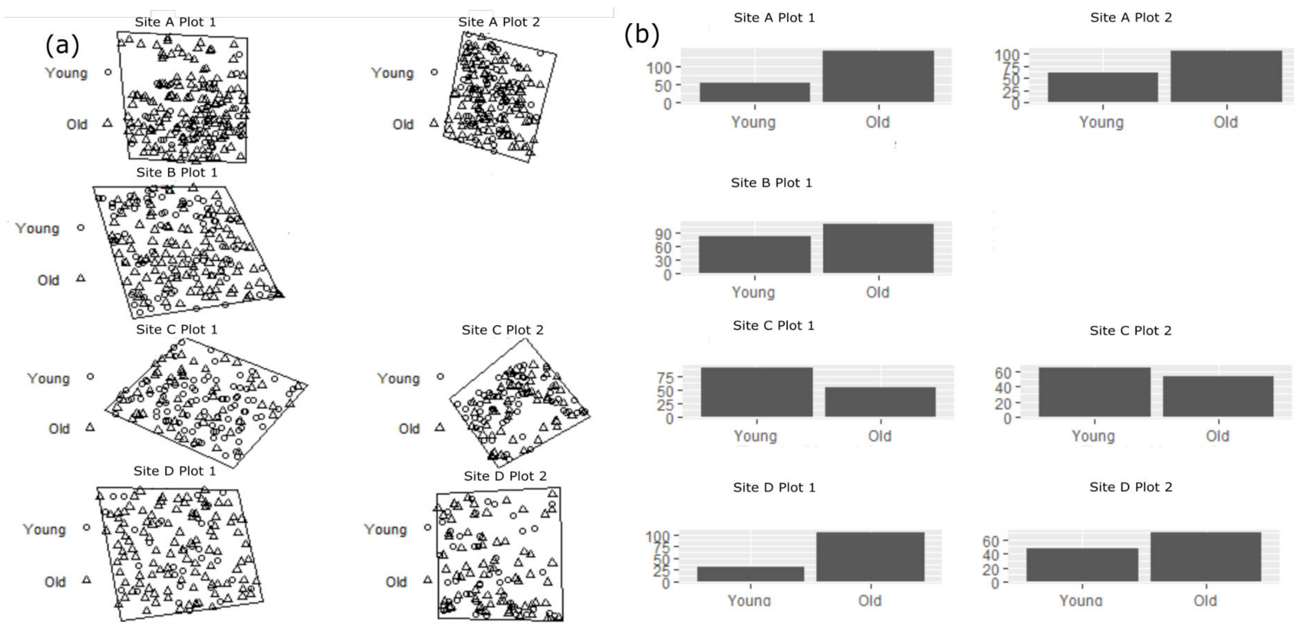

Figure 4.3: Termite mounds at the different study sites and plots. Termite mounds are separated according to basal circumference size on each plot. Old mounds (a) are represented by the triangles and young mounds by the circles. The bar plots (b) show the proportion of old to young mounds on each site on each plot plot.

Mound age is often classified through making use of the basal circumference mean or median (Muvengwi *et al.*, 2018; Davies *et al.*, 2014). According to Korb and Linsenmair (2001); Muvengwi *et al.* (2018) young mounds tend to have small basal circumferences less than the sample mean basal circumference, while older mounds tend to be larger.

Table 4.3: Ground surveyed termite mound height and basal circumference data summary.

		Basal Circumference (m)							Height (m)						
	N	Min	LQ	Med	UQ	Max	mean	Std dev	Min	LQ	Med	UQ	Max	mean	Std dev
Global	1066	1	1.70	2.35	3.00	5.90	2.45	0.90	0.00	0.00	0.25	0.35	1.00	0.22	0.19
A:Plot1	195	1.00	2.00	2.70	3.35	5.00	2.74	0.80	0.00	0.20	0.30	0.35	0.70	0.26	0.17
A:Plot2	166	1.00	1.80	2.50	3.10	4.70	2.52	0.80	0.00	0.00	0.20	0.30	0.55	0.18	0.17
B:Plot1	191	1.00	1.70	2.20	2.70	4.80	2.28	0.79	0.00	0.00	0.00	0.28	1.00	0.15	0.20
C:Plot1	145	1.00	1.50	1.90	2.40	5.10	2.09	0.95	0.00	1.50	1.80	2.50	4.50	0.18	0.71
C:Plot2	117	1.00	1.50	1.80	2.50	4.50	2.03	0.71	0.00	0.00	0.23	0.36	0.80	0.22	0.20
D:Plot1	135	1.20	2.10	2.90	3.45	5.00	2.86	0.95	0.00	0.25	0.30	0.40	0.85	0.31	0.18
D:Plot2	117	1.00	1.70	2.50	3.20	5.90	2.54	1.07	0.00	0.20	0.30	0.45	0.70	0.31	0.18

Since the global basal circumference's distribution experienced skewness (Figure 4.2), the median basal circumference (Table 4.3) instead of the mean, was used as a measure of centrality to classify mounds between old and young (DeCoster *et al.*, 2011; Iacobucci *et al.*, 2015). This is because the median is less susceptible to outliers compared to the mean.

4.1.2 Drone Survey

The DJI Phantom 4 Pro drone (Figure 4.4) was piloted at a 40 m altitude with an image resolution of 1.2-6 cm/pixel at all sites. For the survey, private farmer's land was used and no public land was flown over.

The drone had a built in RGB gimble camera with a 1/2.3 inch CMOS (Complementary Metal-Oxide-Semiconductor).

Drone Image Data Processing

An automated drone flight path was created to survey the plots at the four study sites. This was done through uploading the coordinates of the plots onto the DroneDeploy cloud platform.

For example (Figure 4.4 (a)) Site A plot 1, shows that the planned flight path for 1 hectare needs 142 images and the duration is 8 minutes 21 seconds. One full battery cycle is needed for the 40 m altitude flight, at an image resolution of 1.2 cm/px.

The DJI Phantom 4 Pro drone is known to have good positional accuracy for surveying areas within a kilometer radius (de Sá Rodrigues da Silva *et al.*, 2018). The size of the surveyed plots in this study were all less than a square kilometer.

Once the data had been acquired from the plots by the drone, it was uploaded onto Pix4D software for further processing. In Pix4D, georefrenced orthomosaics and digital surface models (DSM) (Figure 4.6) were created for each plot.

Pix4D allowed for the orthomosaics to be generated through orthorectification instead of photo stitching, in contrast to other image processing softwares.

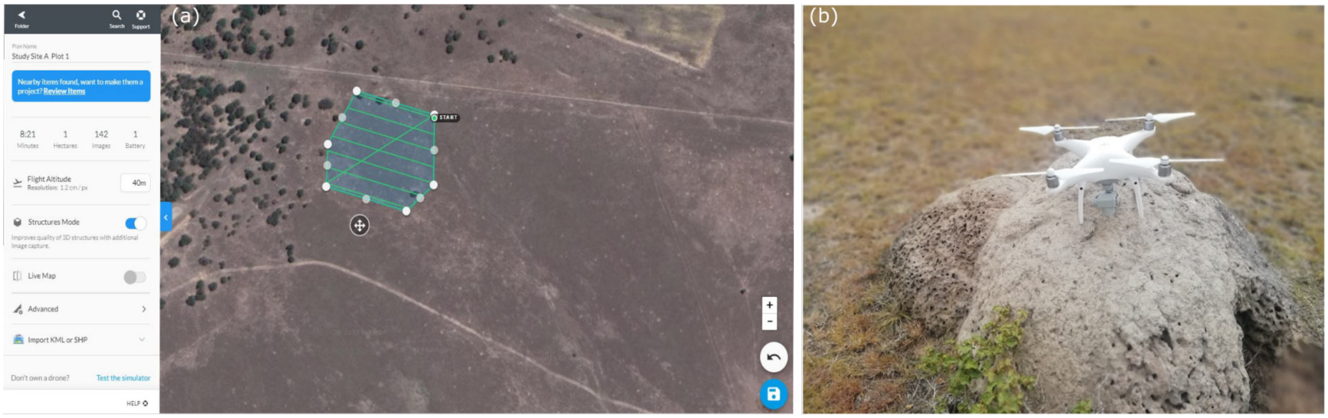

Figure 4.4: (a) DroneDeploy automated flight path. (b) DJI Phantom 4 Pro drone piloted for termite mound data acquisition.

The orthomosaics were generated using DSMs that were created by densified 3D point clouds. Orthorectified orthomosaics and DSMs were then exported to a GIS environment as raster data sets for further processing and analysis.

On the orthomosaic layer, (Figure 4.5), the termite mounds were clearly visible in the RGB frequency band. This was possible due to the high level of resolution at which the data was collected. However, since the orthomosaic is limited to being only 2D, circular bare-patches of soil on the images were not easily distinguishable from termite mounds. This could have potentially lead to them being wrongly classified as mounds.

Also, on the DSM layer (Figure 4.6), features such as shrubs and large rocks within the sampling pots had elevation in contrast to the surrounding ground, much like the termite mounds. This could have also potentially lead to them being wrongfully classified as termite mounds too.

To eliminate these concerns, the DSMs were overlayed with the orthomosaics. The DSM filters everything out of the raster and only preserves the digital surface elevation in greyscale.

Overlaying the DSM and the Orthomosaic

In GIS, on the layer properties dialogue box of the DSM, the colour ramp was set to greyscale. This was to expose surface contrast between the surrounding ground and elevated features.

Contrast in surface was shown by the elevated features having a darker shade of grey in contrast to the light grey surrounding area (Figure 4.5).

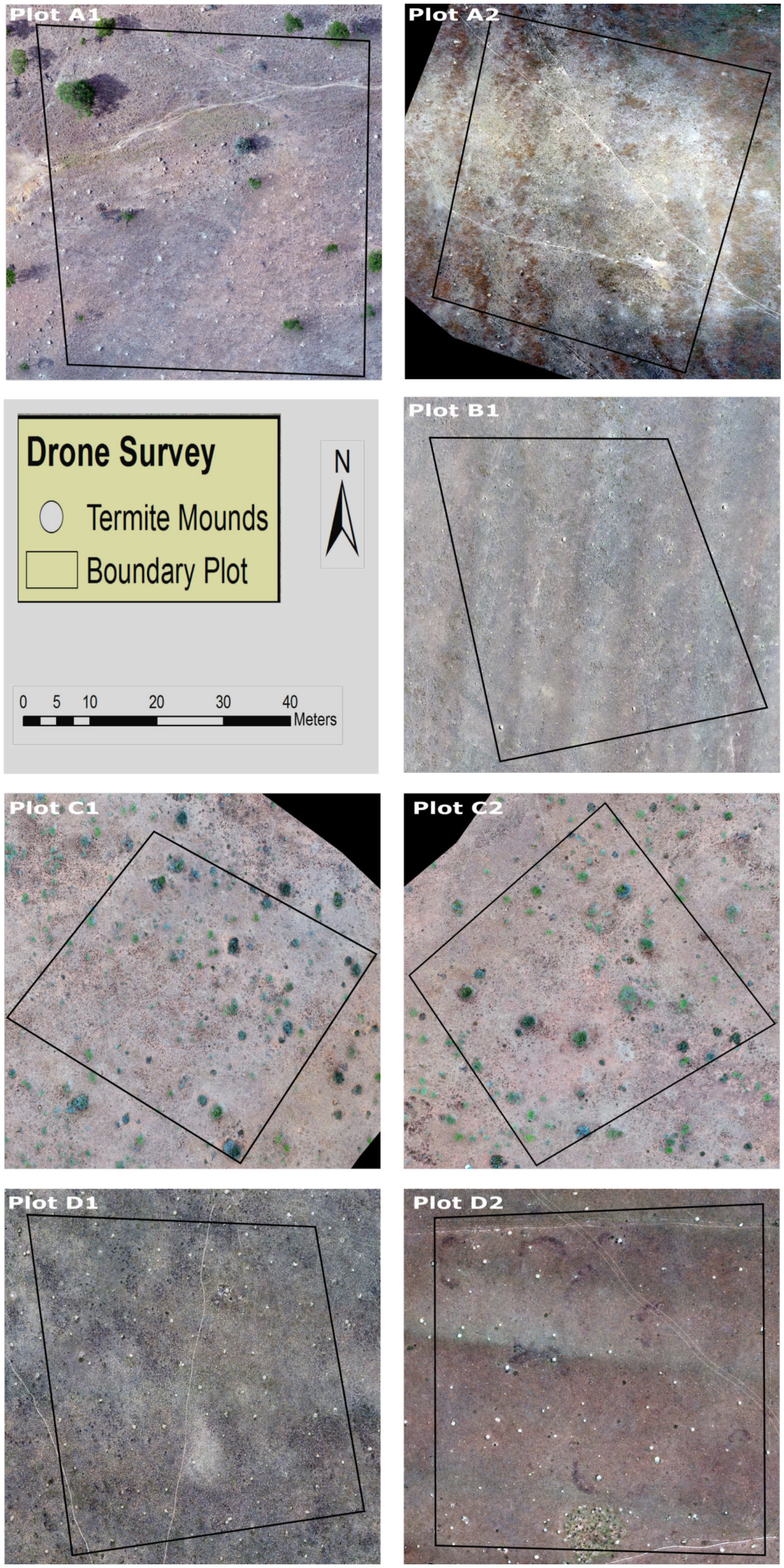

Figure 4.5: Point cloud reconstructed images of the drone surveyed plots.

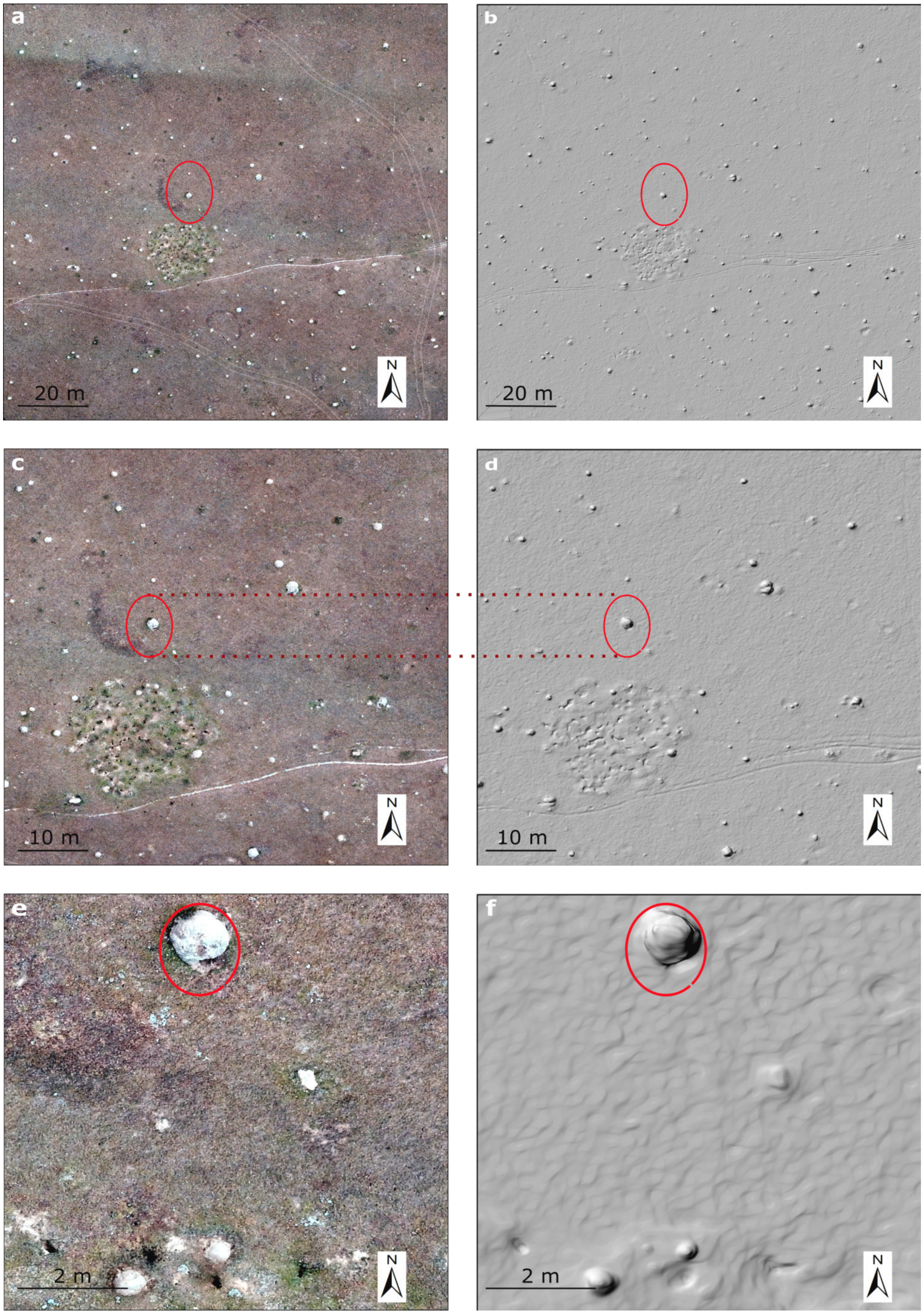

Figure 4.6: Point cloud reconstructed raster outputs showing contrast between the orthomosaics and DSMs for the same area at one of the study sites. The orthomosaics are in RGB on the left and the DSMs are in greyscale on the right. The zoom scale moves from 20 m to 2 m, highlighting the contrasts between both raster types. The orthomosaic and DSM can be overlayed with each other for best object detection.

A Hillshade of the DSM was created to bring about clear contrast in elevation (lessen noise).

In order to distinguish bare-patches from termite mounds on the orthomosaics, transparency on the DSM layer properties dialogue box was adjusted. The DSMs were then overlayed with the orthomosaics.

Bare-patches were exposed through the DSMs exhibiting no elevation over features assumed to be termite mounds on the orthomosaics.

To distinguish between termite mounds and other elevated features on the DSMs, they were overlayed with the orthomosaics.

The orthomosaics being visible in the RGB band, allowed for the distinction between termite mounds and other elevated features thought to be termite mounds on the DSMs.

4.1.3 Aerial Survey

Aerial data received from the NGI was already orthorectified and georefrenced. It was imported onto the ArcGIS 10.6 environment as a raster data set.

The raster data was contained in a RGB composite and had a resolution of 0.5 m/pixel. Vector point layers were created from the raster layer (Figure 4.8), through digitising the termite mounds that fell within the delineated polygons.

The attribute tables of the digitised termite mound point layer only contained spatial location of each mound, with no information recorded for mound heights and basal circumferences.

Positional accuracy discrepancies (Figure 4.7) among the surveying techniques were apparent from the visualisation because some of the mounds from the ground, aerial and drone survey did not overlap directly (Figure 4.7) on top of each other. However, all mounds fell within the greater common boundary plot.

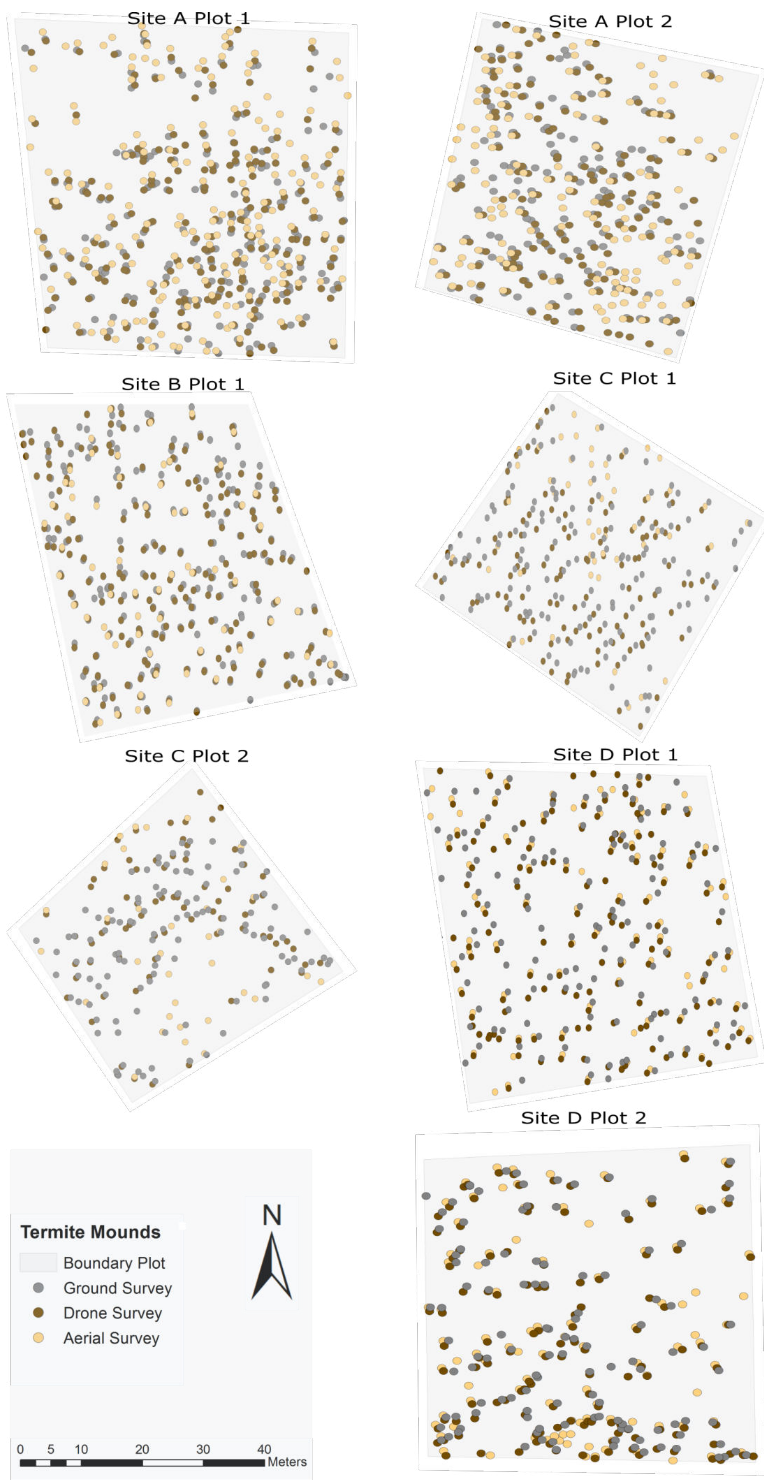

Figure 4.7: Combined Ground, Drone and Aerial surveyed termite mound observations. Positional accuracy discrepancies played a role on those mounds that did not exactly overlap across the surveys.

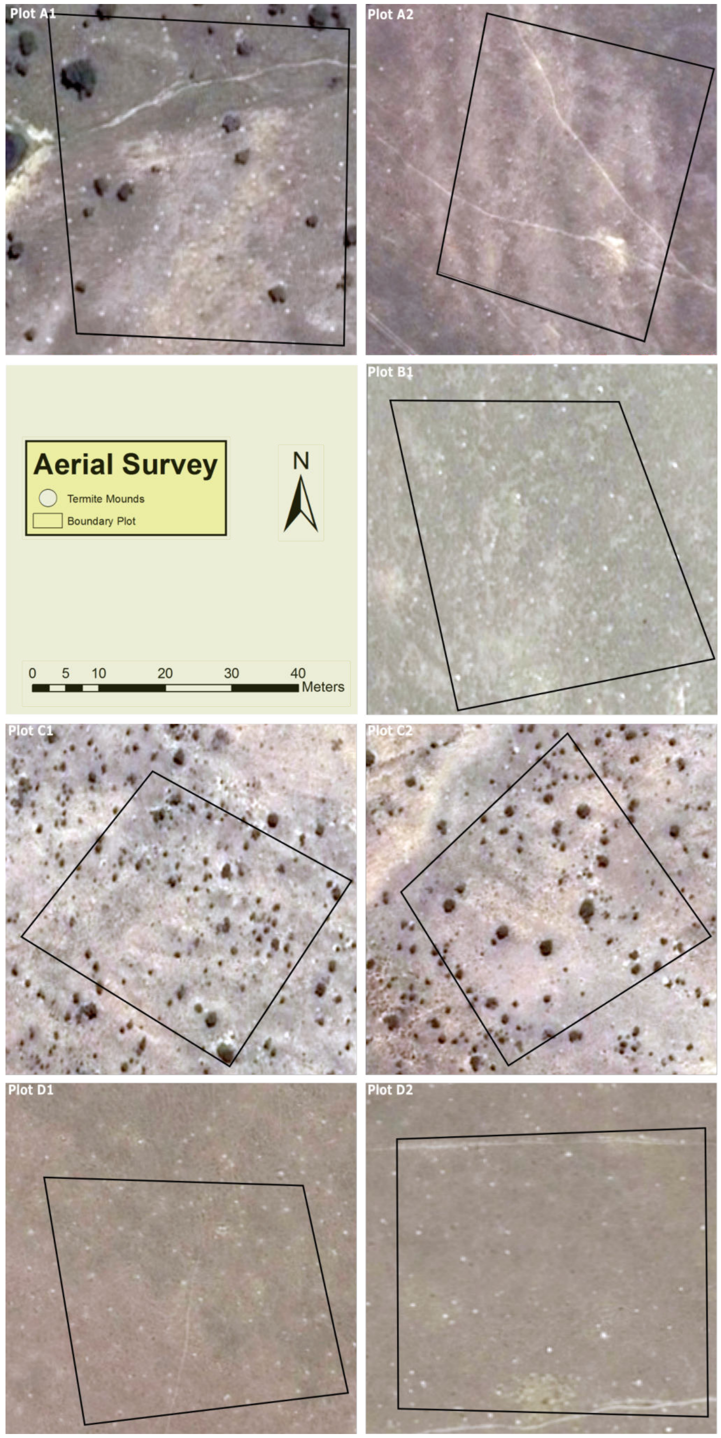

Figure 4.8: Aerial images of the termite mounds at the sampling plots.

Table 4.4: Termite mound data from the Ground (G), Aerial (A) and Drone (D) survey. Area (m^2) indicates area per square meter and Density ($ma.ha^{-1}$) indicates density per hectare and N is the number of observed mounds..

Study Site	**Plot**	**Surveying Technique**	N	**Area** (m^2)	**Density / (ha)** ($ma.ha^{-1}$)
A	1	G	195	8773.81	222.25
		A	181		206.30
		D	197		223.39
	2	G	166	8699.84	190.81
		A	143		164.37
		D	149		170.12
B	1	G	191	8436.66	226.39
		A	66		78.23
		D	195		231.13
C	1	G	145	8777.92	176.95
		A	54		39.87
		D	114		139.12
	2	G	117	8870.14	133.29
		A	35		110.48
		D	73		83.16
D	1	G	135	8870.14	152.20
		A	98		110.48
		D	140		157.83
	2	G	117	8870.14	132.48
		A	99		112.10
		D	124		140.40
Total	7	G	1066	61260.27	3201.35
	7	A	679		
	7	D	992		

A total of 1066 (Table 4.4) termite mounds were recorded on the ground survey across all the study sites recording spatial location, height and basal circumference for each mound.

For the drone and aerial surveys, a total of 992 and 679 (Table 4.4) termite mounds were recorded on all the study sites, with only spatial location being recorded.

Ground surveyed termite mounds had an average density of 176 ma.ha^{-1}, while the drone and aerial had 164 ma.ha^{-1} and 111 ma.ha^{-1} respectively (Table 4.4).

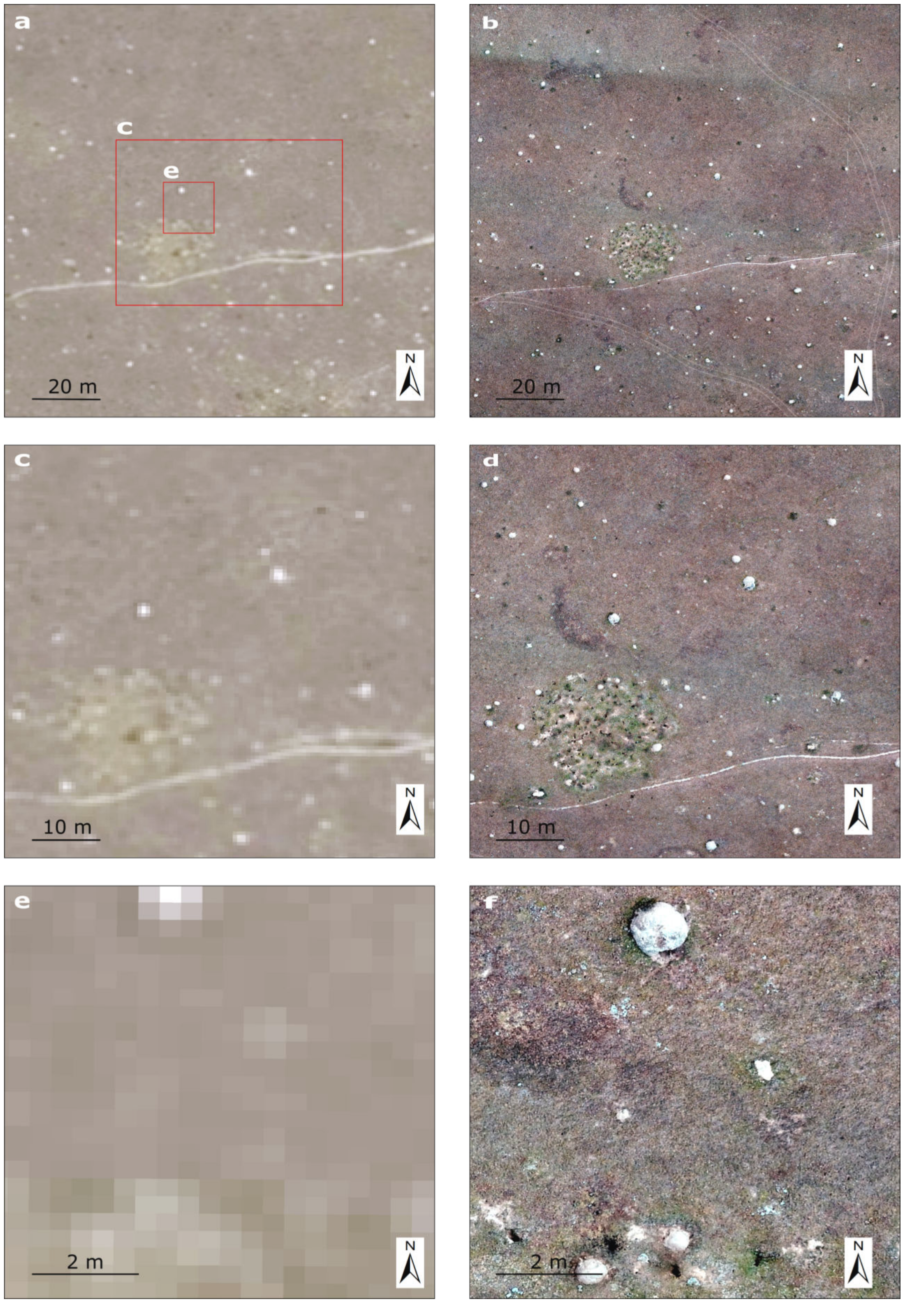

Figure 4.9: Comparing image quality of the drone and aerial survey. Left column are aerial images and right column are drone images of the same area. Each aerial image on the left is compared to that of the drone on the right. As the zoom scale moves from 20 m to 2 m, the aerial imagery gets pixilised faster than the drone imagery.

Comparing Drone and Aerial rasters

Drone and aerial images both have their advantages and disadvantages. One of the objectives of the study was to investigate which, between the aerial and drone survey is the most consistent with the ground survey.

The (Figure 4.9) image quality of the drone and aerial survey for one of the study sites are compared. As stated in the caption (Figure 4.9), the left column represents the aerial imagery and the right, the drone imagery. The two red polygons inside (Figure 4.9(a)), contain (Figure 4.9(c)) and (Figure 4.9(e)) at 10 m and 5 m scale.

Comparing the aerial and drone images, at a zoom of 10 m, both are much clearer and it is possible to better distinguish what is contained on the images. Moving to a zoom of 5 m to 2 m, the aerial image becomes pixilised and it is impossible to make out what it is contained by the image. In contrast, the drone imagery offers a better quality of what is contains.

Overall, the drone images are more pronounced at the different zoom scales due to the high resolution at which they were taken. With decreasing scale, the aerial images get pixilised at a faster rate than the drone images.

Chapter 5

Point Processes

Tobler's first law of geography states that "everything is related to everything else, but near things are more related than distant things"(Tobler, 1970). This law is what drives the need to understand and quantify spatial relationships among earth systems (Baddeley *et al.*, 2015; Miller, 2004; Ripley, 1977).

Individuals generally tend to want to draw conclusions with regards to spatial relationships through simple visual observations. However, persons observing the same distribution in space may draw different conclusions about the patterns formed and the underlying processes responsible for generating them. This is where spatial analysis comes in handy as a scientific method to quantify these observations and provide mathematical and statistical interpretation (Baddeley *et al.*, 2015).

5.1 Point Processes

The analysis of spatial point patterns is based on stochastic models, which assume that the events are generated by some underlying random mechanism. The objective is to investigate the underlying point process that generated a given spatial point pattern, with the null hypothesis being that of Complete Spatial Randomness (CSR) (Ripley, 1977).

The source of large spatial pattern formation is of great interest to earth scientists, with the hope that knowing the emergence or influence of these spatial patterns will bring them closer to the understanding of natural earth systems (Wiegand and Moloney, 2013). Spatial analysis allows for the understanding and characterisation of these earth systems and variations. The spatial structure of naturally occurring species or organisms are known to form as a result of underlying processes or mechanisms. These can be intraspecific competition, pollution exposure, soil geochemistry or historical events such as forest succession (Diggle, 2013).

Spatial patterns are found in a vast range of scales and ratios, from marshes to spatial distributions of biostructures constructed by social insects in ecosystems (Theraulaz *et al.*, 2003). They involve the distribution of events in a space and the geographic relationships that exist among them.

The spatial patterns of interest in this study are the discrete distributions of termite mounds, referred to as spatial point patterns. Termite mounds are treated as discrete random identically independently distributed points or events in a Euclidean plane, whereby their spatial data is quantified to characterise their spatial structure against the model of CSR.

Definition A point process is a stochastic process whose realisation consists of a countable set of points (Diggle, 2013).

The distributional positions of the points are characterised by locations, where

$[x_i = [latitude, longitude] = [u_i, v_i]$] and x_i falls within some domain $D \in R^2$.

- points x_i are known as events.
- $N(B)$ denotes the number of events in a planar region B, $N(B) = \#(x_i \in B \subset D\ )$
- $|B|$ denote the area of B
- $d_{ij} = \| x_j - x_i \|$, d_{ij} denoted the Euclidean distance between point i and j where x is not equal to j and x_i,$x_j \in D$.
- λ is the expected number of events per unit area

- assumption: all properties of pattern are invariant under translation (Stationary)
- assumption: and invariant under rotation (Isotrophic)

The simplest form of a spatial point pattern is a univariate point pattern, whereby all of the events are generated by the same source and the only distinguishing characteristic among them is their spatial location (Wiegand and Moloney, 2013). This can be understood as a point pattern of a single type of specie. A point pattern that involves two distinct types of events is referred to as a bivariate point pattern. This can be thought of as a point pattern of two different types of species. If more than two, it is known as a multivariate point pattern. This study is concerned with univariate spatial point patterns of termite mounds.

Attribute information attached to an event in a point pattern is called a mark. It is the auxiliary information to an event's spatial location that characterises it by traits such as height or diameter. Collectively, a data set comprising of events with marks is referred to as a marked point pattern (Baddeley *et al.*, 2015).

A mark when attached to a single event is known as a univariate marked point pattern. Marks are associated with a single event within the observation window or region of observation (Baddeley *et al.*, 2015). If a point pattern only has spatial location and no marks are present, it is refereed to as an unmarked point pattern (Diggle, 2013).

A marked point pattern is an unordered set given by:

$y = \{(x_1, m_1), \ldots, (x_n, m_n)\}$,$x_i \in W \in D$, $m_i \in M$

where x_i are the event locations and m_i are the marks. W is the observation window of the point process a subset of D and M are existing marks.

In this study we observe both a univariate unmarked (drone and aerial image survey) and a univariate marked point pattern (ground survey) of mound building termites.

When observing spatial point patterns edge effects are observed. Edge effects are experienced when the observation window W on which the observed point pattern falls within forms part of a larger region on which the underlying pattern operates.

The problem associated with edge effects is that events outside of the observation window may interact with events inside, but because events outside are not observed, it is difficult to account for them. Edge correction plays an essential role in spatial statistics and is applied in order to remove bias and improves the stability of results and the sensitivity of the tests. Contemporary statistical tests particularly in the R package spatstat, have been adjusted for edge correction and are applied in this study (Wiegand and Moloney, 2013).

Spatial point patterns consist of three distinguishable patterns, namely being clustered, random and dispersed (eg. Figure 5.1).

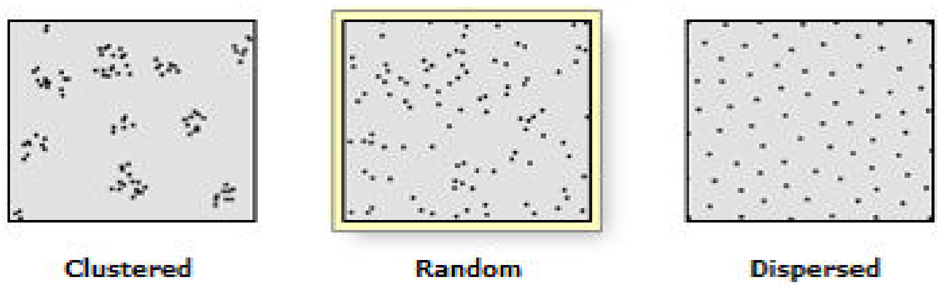

Figure 5.1: Three occurring point patterns in nature. In a clustered pattern, the points of the distribution prefer to arrange closely together (Wiegand and Moloney, 2013) . A random pattern occurs when there is no preferred arrangement that the points of distribution follow. In a dispersed pattern, the points of distribution are regularly spaced among each other.

5.2 Testing for Complete Spatial Randomness (CSR)

Complete spatial randomness implies that events are uniformly distributed, they are independent of each other and that the expected number of events per unit area is the same throughout the region.

A point pattern is CSR if:

- The intensity λ does not vary over the region D (homogeneous process)
- There are no interactions among non-overlapping subregions e.g. the number of events in two subregions are independent

- The number of events in any sub-region follows a Poisson distribution

CSR serves as a standard reference model against which point patterns may be compared, it is the building block of more complex point process models (Wiegand and Moloney, 2013). It is also commonly referred to as a homogeneous Poisson process because the number of points falling within any region D follow a Poisson distribution. The two properties of homogeneity and independence hold true for the Poisson process (Baddeley *et al.*, 2015).

In this study:

- first order homogeneity (intensity λ) of a point pattern is characterised by the unchanging rate of intensity function λ over the planar region or Euclidean space $\mathbb{R}^2$. The assumption being that the density of termite mounds within the planar region is constant as you move across the entire plane (Wiegand and Moloney, 2013).
- Second order homogeneity (independence) on the other hand assesses the relationship that exists between the termite mounds as events e.g. x_i and x_j. It is characterised by understanding that the events x_i and x_j are generated by some point process and are independent of each other.

Given x_i and x_j, the product density $p^{(2)}(x_i, x_j)$ is dependent on their locations. Consider x_i and x_j as the centers of two discs of infinitesimally small size dx_i and dx_j respectively, $p^{(2)}(x_i, x_j)$ approximates the probability that an event of the given point process occurs within dx_i and a second one within dx_j (Wiegand and Moloney, 2013). The events of the point process are independently distributed, which means that there is no interaction between the events influencing their locations.

5.2.1 Distance Based Measures for Testing for CSR

Distance based measures provide a way in which the small scale correlation structures in ecological spatial point patterns can be understood.

This is possible through analysing the mean statistical properties of the distance of separation an observed event x_i has to its nearest neighbour x_j. The commonly employed distance based summary statics are Ripley's K-Function, G-Function and F-Function (Wiegand and Moloney, 2013; Baddeley *et al.*, 2015; Diggle, 2013; Ripley, 1977).

The K-Function measures cumulative distribution of all n event to event distances,

$d(x_i, x_j) = \left\{ d_{ij_{j \# i}} \right\}$

gives the distance d_{ij} between two events x_i and x_j,

$$\hat{K}(d) = \frac{\# \left\{ d(x_i, x_j) \leq d \right\}}{n}. \tag{5.1}$$

The F-Function measures the cumulative distribution of all n event to nearest event distances,

$d_{\min}(t_p, x_j) = \min \left\{ d_{pj} \right\}$

gives the distance d_{pj} between a location t_p and an event at location x_j,

$$\hat{F}(d) = \frac{\# \left\{ d_{\min}(t_p, x_j) \leq d \right\}}{n}. \tag{5.2}$$

.

The G-Function measures the cumulative distribution of all n event to nearest neighbour event distances.

$d_{\min}(x_{i,} x_j) = \min \left\{ d_{ij_{j \# i}} \right\}$

gives the distance between an event at location x_i and its nearest neighbour event x_j,

$$\hat{G}_{\text{obs}}(d) = \frac{\# \left\{ d_{\min}(x_i, x_j) \leq d \right\}}{n} \tag{5.3}$$

Since this study is interested in the "event to nearest neighbour event distance" between termite mounds, the G-Function will be applied coupled by the R index discussed later in this Chapter.

$\hat{G}_{\text{obs}}(d)$ is the empirical distribution function of the *observed* nearest neighbour distances.

Under CSR, the *theoretical* value of the G-Function is given by $G_{\text{theo}}(d) = 1 - e^{\lambda \pi r^2}$.

The G-Function is inspected by plotting the empirical distribution function $\hat{G}_{\text{obs}}(d)$ against the theoretical $G_{\text{theo}}(d)$ of the homogeneous Poisson process with constant intensity λ, over distance d. Since the R-software uses the letter r instead of d to represent the distance when computing the G-Function, we simply replace the letter d with r for consistency.

To address edge correction adjustment arising from the unobserved events outside the observation window W, the Kaplan-Meier and Hanisch estimators are applied. Detailed work on edge correction estimators can be found in (Baddeley and Gill, 1993; Baddeley *et al.*, 2015).

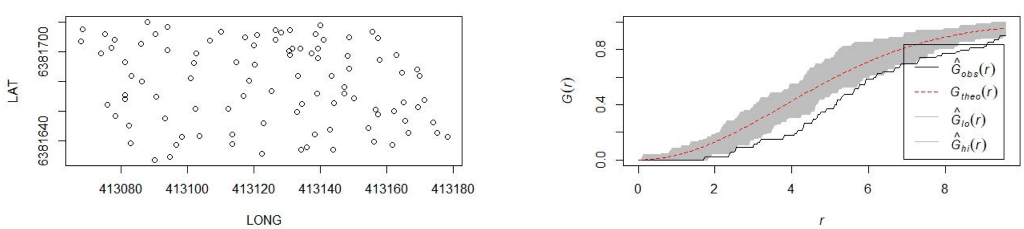

(a) Ecological spatial point pattern. (b) A visualisation of the G-function (a).

Figure 5.2: Illustration of an observed ecological spatial point pattern (a) and its G-Function (b). $\hat{G}_{\text{obs}}(r)$ is represented by the solid line and $G_{\text{theo}}(r)$ is the theoretical function represented by the dashed lines. $\hat{G}_{\text{lo}}(r)$ and $\hat{G}_{\text{hi}}(r)$ envelopes represent the minimum and maximum variation of $G_{\text{theo}}(r)$.

In figure 5.2 for the observed ecological spatial pattern :

- If $\hat{G}_{\text{obs}}(r) = G_{\text{theo}}(r)$, then the observed point pattern exhibits CSR
- If $\hat{G}_{\text{obs}}(r) > G_{\text{theo}}(r)$, then the point pattern exhibits "clustering", an indication that the observed nearest neighbour distances are shorter than those of a Poisson process
- If $\hat{G}_{\text{obs}}(r) > G_{\text{theo}}(r)$, than the point patterns exhibits "dispersion"

Since the G-function returns the results in graphical form, it is intuitive in distinguishing deviation of the point pattern from CSR. However in some instances due to variations in randomness of the process generating the data there are large discrepancies within the theoretical Poisson process $G_{\text{theo}}(r)$.

In order to account for the entire variability, Monte Carlo simulation envelopes are introduced. Monte Carlo simulation is repeated random sampling to predict the probability of different outcomes (Bird, 1981).

The envelopes reflect the minimum and maximum variation of the process under CSR. It is important to note however, that the simulation envelopes reflect the minimum and maximum variation of the $G_{\text{theo}}(r)$ process under CSR and not the actual expected process itself.

The number of simulations that are run determines the significance level of critical bands. The greater the simulations run, the lower the significance of the critical bands. Details on selecting the number of simulations are found in (Baddeley *et al.*, 2015). Therefore there is a trade-off between the simulations and the level of significance of the critical bands.

The R Aggregation Index

The aforementioned distance based measures lack an index that is able to quantify the overall distribution under a discrete value. The R index as a discrete mathematical quantifier of the spatial arrangement between events x_i and x_j is able to achieve this Baddeley *et al.* (2015). An advantage of the R index is that it makes use of the precise information about spatial location and is independent of shape and size of the observation window W.

The R index provides a natural test statistic and requires no artificial partitioning (Smith, 2016; Protazio, 2008). Its test for CSR is based on minimum inter event distance, thus removing the need for simulation unless it is for convoluted regions in which simulations such as Monte Carlo are implemented (Diggle, 2013).

The R index and the G-Function play complementary roles (Wiegand and Moloney, 2013).

The G-Function computes a distribution function of the mean nearest neighbour distances, while the aggregation index R, computes the mean nearest neighbour distance as a discrete value. It gives information about the spatial point pattern across the entire observation window.

In computing the R index, the *observed* mean distance from a randomly selected termite mound x_i to its nearest neighbour x_j in a spatial point pattern is given by $\bar{d}_o = \frac{\sum \min\left\{d_{ij_{j\#i}}\right\}}{n}$, where $\min\left\{d_{ij_{j\#i}}\right\} = d_{\min}(x_i, x_j)$

and n is the sample size (see section 5.2).

The *expected* mean nearest neighbour distance from a randomly selected termite mound to its nearest neighbour under CSR is given by $E(r) = \frac{1}{2}\frac{1}{\sqrt{\lambda}}$ (e.q A.1), where $E(r) = \bar{d}_e = \frac{1}{2\sqrt{\lambda}}$, and λ is the intensity of the distribution in a given region (Clark and Evans, 1954). Both the number of mounds and area is not fixed. R is the measure of the degree to which the observed point pattern approaches or departs from CSR. It is represented by

$$R = \frac{\bar{d}_o}{\bar{d}_e} = \frac{\frac{\sum_{i=1}^{n}\sum_{j\#i}^{n} \min\left\{d_{ij_{j\#i}}\right\}}{n}}{\frac{1}{2\sqrt{\lambda}}}. \tag{5.4}$$

.

- If the point pattern is random, the aggregation index will be $R = 1$
- If clustered, the aggregation index will $R < 1$
- and if dispersed, the aggregation index will be $R > 1$
- The p-value used here is of 0.05 based of previous literature related to this study (Clark and Evans, 1954; Baddeley *et al.*, 2015; Wiegand and Moloney, 2013) . It is used to test whether a spatial point pattern is significantly clustered, dispersed or random from the value returned by the R index.

The expected variance of a randomly selected termite mound to its nearest neighbour under CSR is given by $\text{Var}(\bar{r}) = \frac{4-\pi}{4\lambda\pi}$ (e.q A.2).

Chapter 6

Results

In the study area, two plots were sampled on each site with the exception of Site B as explained in Chapter 2 section 2.1. Each site had a ground, drone and an aerial survey conducted. A total of 1066 termite mounds were recorded on the ground survey with 992 on the drone and 679 on the aerial survey.

Complete Spatial Randomness Hypothesis

On each site and for all surveying techniques, termite mound distributions were observed in order to understand the spatial point patterns they formed. This was done through testing for CSR, explained in Chapter 5 section 5.2.

CSR Hypothesis

H_o : Observed termite mound spatial point patterns exhibit CSR

H_a : Observed termite mound spatial point patterns do not exhibit CSR

6.1 Drone, Aerial and Ground Survey

The drone and aerial survey results were compared to those of the ground survey to see how well they performed in detecting termite mounds and their spatial point patterns.

This included mound counts, mean nearest neighbour distances and densities.

Comparing mound counts (Table 6.1), the ground (195), drone (197) and aerial (181) surveys all recorded high amounts of termite mounds in plot A1. Low counts (177) for the ground survey were equally recorded in plot C2 and D2, while the drone and aerial survey's low mound counts were recorded (73 and 35) in plot C2.

High mound densities (226.39 ma.ha^{-1} and 231.13 ma.ha^{-1}) for the ground and drone survey were recorded in plot B1, whereas the aerial survey's (206.30 ma.ha^{-1}) were found in plot A1. Low densities (132.48 ma.ha^{-1}) for the ground survey were found in plot D2, whereas both the drone and aerial survey recorded low densities (83.16 ma.ha^{-1} and 39.87 ma.ha^{-1}) in plot C2.

Considering mean nearest neighbour distances for all mounds, the ground survey recorded long distances (5.13 m) in plot D1. The drone and aerial survey's long mean nearest neighbour distances were recorded (5.99 m and 9.71 m) in plot C2. Short mean nearest neighbour distances (3.19 m, 3.53 m and 4.04 m) for the ground, drone and aerial surveys were all found in plot A1.

Correlation for basal circumference and height was only calculated for the ground survey represented by "G" on Table 6.1 since no height and basal circumference was recorded for the drone and aerial surveys. This was done in order to understand the relationship between termite mound basal circumference and height. Plot C2 (0.71) (Table 6.1) recorded high correlations between basal circumference and height, while small correlation overall was recorded in plot A1 (0.46) (Table 6.1).

6.1.1 Clark and Evans Aggregation Index (R)

Combining all the surveys, 16 out of 21 surveyed plots (Table 6.1) recorded $R > 1$, suggesting that the observed mound point patterns were largely dispersed. However, when assessing the p-values (Table 6.1) it was found that only 9 of the 21 plots were dispersed. Since the value of R determines whether a point pattern is clustered or dispersed against randomness. For plot A1 (Table 6.1), the ground survey observed a clustered spatial point pattern, while the drone was random and the aerial dispersed. Plot A2's (Table 6.1) ground and drone surveys, both observed random point patterns, whereas the aerial survey was dispersed.

Table 6.1: Summary of Ground (G) , Drone (D), and Aerial (A) surveyed termite mound data and their point patterns on each plot. R, indicates Clark and Evans Aggregation Index and $\bar{r_o}$(m) indicates the observed mean nearest neighbour distance represented in Chapter 5 by $\bar{d}_o$.

Study Site	**Plot**	**Surveying Technique**	N	**Area (m^2)**	**Density / (ha) (ma.ha^{-1})**	$\bar{r}_o$**(m)**	R	$p-value$	**Observed Point Pattern**	**Corr Height (m) vs Basal Circ (m)**
A	1	G	195		222.25	3.19	0.91	0.04	Clustered	0.46
		A	181	8773.81	206.30	4.04	1.10	0.01	Dispersed	
		D	197		223.39	3.53	1.03	0.47	Random	
	2	G	166		190.81	3.83	0.98	0.70	Random	
		A	143	8699.84	164.37	4.71	1.17	0.00	Dispersed	0.58
		D	149		170.12	4.28	1.06	0.16	Random	
B	1	G	191		226.39	3.71	1.10	0.03	Dispersed	0.51
		A	66	8436.66	78.23	6.81	1.14	0.05	Dispersed	
		D	195		231.13	3.78	1.10	0.01	Dispersed	
C	1	G	145		176.95	4.19	1.06	0.21	Random	0.59
		A	54	8777.92	39.87	6.71	1.02	0.77	Random	
		D	114		139.12	4.58	1.00	0.92	Random	
	2	G	117		133.29	4.18	0.91	0.13	Random	0.71
		A	35	8870.14	110.48	9.71	1.14	0.16	Random	
		D	73		83.16	5.99	0.95	0.60	Random	
D	1	G	135		152.20	5.13	1.21	0.00	Dispersed	0.61
		A	98	8870.14	110.48	6.02	1.26	0.00	Dispersed	
		D	140		157.83	4.99	1.21	0.00	Dispersed	
	2	G	117		132.48	3.95	0.91	0.14	Random	0.70
		A	99	8870.14	112.10	5.74	1.11	0.01	Dispersed	
		D	124		140.40	4.34	1.01	0.83	Random	
Total	7	G	1066							
	7	A	679	61260.27	3201.35					
	7	D	992							

For plot B1 (Table 6.1), all surveys observed dispersed point patterns. Spatial point patterns observed in plot C1 and C2 (Table 6.1) were random for all surveys. In plot D1 (Table 6.1), dispersed point patterns were observed for all surveys. For plot D2 (Table 6.1), the ground and drone surveys observed random point patterns, wheres the aerial survey was dispersed.

6.2 Young and Old Termite Mound Spatial Point Patterns

All ground surveyed termite mounds were separated and categorised as young and old. The G-Function was then used to classify the point patterns they formed at various distances scales within each plot.

6.2.1 Site A

Analysing the point patterns formed by all termite mounds for plot A1 (Table 6.1), all mounds were clustered. Separating the mounds (Figure 6.1) according to age, old termite mounds were mostly dispersed, experiencing random patterning at distances < 2 m and clustering > 5 m. Young mounds (Figure 6.1) were observed to be clustered everywhere. The recorded R (Table 6.2) for old mounds suggested that the mounds were dispersed overall while young mounds were clustered.

In plot A2 (Table 6.1), all mounds were random. Separating the mounds (Figure 6.1) according to age, old mounds were observed to be clustered at distances of < 1.5 m and >4 m, and dispersed at > 2.5 m to 4 m. Young mounds (Figure 6.1) were observed to be clustered everywhere. The recorded R (Table 6.2) for old mounds suggested that the mounds were clustered overall with young mounds also clustered.

6.2.2 Site B

In plot B1 (Table 6.1), the spatial point patterns formed by all mounds were dispersed throughout.

Separating the mounds (Figure 6.1) according to age, old mounds (Figure 6.1) were observed to be clustered at distances < 4.5 m, dispersed between 4.5 m and 6.2 m and random > 8 m. Young mounds (Figure 6.1) were found to be mostly clustered, although alternating between randomness at small distance scales. The recorded R (Table 6.2) for old mounds suggested that the mounds were clustered overall with young mounds also clustered.

6.2.3 Site C

In plot C1 (Table 6.1), all mounds were observed to be random throughout. Separating the mounds (Figure 6.1), old mounds (Figure 6.1) in this plot were dispersed throughout, whereas younger mounds were observed to be random. The recorded R (Table 6.2) for old mounds suggested that the mounds were dispersed overall while young mounds were random.

In plot C2 (Table 6.1), all mounds were observed to be random.

Separating the mounds (Figure 6.1) according to age, old mounds (Figure 6.1) in this plot were observed to be clustered for distances < 5 m and random at distances > 5 m and dispersed > 8 m. Young mounds (Figure 6.1) were observed to be dispersed for distances < 4.5 m and clustered for all distances > 4.5 m. The recorded R (Table 6.2) for old mounds suggested that the mounds were random overall while young mounds were clustered.

6.2.4 Site D

In plot D1 (Table 6.1) all mounds were observed to be dispersed at all distance scales. Separating the mounds (Figure 6.1) according to age, old mounds (Figure 6.1) were also dispersed, whereas young mounds were dispersed at distances <5 m and > 7 m, clustered at > 5 m to 7 m. The recorded R (Table 6.2) for old mounds suggested that the mounds were dispersed overall with young mounds also dispersed.

In plot D2 (Table 6.1), all mounds were observed to be random.

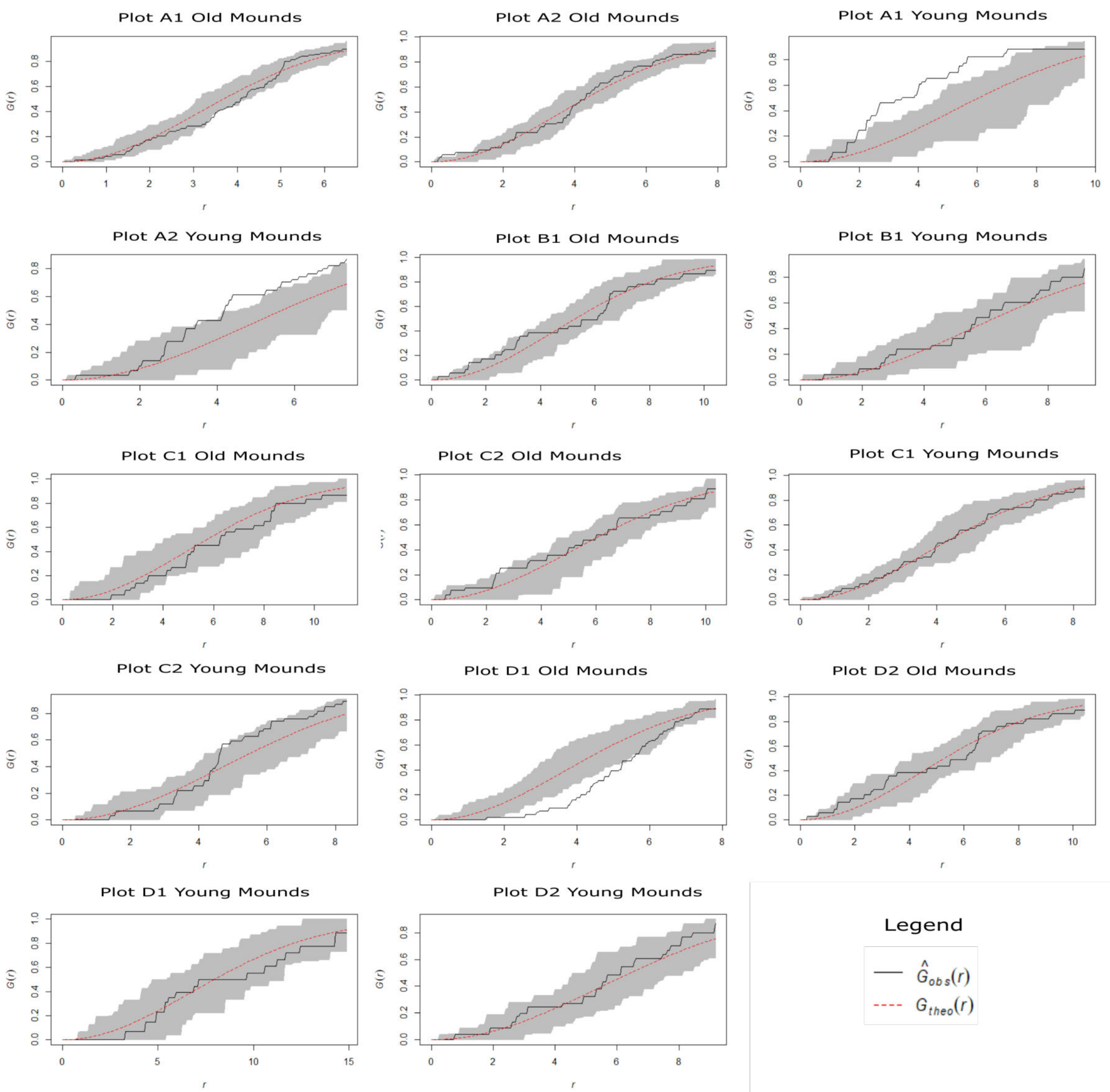

Figure 6.1: Ground surveyed termite mound spatial point patterns for young and old mounds. $\hat{G}_{\text{obs}}(r)$ represents the observed point pattern, with the solid line and $G_{\text{theo}}(r)$ is the expected theoretical point pattern represented by the dashed lines. $\hat{G}_{\text{obs}}(r) > G_{\text{theo}}(r)$; clustered, $\hat{G}_{\text{obs}}(r) < G_{\text{theo}}(r)$; dispersed and $\hat{G}_{\text{obs}}(r) = G(r)$; random. The shaded regions are simulation envelopes, accounting for maximum and minimum variation of $G_{\text{theo}}(r)$ under CSR. (It is important to note however, that the simulation envelopes reflect the minimum and maximum variation of the process under CSR and not the actual expected theoretical process itself).

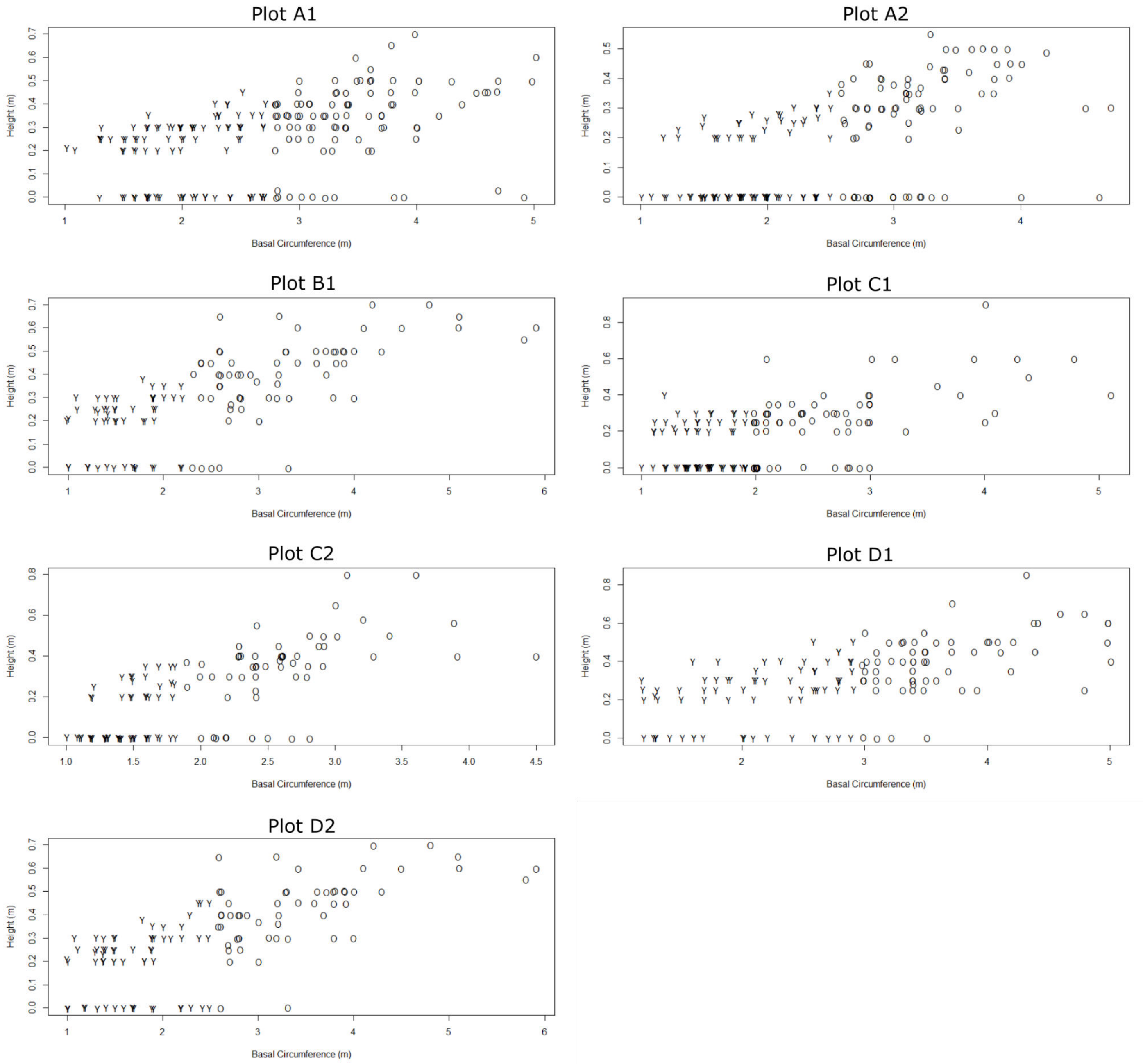

Figure 6.2: Scatter plot showing the distribution of young and old termite mound height against basal circumference. Old mounds are represented by "O" and young mounds are represented by "Y".

Separating the mounds (Figure 6.1) according to age, old mounds (Figure 6.1) in this plot were observed to be clustered at distances < 4 m and dispersed at > 4.5 m to 6.2 m. Young mounds (Figure 6.1) were random at distances < 2.5 m, dispersed at > 4 m and clustered at distances $>$ 6 m.

The recorded R (Table 6.2) for old mounds suggested that the mounds were clustered overall with young mounds also clustered.

From the seven plots in the study, old mounds recorded three dispersed, three clustered and one random point pattern.

Young mounds recorded five clustered, one random and one dispersed point pattern.

In plot A1 (Figure 6.2) the scatter plot distribution shows more young mounds recorded zero height compared to old mounds. Majority of old mounds had basal circumferences above 3 m and were taller than young mounds. In plot A2's (Figure 6.2) distribution, it was found that old mounds mostly consisted of basal circumferences of around 3 m and were mainly distributed above a height of 0.2 m. In this plot old mounds with large basal circumferences were generally taller than those with small basal circumference.

In plot B1's (Figure 6.2) distribution, old mounds were taller than young mounds and majority of young mounds basal circumference distributions were less than 2 m. Old mound basal circumferences observed here were large compared to the rest of the plots and corresponded with tall heights.

For plot C1 (Figure 6.2), majority of old mound basal circumference distributions were between 2 and 3 m with young mounds mainly distributed at close to zero height. Plot C2's (Figure 6.2) distribution had more young mounds with zero height in comparison to old mounds. Young mounds here showed consistency both in height and basal circumference. In plot D1 (Figure 6.2) young mounds had larger basal circumferences compared to those in other plots. In plot D2's (Figure 6.2) distribution, old mounds recorded the least zero height, with large basal circumferences corresponding with tall heights. Young mound heights were mainly between 0 and 0.4 m with only a few being beyond 0.4 m.

Table 6.2: Association of termite mounds with auxiliary data. DM, EM and MF indicate Daggaboersnek Member, Elandsberg Member and Middleton Formation. BDG, AMG and GFT indicate Bedford Dry Grassland, Amathole Montane Grassland and Great Fish Thicket. ER, LL and LR indicate Eutric Regosols, Lithic Leptosols and Leptic Regosols. NN dst indicates the mean nearest neighbour distance. IQR indicates the inter-quartile range. Median basal circumference and height was used. Average distance was used for the auxiliary data.

	Plot A1		Plot A2		Plot B1		Plot C1		Plot C2		Plot D1		Plot D2	
Geology	DM		DM		EM		MF		MF		DM		DM	
Vegetation	BDG		BDG		AMG		GFT		GFT		BDG		BDG	
Soil	ER		ER		LL		ER		ER		LR		LR	
Elevation (m)	671 [670.7 - 671.5]		692 [691.6 - 692]		1048 [1048 - 1049]		435 [434.7 - 435.3]		438 [437.8 - 438.4]		755 [754.8 - 755.5]		764 [763.4 - 764]	
Karo Dol dst (m)	1878 [1875 - 1881]		3881 [3877 - 3885]		2093 [2089 - 2097]		6651 [6647 - 6654]		6650 [6646 - 6655]		4617 [4612 - 4621]		3421 [3416 - 3425]	
Road dst (m)	2566 [2563 - 2570]		669 [665.1 - 673.3]		17919 [17916 - 17922]		13033 [13030 - 13037]		13153 [13148 - 13159]		1999 [1995 - 2003]		1684 [1678 - 1689]	
River dst (m)	841 [837.6 - 844.1]		1216 [1212 - 1219]		893 [888.6 -896.5]		499 [495.4 - 502.9]		442 [437.1 - 446.4]		2911 [2907 - 2915]		2262 [2257 - 2267]	
Hum Settl dst (m)	1404 [1401 - 1407]		786 [781.6 - 790.1]		763 [759.6 - 766.2]		1961 [1956 - 1966]		1814 [1808 - 1819]		772 [767.4 - 775.7]		341 [336.5 - 346.4]	
Mound Age	**Old**	**Young**	**Old**	**Young**	**Old**	**Young**	**Old**	**Young**	**Old**	**Young**	**Old**	**Young**	**Old**	**Young**
Density (ma.ha^{-1})	161.85	60.41	121.84	68.97	129.20	97.19	68.34	108.61	60.38	72.91	117.25	34.95	79.26	53.22
R	1.12	0.90	0.91	0.87	0.90	0.90	1.17	1.00	0.92	0.90	1.19	1.11	0.90	0.92
$p-$ **value**	0.03	0.01	0.04	0.00	0.03	0.03	0.02	0.60	0.47	0.01	0.00	0.04	0.02	0.04
Basal Circ(m)(IQR)	3.0 - 3.8	1.7 - 2.4	2.8 - 3.4	1.6 - 2.1	2.5 - 3.3	1.5 - 2.0	2.1 - 3.0	1.4 - 1.7	2.3 - 2.8	1.3 - 1.6	3.2 - 4.0	1.7 - 2.6	2.80 - 3.83	1.4 - 2.0
(Median)	3.4	2	3.1	1.8	2.8	1.7	2.5	1.5	2.55	1.5	3.5	2.1	3.25	1.7
Height (m)(IQR)	0.30 - 0.45	0.0 - 0.3	0.2 - 0.4	0.0 - 0.2	0.0 - 0.34	0.0 - 0.21	0.10 - 0.35	0.0 - 0.2	0.3 - 0.4	0.0 - 0.2	0.3 - 0.5	0.0 - 0.3	0.3 - 0.5	0.0 - 0.3
(Median)	0.35	0.25	0.3	0.0	0.24	0.0	0.25	0.0	0.37	0.0	0.4	0.0	0.45	0.24
Corr Height vs Basal Circ	0.26	0.06	0.27	0.27	0.53	0.17	0.56	-0.07	0.51	0.46	0.47	0.35	0.55	0.24
NN dst (m)	5.37	4.21	5.32	4.79	6.00	4.33	6.42	5.54	6.40	6.22	7.03	6.45	6.87	5.41

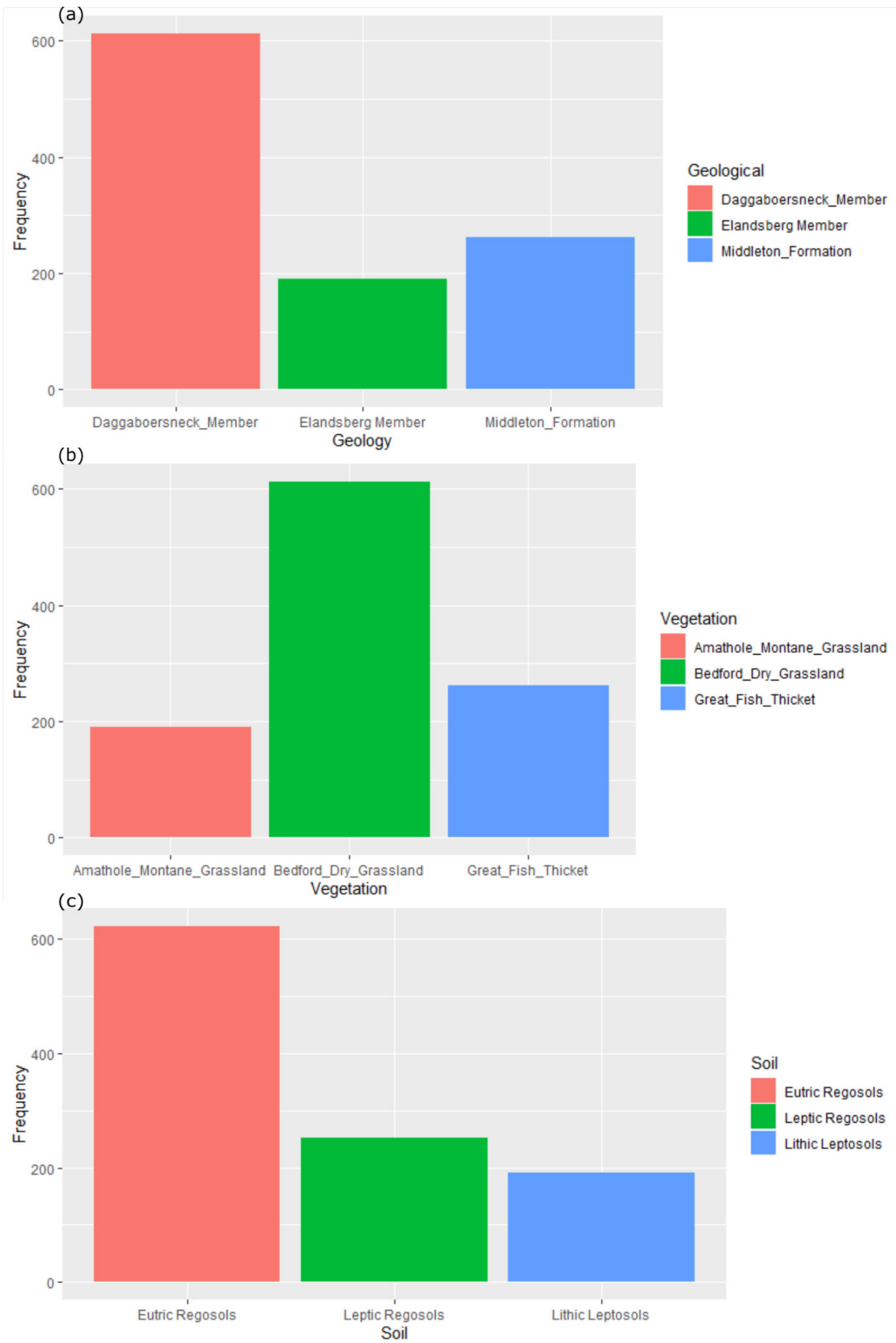

Figure 6.3: Termite mounds observed on the different geology, soil and vegetation types.

6.3 Association between Termite Mounds and Auxiliary Data

The recorded termite mound data was overlayed by auxiliary data (natural and anthropogenic features) to perform a spatial join in order to understand their relationship with these features. Below is the summary of the table (Table B.2) that contains visual information of the spatial join. Means are used to summarise the behaviour of terminate mounds on the different auxiliary data. In the event of long and short mean nearest neighbour distances, they depict the longest and shortest recorded means.

All mounds recorded by the ground survey including their heights (Table B.2) and basal circumeference (Table B.1) made up a total of 1066. Separating them according to age using basal circumference as a proxy, 640 (60.04%) (Table 6.2) were classified as old and 426 (39.96%) as young.

Considering termite mound interactions with geology and vegetation, high mound counts (613) were recorded on (Figure 6.3) the Daggaboersnek Member, Bedford Dry Grassland followed by the Middleton Formation, Great Fish Thicket (262) and then the Elandsberg Member, Amathole Montane Grassland (191).

All mounds (Table 6.2) recorded high densities on the Elandsberg Member, Amathole Montane Grassland (226.39 ma.ha^{-1}) and low densities (155.11 ma.ha^{-1}) on the Middleton Formation and Great Fish Thicket. Separating all mounds between young and old (Table 6.2), high densities (97.19 ma.ha^{-1} and 129.20 ma.ha^{-1}) of young and old mounds were recorded on the Elandsberg Member, Amathole Montane Grassland, with low densities (54.39 ma.ha^{-1} and 64.36 ma.ha^{-1}) recorded on the Middleton Formation and Great Fish Thicket.

Termite mound basal circumferences were positively correlated with height across all the geology and vegetation. High correlations (0.65) among basal circumference and height for all mounds (Table 6.2) were recorded on the Middleton Formation, Great Fish Thicket and the lowest (0.51) on the Elandsberg Member and Amathole Montane Grassland. Old mounds (Table 6.2) recorded the highest correlations (0.54) on the Middleton Formation, Great Fish Thicket and the lowest (0.39) on the Daggaboersnek Member and Bedford Dry Grassland.

Young mounds (Table 6.2) recorded the highest correlations (0.39) on the Middleton Formation, Great Fish Thicket and lowest (0.17) on the Elandsberg Member and Amathole Montane Grassland. All mounds recorded tall heights (0.30 m) on the Daggaboersnek Member and short heights (0.0 m) on the Elandsberg Member.

Separating all mounds between young and old, tall young (0.12 m) and old (0.38 m) mounds (Table 6.2) were recorded on the Daggaboersnek Member, Bedford Dry Grassland. Short old mounds (0.24 m) were recorded on the Elandsberg Member, Amathole Montane Grassland (Table 6.2), with short young mounds (0.0 m) on the Daggaboersnek Member, Bedford Dry Grassland, Elandsberg Member, Amathole Montane Grassland, Middleton Formation and Great Fish Thicket.

All mounds (Table 6.2) recorded large basal circumferences (2.90 m) on the Daggaboersnek Member and small basal circumferences (1.80 m) on the Middleton Formation and Great Fish Thicket. Separating all mounds between young and old, large basal circumferences for young (1.9 m) and old (3.31 m) mounds (Table 6.2) were recorded on the Daggaboersnek Member, Bedford Dry Grassland with small basal circumferences for old (2.53 m) and young (1.5 m) mounds recorded on the Middleton Formation, Great Fish Thicket.

All mounds (Table 6.2) recorded long mean nearest neighbour distances (4.19 m) on the Middleton Formation, Great Fish Thicket and short ones on the (3.17 m) Elandsberg Member, Amathole Montane Grassland. Mean nearest neighbour distances among young mounds (Table 6.2) were longer on the Middleton Formation, Great Fish Thicket (5.88 m) and shorter (4.33 m) on the Elandsberg Member, Amathole Montane Grassland. This was also true (6.21 m and 6 m) for old mounds.

Among the different soil types (Figure 6.3), Eutric Regosols recorded high mound (623) counts followed by Leptic Regosols (252), with Lithic Leptosols (191) having the lowest. All mounds had high densities (226.39 m) on Lithic Leptosols and low (142.34 m) on Lithic Regosols. Dividing all mounds between young and old, high densities of old (129.20 ma.ha^{-1}) and young (97.19 ma.ha^{-1}) mounds were recorded on Lithic Leptosols, whereas low densities (98.26 ma.h$a^{-1}$and 44.09 ma.ha^{-1})

were recorded on Leptic Regosols.

Mound height and basal circumference was also correlated with height across all soil types. High correlations (0.66) among basal circumference and height of all mounds were recorded on Leptic Regosols and low correlations (0.51) on Lithic Leptosols. Old mounds recorded high correlations (0.53) on Lithic Leptosols and low correlations (0.41) on Eutric Regosols. Young mounds had high correlations (0.30) on Leptic Regosols and low correlations (0.17) on Lithic Leptosols. Young tall mounds (0.13 m) were recorded on Eutric Regosols and old tall mounds (0.43 m) on Leptic Regosols.

Large basal circumferences among young (1.9 m) and old (3.38 m) mounds were recorded on Leptic Regosols. Young mounds with small (1.7 m) basal circumferences were recorded equally on Eutric Regosols and Lithic Leptosols, whereas old mounds (2.8 m) were recorded on Lithic Leptosols. All mounds recorded long (4.54 m) mean nearest neighbour distances on Leptic Regosols and short (3.71 m) on Lithic Leptosols. Mean nearest neighbour distances among young mounds were long (5.93 m) on Leptic Regosols and short (4.33 m) on Lithic Leptosols. Among old mounds they were long (6.95 m) on Lithic Regosols and short (5.88 m) on Eutric Regosols.

Here (Figure 6.4) the euclidean distances of the auxiliary features together with basal circumferences and height for termite mounds were correlated in order to understand existing relationships. In plot A1 (Figure 6.4), there was a positive moderate correlation between basal circumference and height for all mounds. Height had no observed relationship with any of the features. Basal circumference had a fairly positive relationship with rivers, human settlements and Karoo dolerite. Karoo dolerite had a strong positive relationship with rivers and human settlements, whereas main roads had a strong negative relationship with rivers, human settlements and Karoo dolerite.

In plot A2 (Figure 6.4), height and basal circumference had a moderate positive relationship. Basal circumference had a fairly positive relationship with Karoo dolerite, rivers, main roads and human settlements. Height had a fairly positive relationship with main roads, rivers, elevation and human settlements. Human settlements had a strong positive correlation with main roads, elevation and rivers, whereas Karoo dolerite had a strong negative correlation with roads and human settlements.

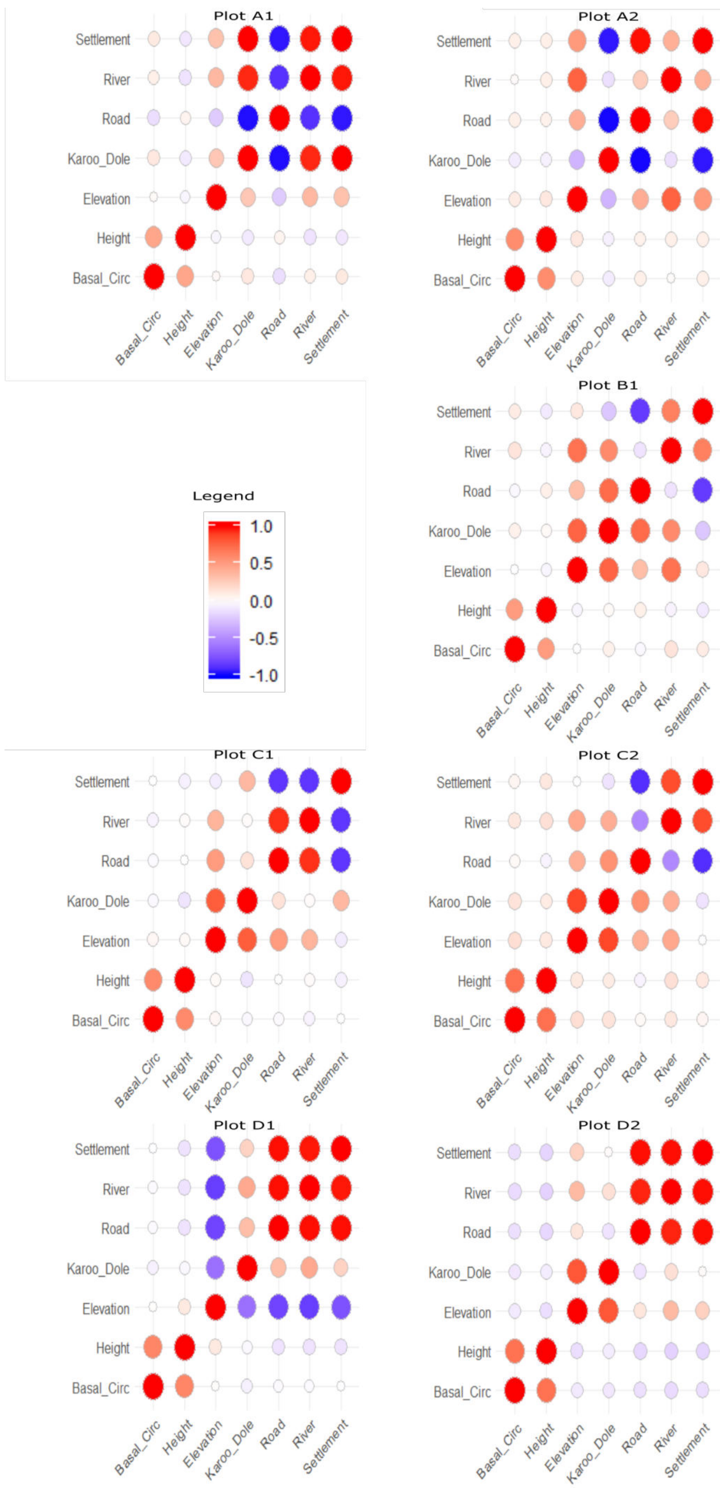

Figure 6.4: Relationship between ground surveyed termite mounds and auxiliary features. Red and blue circles represent high and low correlations respectively, the stronger the correlation the bigger the circle and stronger the colour.

At this site both young and old mounds (Table 6.2) recorded the shortest nearest neighbour distances, suggesting an abundance of resources at the site.

This is also apparent in the site recording the second closest distance to a Karoo dolerite and river, indicating good water availability.

In plot B1 (Figure 6.4), there was a moderate positive relationship between height and basal circumference. Height had a fairly positive relationship with main roads. Basal circumference had a fairly positive relationship with Karoo dolerite, rivers and human settlements. Rivers had a strong positive relationship with Karoo dolerite, settlements and elevation. At this site, old mounds (Table 6.2) recorded the highest densities. These mounds occupied the highest elevation and were relatively close to a river and to Karoo dolerite, suggesting that old mounds prefer regions of high elevation and a relatively close water source.

In plot C1 (Figure 6.4), there was a moderate positive relationship between height and basal circumference. Basal circumference and height had no observed relationship with any of the features. Elevation had a strong positive relationship with Karoo dolerite and a moderate positive relationship with main roads and rivers.

In plot C2 (Figure 6.4), there was a strong positive relationship between basal circumference and height. Basal circumference had a fairly positive relationship with elevation, Karoo dolerite and rivers. Height shared the same relationship with human settlements, rivers and elevation.

Human settlements had a strong negative relationship with main roads and a strong positive relationship with rivers. This site (Table 6.2) was the only site where young mounds were more abundant than old mounds. This can be attributed to the low elevation and shortest distance to a river, suggesting that young mounds prefer low elevations and being close water source to old mounds.

In plot D1 (Figure 6.4), basal circumference had a moderate positive relationship with height. There appeared to be no relationship between basal circumference and the features, with height having a fairly positive relationship with elevation. Rivers had a strong positive relationship with main roads and human settlements and a strong negative relationship with elevation. In plot D2 (Figure 6.4), there was a strong positive relationship between basal circumference and height. For both basal circumference and height there was no relationship observed with the features.

There was a strong positive relationship observed between rivers, main roads and human settlements. At this site both young and old mounds (Table 6.2) recorded the longest nearest neighbour distances, suggesting a lack of resources as nearest neighbour distances signify foraging boundaries. These mounds were the closest to human settlements and roads, recording the largest basal circumference and height, suggesting resilience of the mounds to anthropogenic disturbance.

Chapter 7

Discussion

7.1 Comparing the Surveys

The drone and aerial surveys observed both high and low termite mound counts on the same plots which was consistent with the ground survey. Recorded termite mound count over all the polygons in the global study area per plot was 152, 29 for the ground survey, 141.71 for the drone and 96.57 for the aerial. Concerning density, the drone survey recorded high termite mound densities on the same plot as the ground survey, different to those of the aerial survey. Low densities for both the drone and aerial survey were recorded on the same plot, inconsistent with the ground survey. Overall mound densities were 176.34 ma.ha^{-1} for the ground survey, 163.59 ma.ha^{-1} for the drone and 111.04 **ma.h**a^{-1} aerial survey. Long mean nearest neighbour distances for the drone and aerial survey were both recorded on the same plot, different to those of the ground survey. Short mean nearest neighbour distances for the drone and aerial survey were recorded on the same plot, this time consistent with those of the ground survey. Mean nearest neighbour distances were 4.03 m, 4.50 m and 6.25 m for the ground, drone and aerial surveys.

The drone survey in all the plots tended to overestimate the termite mounds detected in relation to the ground survey, whereas the aerial survey underestimated. Overestimation of the drone survey can be a consequence of the drone survey detecting termite mounds which fell out of the specified surveying criteria, due to its high image resolution ability.

This is because in Chapter 4, it was stated that the ground survey ignored mounds that were less than 1 m in basal circumference. The drone survey picked up these ignored mounds by the ground survey, hence the overestimation.

Low mound counts, densities and large mean nearest neighbour distances detected on the drone and aerial surveys of Site C in relation to the ground survey can be attributed to dense tree cover present at the site in contrast to other sites in the study. Dense tree cover in these plots made it difficult for remote detection of termite mounds.

Another reason why the aerial survey recorded low densities of mounds on Site C is because young mounds had a higher density than old mounds on the site, which made remote detection difficult due to size. Considering mound density and count on each plot, the drone survey was found to have been more consistent with the ground survey in detecting termite mounds than the aerial survey. This was to the extent that in plot C1 and C2 the drone survey recorded twice as many observations in contrast to the aerial survey.

It is important to recall that the resolution of the drone and aerial survey were not the same, including a time lag difference in surveying. This may have lead to geometrical attributes of mounds being less accurately recorded in the aerial images. This would have been more influential in the case of young mounds. However, with old mounds, these discrepancies would have been negligible, since the lag was three years and it takes about five years for an average colony to grow. Also, the precise autonomy the drone provides in real time, allows the researcher more control of over the survey, which is an advantage being observed here.

This is because in Chapter 4, when comparing the image resolution between the aerial images and drone images, it was apparent how well the drone imagery outperformed the aerial imagery with regards to image resolution. An added advantage of the drone imagery was that it could reproduce Digital Surface Models which could be used in tandem with orthomosaics to enhance mound detection abilities of the drone survey. Although aerial surveys can also produce DSMs, there are barriers such as cost and surveying time. This is apparent in this study, as no DSMs or real time aerial imagery could be procured.

The drone survey's recorded mean nearest neighbour distances and spatial point patterns were more consistent to the ground survey's than those of the aerial survey.

Throughout the study, the aerial survey recorded long mean nearest neighbour distances more than both the ground and drone survey, an indication of its inconsistency in detecting termite mounds. This is informed by the understanding that frequent mound detection leads to shortened mean nearest neighbour distances between the mounds, which is not the case with the aerial survey. An influencing factor of the poor performance of the aerial survey was its low image resolution compared to the drone and ground surveys.

Out of the seven plots, the drone survey recorded six plots having consistent point patterns with the ground survey, with the aerial survey recording four plots consistent with the with the ground survey.

The percentage distribution of spatial point patterns recorded for the ground survey was, 57.14% random, 28.57% dispersed and 14.29% clustered. The percentages are calculated from the mound counts. The drone and the aerial survey were 85.71% and 57.14% accurate in recording consistent point patterns with those observed by the ground survey on each plot. A contributing factor to the poor performance of the aerial survey besides the resolution, is the time difference when the images where taken, they are were taken three years ahead those of the drone. This was because there were no updated images available at the time as aerial surveys are quite costly to conduct meaning images are not readily available.

7.2 Young and Old Termite Mound Behaviour

During the ground survey, separation of all mounds into young and old exposed their different characteristics and brought about unique information that would have otherwise been missed about their spatial structure. Throughout the plots, there was a higher density of old mounds (105.51 ma.ha^{-1}) compared to young mounds (70.89 ma.ha^{-1}), suggesting that the termite mound population largely consisted of mature colonies. This was true with the exception of Site C, where young mounds were more abundant than old mounds. This and the fact that this site's ground survey recorded the second largest mean nearest neighbour distance in the study 6.41 m could be a consequence of fierce intraspecfic competition among old mound colonies at this site. Mean nearest neighbour distances recorded overall in the study revealed that old mounds (6.20 m) had longer foraging boundaries than young mounds (5.28 m). This can be expected as mature colonies have more populations to support than younger colonies and hence the need for longer foraging distances. Basal circumference and height for both young and old mounds were correlated throughout, with old mounds (0.45) experiencing higher correlations than young (0.21) mounds. This suggests consistency between mound height and basal circumference. This occurs because as the mound ages, the wider and taller it becomes (Davies *et al.*, 2014).

Throughout the study, old mounds favoured patterns of dispersion and clustering; 42.86% exhibited dispersion, 42.86% were clustered and 14.29% were random. The number old mounds at the different plots that were clustered and dispersed were evenly matched, hence the ratio, with the rest of the mounds forming random patterns. The high percentages of clustering and dispersion among old colonies suggests both favourable conditions and high intraspecific competition within the ecosystem.

This is because old mounds are usually expected to be dispersed as a result of established foraging networks in competition for resources, which signals favourable environmental conditions (Korb and Linsenmair, 2001).

However, in all clustering cases among old mounds, dispersion was always present, but only for short distance scales and at large mean nearest neighbour distances. This can be a consequence of uneven resource distribution across the study site.

Young mounds in the study favoured clustered spatial patterns 71.43% , with the rest being dispersed and random at 14.29% each. At an intraspecific level, clustering among young mounds usually suggests a patchily distributed micro climate and a localised abundance of resources (Cramer and Midgley, 2015). With small mounds only a few colony members need to be maintained in each mound. Dispersion among young mounds is uncommon, this could be attributed to uneven resource distribution at different distance scales in the study site. Randomness could be a result of transitioning of young mounds into mature old mounds through colony clashes informed by resource competition. In the field young mounds were observed to be usually clustered close to old mounds, which suggests mutual existence, but it was uncommon to see old mounds clustered together. This is understandable as older mounds have established foraging boundaries which they fight to maintain.

7.3 Spatial Join of Anthropogenic and Natural Factors

Rivers as a water source were a common feature in the study, their proximity to termite mounds ranged round 470 m to 2000 m. The closest site to a river was found to be Site C where termite mounds recorded a distance of 470 m to a river. This close water source could explain the canopy that was created by the vegetation which made it hard to detect mounds remotely at this site. Mound density here was the least in the entire study, which may suggest that mounds prefer areas further away from a river. This was further supported by high mound densities in the study being recorded in Site A which had the second furthest distance to rivers but the nearest to Karoo dolerite. Karoo dolerite and dolerites being a proxy for a water source was covered in Chapter 3.

Termite mound basal circumferences had a fairly positive relationship with the presence of rivers for four out of the seven plots in the study. Height had a fairly positive relationship with the presence rivers for two out of the seven plots.

The elevation profile of the study ranged from around 400 m in Site C to 1000 m above sea level in Site B. In terms of elevation it didn't appear that termite mounds had a clear preference. This is because mounds with high densities were recorded at around 600 m and 1000 m above sea level, with low densities being recorded at around 700 m and 400 m above sea level. However, concerning basal circumference, it did appear that they tended to be larger at higher elevations. Termite mound basal circumferences appeared to have a fairly positive relationship with elevation for one out of the seven plots in the study. Height had a fairly positive relationship with elevation for two out of the seven plots.

Roads as a proxy for present anthropogenic disturbance were also a common feature in the study, ranging from around 600 m to 17000 m near or away from termite mounds. Sites A and D were the closest sites to main roads where sampling was performed. Here both termite mound basal circumferences and height were the largest and tallest in the study, demonstrating the resilience of termite mounds to present anthropogenic disturbance. Termite mound basal circumferences appeared to have a fairly positive relationship with the presence of roads for one out of the seven plots in the study. Height had a fairly positive relationship with the presence of roads for two out of the seven plots.

Human Settlements as a proxy for present anthropogenic disturbance much like roads were also a common feature in the study, with the nearest to a site ranging from around 300 m and the furthest 1900 m. Sites D and B were the closest sites to human settlements, with the latter together with Site A recording the largest termite mound basal circumferences and heights in the study, again showing resilience of termite mounds to present anthropogenic disturbance. Here, established foot paths and tire tracks leading from human settlements to the the plots were also visible on the aerial and drone images, showing common interaction between humans and the termite mounds. Termite mound basal circumferences appeared to have a fairly positive relationship with the presence of human settlements for three out of the seven plots in the study. Height had a fairly positive relationship with presence of human settlement for two out of the seven plots.

The presence of Karoo dolerite as a potential water source in the study area, ranged around 1000 m from the nearest mound to 6000 m to the furthest.

Sites A and B were the closest sites to Karoo dolerite, here termite mounds recorded the highest density including basal circumference and height in the the study. Understanding that the presence of dolerite is commonly associated with fractured aquifers (Woodford and Chevallier, 2002). This may suggest the need of a good water source presence by termite mounds but not too close within their immediate surrounding. It is also important to note that in sites A, B and D there were man made or naturally occurring dams not to far from the plots, which further suggests a preference or dependency on areas with water availability by termite mounds. Termite mound basal circumferences appeared to have a fairly positive relationship with the presence of Karoo dolerite for four out of the seven plots in the study and none with height.

7.3.1 Geology and Vegetation

Termite mound behaviour was the same both on geology and vegetation because the two layers overlayed each other completely. High densities for all mounds were recorded on the Elandsberg Member, Amathole Montane Grassland, including those of young and old mounds. Low densities for all mounds, including young and old were recorded on the Middleton Formation, Great Fish Thicket. All mounds, including young and old mounds found on the Daggaboersnek Member, Bedford Dry Grassland were taller and larger than those on other geology and vegetation. This can be attributed to a moderate population density, thus allowing for enough resources enabling them to grow further on this geology and vegetation. Here, the dominant spatial point patterns recorded for old mounds were dispersed, while clustered for young mounds. Young and old mounds experienced variations in their mean nearest neighbour distances across the different geology and vegetation. Long mean nearest neighbour distances for old and young mounds were recorded on the Middleton Formation and Great Fish Thicket. The large spacing between the mounds here was expected due to the low mound densities. Here, young and old mounds experienced high correlation between basal circumference and mound height.

Additionally, point patterns formed by young mounds were clustered while old mounds were split equally between dispersion and clustering. Termite mounds across the different geology and vegetation behaved differently, suggesting a strong influence of environmental heterogeneity (Muvengwi *et al.*, 2018).

Short mean nearest neighbour distances among old and young mounds were observed on the Elandsberg Member and Amathole Montane Grassland. The short distances between these mounds could be a consequence of the high density of mounds compared to the other geology and vegetation layers. These mounds also recorded low correlations between basal circumference and mound height. This was expected as mounds that are close together tend to be smaller in size because the populations they support are spread evenly across the colonies. As a result, spatial point patterns recorded on here were clustered for both young and old mounds.

7.3.2 Soil

Much like on the geology and vegetation, termite mound behaviour varied across soil types (Muvengwi *et al.*, 2018). Mounds, old and young were abundant on Lithic Leptosols followed by Eutric Regosols and then Leptic Regosols. Lithic Leptosols was where old and young mounds recorded low basal circumferences. This reduction in size may have been caused by the high abundance of mounds on this type of soil, limiting the growth of each colony population. Young mounds here, recorded short mean nearest neighbour distances. This could be attributed to the high densities experienced by these young mounds. Additionally, the spatial point patterns formed by young and old mounds here were clustered.

Large basal circumferences for young and old mounds were recorded on Leptic Regosols. These mounds also recorded long mean nearest neighbour distances compared to other mounds. Large spacing between the mounds can be explained by the low density of mounds observed here, allowing for greater mound growth. This could also suggest heightened intraspecfic competition among old mounds and young mounds transitioning to old mounds. Old mounds on Leptic Regosols were also taller than those of surrounding soils. Observed point patterns formed by young mounds here were split equally between dispersed and random and the same was recorded for old mounds.

Chapter 8

Conclusion

Chapter 6 and 7 presented the results and discussion from the work carried out in order to address the aims and objectives of this study.

8.1 Summary of Findings

Comparing the aerial and drone survey's results to those of the ground, it was established that overall, the drone survey outperformed the aerial survey. This could be attributed to the scale of the study which gave the drone a competitive advantage. It allowed for the drone images to be collected at a centimeter per pixel resolution. In addition, drone detection accuracy was improved through the generation of digital surface models from point clouds and contrasting them against the Orthomosaics.

The acquired aerial images, were half a meter resolution per pixel and digital surface models could not be generated from them. The time lag involved in flying aerial surveys was also a pitfall. There was a site however, where both the drone and aerial survey performed poorly. The performance here was due to large tree cover on the site which made remote detection of mounds difficult. This is one of the current challenges faced by remote-sensing.

However, considering the spatial point patterns observed, both surveys were more than 50% consistent with the ground survey, although the drone survey detected 28.57 % more accurate spatial point patterns than the aerial survey. From these findings in the study and being mindful of the constraints encountered, it appears that that for remote spatial data collection for small features such as termite mounds and at small spatial distance scales, the drone survey outperformed the aerial survey. This is with of cause understanding the limitations of the aerial survey in this study as a consequence of cost implications that were experienced.

Data for the ground survey was collected for all mounds on the sites and then separated according to age, as explained in Chapter 4. Old mounds recorded 20.08% more sightings than young mounds in the study. Foraging distances for young colonies were much shorter than those of older colonies. Overall, mature (old) colonies were bigger in size and had longer foraging boundaries than young ones. Before all mounds were classified according to age, majority of the spatial point patterns observed were random. Post classification, the leading spatial point patterns formed by old mounds were equally split between dispersion and clustering, with only a small fraction random, a result of clear intraspecific competition. In comparison to old mounds, over 70% of young mound spatial point patterns were clustered. However, as young mounds are still to mature into older mounds as the colonies grow, this leads to increased intraspecific competition resulting in the destruction of some young colonies, with the new emerging mature mounds establishing different point patterns. For this reason, it is intuitive to record old mound data for monitoring purposes because their spatial point patterns are more resilient.

Classifying mounds according to age proved to be a determining factor of their behaviour and structure as there were stark differences between old and young mounds in the study, which also informed the differences in the observed spatial point patterns.

Auxiliary data, in proximity to or underlying the sites where termite mounds were observed was collected to further understand their behaviour. Old mounds in the study proved more resilient to anthropogenic disturbance in the form of roads and human settlements and also favoured regions of higher elevation. Young mounds in contrast to old mounds seemed to thrive at low elevations further away from roads and human settlements. Mounds although they generally have a preference for areas with water availability, seemed to not to thrive in sites close to rivers.

The Elandsberg Member and Amathole Montane Grassland were the geology and vegetation where old and young mounds were most abundant.

Considering size, conditions on the Daggaboersnek Member and Bedford Dry Grassland were favourable for both young and old colonies to grow large. Colonies on the Middleton Formation and Great Fish Thicket had longer foraging networks, an indication of high intraspecific competition and scarce resources.

Concerning soils, old and young mounds had a preference for Lithic Leptosols. This was evident in their abundance. Conditions on Leptic Regosols were more favourable in allowing for colony size growth, as large young and old mounds were present with extended foraging distances. In essence, larger mounds tended to have longer foraging networks than smaller mounds. Eutric Regosols provided more favourable conditions for old mounds as their colony distances were considerably shorter compared to the other soils. Spatial point patterns observed after mounds were separated according to age on geology, vegetation and soil, differed greatly to those pre-seperation. Older mounds were largely dispersed and young mounds clustered. The introduction of natural and anthropogenic features allowed for a more complex understanding of termite mounds and how they behave on various environmental gradients.

8.2 Limitations

- The study was exploratory in nature and no modeling or post-monitoring was performed to assess how termite mound spatial point patterns and general behaviour was after study. This was largely due to the fact that in order to detect considerable change in termite mounds, sufficient time would have to pass, of which the study could not cater for.
- Financial constraints, prevented acquisition of the most recent aerial data. This limitation could have had an impact on the performance of the aerial survey.
- The time and scale at which the aerial images were collected as opposed to the other methods is a possible limitation.

- The aerial and drone survey experinced a short fall in one of the sites were there was a canopy of tree cover. In this instance, vegetation penetrating sensors like Synthetic Aperture Radars (SAR) could be used.
- Plot sizes at the study sites were of a small scale because the drone's battery power and coverage is limited and a more expensive drone model would have been needed to cover a more expansive area. A more expansive area would also have needed much more cloud computing resources to processes the drone images into digital surface models.

8.3 Contribution and Impact

The results suggest that long, resource consuming data collection using field surveys could be reduced and costs saved through the potential benefits of satellite, remote-sensing, such as the drone and aerial survey. Furthermore, the methodology of overlying drone generated othormosaics and digital surface models, demonstrated the added accuracy offered to remote sensing and object detection. Although remote-sensing cannot completely replace field surveys as they also serve a purpose, they can eliminate the mundane monitoring work. In this case, drones could be dispatched to collect data at the different sites to monitor the termite mounds post the study. Advancements in technologies such as drones prove useful in terms of real-time data collection and give greater control to the researcher to conduct their own primary data collection in contrast to traditional secondary data from aerial and satellite surveys. Drones are a low cost option when it comes to remote data collection and detection of small features. They also have readily available cloud services for point cloud and digital surface model generation.

Termites are sensitive to changes in their ecosystem, this was evident in how the mounds behaved at the different sites. Separating the mounds between young and old, further revealed the potential benefits of additional information that can be induced from their age. Understanding the differences between old and young mounds, can help infer the spatial point patterns they follow and establish intraspecific competition and environmental heterogeneity existing at particular regions. Introducing environmental and anthropogenic factors lead to the understanding that young and old mounds behave differently on various environmental gradients. The study suggested that younger mounds have more dynamic point patterns than old mounds because as they mature into older mounds, new point patterns emerge. For this reason it is much more beneficial to use older mound colonies for ecosystem monitoring due to their resilience and ability to maintain spatial point pattern integrity. Older mounds were also more resilient to present anthropogenic disturbance at the sites.

This baseline study could be used as a cost effective way in which to monitor for potential shale gas leakage. An increase in the sampling area could also allow for more data collection which could have an influence on the outcome. However, the selection of the specific sites was on a to uncover most of the diverse topography, vegetation and elevation of the region. Also, Site B could only have one site represented which may have provided a different outcome had a second plot been recorded . Post shale gas implementation, termite mound spatial data could be re-collected and the same investigation repeated to determine whether there have been any significant deviations from the established exploratory data. If so, then the existing environmental and anthropogenic factors would be evaluated to understand if there have been any considerable changes that could have induced deviation in the known established spatial point patterns.

8.4 Future Work

- Modeling could be introduced to expand on the exploratory nature of the study. This could allow for introduction of different variables to understand how mound spatial patterns could potentially react to them.
- Satellite images with high resolution could be used in conjunction with high resolution aerial images to collect termite mound spatial data at larger scales.
- Machine learning object detection could be trained to classify and automatically detect the termite mounds against other environmental features in the images. This could potentially increase the accuracy and speed in mound detection.

Bibliography

Academy of Science of South Africa (ASSAF) (2016). *South Africa Technical Readiness to Support the Shale Gas Industry* . [online]. Available at: DOI http://dx.doi.org/10.17159/assaf.2016/0003 (Accessed: 15 2019 August).

AEON (2018). *(T)(C)Racking the Shale-Gas Debate: Baseline Data and Citizen Science @KarooCommons.za*. AEON Report Series No. 4. AEON, Port Elizabeth, South Africa. [online].Available at: http://aeon.org.za/wp-content/uploads/2018/12/AEON-Shale-Gas-Report-2018.pdf (Accessed: 10 January 2019).

Ahmed, I., Bala, J. and Pradhan, B. (2018). 'Termite Mounds as Bio-Indicators of Groundwater: Prospects and Constraints'. *Pertanika Journal of Science & Technology*, **26**(2), p479–498.

Alves, W, d. F., Mota, A., De Lima, R., Bellezoni, R. and Vasconcellos, A. (2011). 'Termites as Bioindicators of Habitat Quality in the Caatinga, Brazil: Is there Agreement between Structural Habitat Variables and the Sampled Assemblages'. *Neotropical Entomology*, **40**(1), p39–46.

Atkinson, D., Wolpe, R., Kotze, H., Madyo, S., Poole, C., Fikizolo, L., Leiman, T., van der Merwe, S., van der Merwe, H., Lochner, P. and Cape, L. (2017). *Socio-economic Assessment of SKA Phase 1 in South Afria*. Strategic Environmental Assessment. [online]. Available at: https://sahris.sahra.org.za/sites/default/files/additionaldocs/SocioEconomic-Assessment.pdf (Accessed: 5 October 2017).

Aucamp, A. and Tainton, N. M. (1984). *Veld Management in the Valley Bushveld of the Eastern Cape [South Africa]*. Department of Agriculture. [online]. Available at:https://agris.fao.org/agris-search/search.do?recordID=ZA9500209 (Accessed 15 January 2020).

Austailian Government (2014). *Hydraulic Fracturing Techniques, Including Reporting Requirements and Governance Arrangements*. Department of the Environment. [online]. Available at: https://www.environment.gov.au/system/files/resources/de709bdd-95a0-4459-a8ce-8ed3cb72d44a/files/background-review-hydraulic-fracturing$_0$*.pdf*(*Accessed* : 21*May*2017).

Baddeley, A. J. and Gill, R. D. (1993). *Kaplan-Meier Estimators of Interpoint Distance Distributions for Spatial Point Processes*. CWI.

Baddeley, A., Rubak, E. and Turner, R. (2015). *Spatial Point Patterns: Methodology and Applications with R*. Chapman and Hall/CRC.

Bird, G. (1981). 'Monte-Carlo simulation in an engineering context'. *Progress in Astronautics and Aeronautics*, **74**(1), 239–255.

Bordy, E. M., Linkermann, S. and Prevec, R. (2011). 'Palaeoecological Aspects of Some Invertebrate Trace Fossils from the Mid to Upper Permian Middleton Formation (Adelaide Subgroup, Beaufort Group, Karoo Supergroup), Eastern Cape, South Africa'. *Journal of African Earth Sciences*, **61**(3), p238–244.

Botha, J., Woodford, A. and Chevallier, L. P. (2002). *Hydrogeology of the Main Karoo Basin: Current Knowledge and Future Research Needs*. Water Research Commission. [online]. Available at: http://www.wrc.org.za/wp-content/uploads/mdocs/TT179-02.pdf (Accessed: 1 August 2017).

Brown, K. S. (1997). 'Diversity, Disturbance, and Sustainable use of Neotropical Forests: Insects as Indicators for Conservation Monitoring'. *Journal of Insect Conservation*, **1**(1), p25–42.

Burns, R. (1984). *Importance of Baseline Information to the Research Natural Area Program*. Symposium on Research Natural Areas: Baseline Monitoring and Management. [online]. Available at: https://agris.fao.org/agris-search/search.do?recordID=US8538925 (Accessed: 3 March 2019).

Cairns, J. and Pratt, J. R. (1993). 'A History of Biological Monitoring Using Benthic Macroinvertebrates'. *Freshwater Biomonitoring and Benthic Macroinvertebrates*, **10**(2), p11–27.

Carignan, V. and Villard, M. (2002). 'Selecting Indicator Species to Monitor Ecological Integrity: A Review'. *Environmental Monitoring and Assessment*, **78**(1), p45–61.

Catuneanu, O. and Elango, H. N. (2001). 'Tectonic Control on Fluvial Styles: The Balfour Formation of the Karoo Basin, South Africa'. *Sedimentary Geology*, **140**(3), p291–313.

Chere, N. (2015). *Sedimentological and Geochemical Investigations on Borehole Cores of the Lower Ecca Group Black Shales, for Their Gas Potential-Karoo Basin, South Africa*. Master's thesis. Nelson Mandela University.

Clancy, S., Worrall, F., Davies, R. and Gluyas, J. (2018). 'The Potential for Spills and Leaks of Contaminated Liquids from Shale Gas Developments'. *Science of the Total Environment*, **626**(143), p1463–1473.

Clark, P. J. and Evans, F. C. (1954). 'Distance to Nearest Neighbor as a Measure of Spatial Relationships in Populations'. *Ecology*, **35**(4), p445–453.

Cole, D. (1994). 'Southern Africa: Karoo Basin and Cape Fold Belt'. *Permian-Triassic Pangean Basins and Foldbelts Along the Panthalassan Margin of Gondwanaland*, **184**(1), p223–279.

Constantino, R. (1998). 'Catalog of the Living Termites of the New World (Insecta: Isoptera)'. *Arquivos de Zoologia*, **35**(2), p135–230.

Cramer, M. D. and Midgley, J. J. (2015). 'The Distribution and Spatial Patterning of Mima-like Mounds in South Africa Suggests Genesis Through Vegetation Induced Aeolian Sediment Deposition'. *Journal of Arid Environments*, **119**(6), p16–26.

Cramer, M. D., Von Holdt, J., Khomo, L. and Midgley, J. J. (2016). 'Evidence for Aeolian Origins of Heuweltjies from Buried Gravel Layers'. *South African Journal of Science*, **112**(1-2), p1–10.

Davies, A. B., Levick, S. R., Asner, G. P., Robertson, M. P., van Rensburg, B. J. and Parr, C. L. (2014). 'Spatial Variability and Abiotic Determinants of Termite Mounds Throughout a Savanna Catchment'. *Ecography*, **37**(9), p852–862.

de Sá Rodrigues da Silva, M., Eger, R. A., Rosenfeldt, Y. A. Z. and Loch, C. (2018). 'Testing DJI Phantom 4 Pro for Urban Georefrencing'. *International Archives of the Photogrammetry, Remote Sensing & Spatial Information Sciences*, **42**(1), p407–411.

de Wit, M. and Jeffery, M. (1988). *Geological Map of Sectors of Gondwana: Reconstructed to Their Disposition-150 Ma Scale 1: 10.000. 000: Lambert Equal Area Prjection-Centred at 20Â° S, 40Â° E*. American Association of Petroleum Geology.

DeCoster, J., Gallucci, M. and Iselin, A.-M. R. (2011). 'Best Practices for Using Median Splits, Artificial Categorization, and their Continuous Alternatives'. *Journal of Experimental Psychopathology*, **2**(2), p197–p209.

Diggle, P. J. (2000). *Spatial Statistics for Environmental Epidemiology*. Medical Statistics Unit, University of Lancaster. [online]. Available at: https://www.lancaster.ac.uk/staff/diggle/spatialepi/notes.pdf (Accessed: 15 August 2018).

Diggle, P. J. (2013). *Statistical Analysis of Spatial and Spatio-Temporal Point Patterns*. Chapman and Hall/CRC.

Driscoll, J. and Maclachlan, J. (2017). 'Monitoring Methane from Fracking Operations: Leak Detection and Environmental Measurements'. *ACS Energy Letters*, **2**(10), p2436–2439.

Henschel, J. R., Hoffman, M. T. and Walker, C. (2018). 'Introduction to the Karoo Special Issue: Trajectories of Change in the Anthropocene'. *African Journal of Range & Forage Science*, **35**(3-4), p151–156.

Hoare, D. (2003). Biodiversity and Performance of Grassland Ecosystems in Communal and Commercial Farming Systems in South Africa. *Biodiversity and the Ecosystem Approach in Agriculture, Forestry and Fisheries*. Food and Agriculture Organization of the United Nations,Rome, Italy. [online]. Available at: https://www.cabdirect.org/cabdirect/abstract/20033095661 (Accessed: 5 November 2018).

Howarth, R. W., Ingraffea, A. and Engelder, T. (2011). 'Should Fracking Stop?'. *Nature*, **477**(7364), p271–275.

Huntley, B. J. (1984). Characteristics of South African Biomes. *in* de Booysen , P.V and Tainton, N.M (ed.), *Ecological Effects of Fire in South African Ecosystems*. Vol. 48 of *Ecological Studies (Analysis and Synthesis)*. Springer, Berlin, Heidelberg. [online]. Available at: https://www.springer.com/gp/book/9783642698071 (Accessed: 12 September 2018).

Iacobucci, D., Posavac, S. S., Kardes, F. R., Schneider, M. J. and Popovich, D. L. (2015). 'The median split: Robust, refined, and revived'. *Journal of Consumer Psychology*, **25**(4), p690–p704.

Ibe, O. (2013). *Markov Processes for Stochastic Modeling*. Newnes.

IUSS Working Group WRB (2014). *World Reference Base for Soil Resources 2014: International Soil Classification System for Naming Soils and Creating Legends for Soil Maps*. World Soil Resources Reports No. 106. Food and Agriculture Organization of the United Nations, Rome, Italy. [online]. Available at: http://www.fao.org/3/i3794en/I3794en.pdf (Accessed: 23 September 2019).

Jackson, R. B., Vengosh, A., Carey, J. W., Davies, R. J., Darrah, T. H., O'Sullivan, F. and Pétron, G. (2014). 'The Environmental Costs and Benefits of Fracking'. *Annual Review of Environment and Resources*, **39**(1), p327–362.

Jean-Pierre, B., Moise, A. A. A., Sylvain, T. C., Philippe, K. K., Yao, T. and Ahoua, Y. (2015). 'Spatial Distribution and Density of Termite Mounds in a Protected Habitat in the South of Cote d'ivoire: Case of National Floristic Center (CNF) of UFHB of Abidjan'. *European Scientific Journal*, **11**(3), p241–259.

Johson, M. (1976). *Stratigraphy and Sedimentology of the Cape and Karoo Sequences*. PhD thesis. Rhodes University.

Juergens, N., Vlieghe, K. E., Bohn, C., Erni, B., Gunter, F., Oldeland, J., Rudolph, B. and Picker, M. D. (2015). 'Weaknesses in the Plant Competition Hypothesis for Fairy Circle Formation and Evidence Supporting the Sand Termite Hypothesis'. *Ecological Entomology*, **40**(6), p661–668.

Keeler, H. P. (2016). *Notes on the Poisson Point Process*. Weierstrass Institute, Berlin, Germany. [online]. Available at: https://researchers.ms.unimelb.edu.au/ hp-keeler@unimelb/PoissonPointProcess.pdf (Accessed: 16 June 2018).

Kiran, R., Teodoriu, C., Dadmohammadi, Y., Nygaard, R., Wood, D., Mokhtari, M. and Salehi, S. (2017). 'Identification and Evaluation of Well Integrity and Causes of Failure of Well Integrity Barriers (A Review)'. *Journal of Natural Gas Science and Engineering*, **45**(3), p511–526.

Kiviat, E. (2013). 'Risks to Biodiversity from Hydraulic Fracturing for Natural Gas in the Marcellus and Utica Shales'. *Annals of the New York Academy of Sciences*, **1286**(1), p1–14.

Korb, J. and Linsenmair, K. E. (2001). 'The Causes of Spatial Patterning of Mounds of a Fungus-Cultivating Termite: Results from Nearest-Neighbour Analysis and Ecological Studies'. *Oecologia*, **127**(3), p324–333.

Krupp, F. (2014). 'Don't Just Drill, Baby-Drill Carefully: How to Make Fracking Safer for the Environment'. *Foreign Affairs*, **93**(3), p15–20.

Lindeque, A., de Wit, M. J., Ryberg, T., Weber, M. and Chevallier, L. (2011). 'Deep Crustal Profile Across the Southern Karoo Basin and Beattie Magnetic Anomaly, South Africa: An Integrated Interpretation with Tectonic Implications'. *South African Journal of Geology*, **114**(3-4), p265–292.

Linol, B. and De Wit, M. J. (2016). *Origin and Evolution of the Cape Mountains and Karoo Basin*. Springer.

Linol, B., Miller, W., Rensburg, C., Schoeman, R., Bezuidenhout, L., Genin, F., Morkel, B., Dhliwayo, N., Jeppesen, K., Dlakavu, S. and Mngcele, L. (2020). 'Earth Stewardship Science–Transdisciplinary Contributions to Quantifying Natural and Cultural Heritage of Southernmost Africa'. *Remote Sensing*, **12**(3), p420–428.

Martin, K. (2017). *Potential Eco-physiological and Phytosociological Impacts of Fracking on the Vegetation of the Karoo, Eastern Cape, South Africa*. PhD thesis. University of Bremen.

Meng, Q. (2016). 'The Impacts of Fracking on the Environment: A Total Environmental Study Paradigm'. *Science of the Total Environment*, **580**(100), p953–957.

Miller, H. J. (2004). 'Tobler's First Law and Spatial Analysis'. *Annals of the Association of American Geographers*, **94**(2), p284–289.

Mngcele, L. (2017). *A Scientific Study on the Effects of Selected Macroeconomic Variables on the GDP of South Africa Using Principal Component Regression.* Honours Treatise. Nelson Mandela Uinversity.

Mucina, L. and Rutherford, M. e. (2006). *The vegetation of South Africa, Lesotho and Swaziland*. Strelitzia 19. South African National Biodiversity Institute, Pretoria. [online]. Available at: https://www.sanbi.org/wp-content/uploads/2018/05/Strelitzia-19.pdf (Accessed: 29 October 2018).

Mujinya, B. B., Adam, M., Mees, F., Bogaert, J., Vranken, I., Erens, H., Baert, G., Ngongo, M. and Van Ranst, E. (2014). 'Spatial Patterns and Morphology of Termite (Macrotermes Falciger) Mounds in the Upper Katanga, DR Congo'. *Catena*, **114**(10), p97–106.

Muvengwi, J., Davies, A. B., Parrini, F. and Witkowski, E. T. (2018). 'Geology Drives the Spatial Patterning and Structure of Termite Mounds in an African Savanna'. *Ecosphere*, **9**(3), p1–17.

National Geo-Spatial Information (2013). National Aerial Photography and Imagery Programme. [online]. Available at: http://www.ngi.gov.za/index.php/what-we-do/aerial-photography-and-imagery (Accessed: 20 July 2017).

Nengovhela, V. (2018). *Petrophysical Analysis of Thermo-Tectonic Effects Linked to Lower Jurassic Dolerite Intrusions in Sedimentary Rocks of the Main Karoo Basin Sedimentary Rocks of the Main Karoo Basin, with Implications for Shale Gas Development in South Africa: Implications for Shale Gas Development in South Africa*. Master's thesis. Nelson Mandela University.

Neumann, E., Svensen, H., Galerne, C. Y. and Planke, S. (2011). 'Multistage Evolution of Dolerites in the Karoo Large Igneous Province, Central South Africa'. *Journal of Petrology*, **52**(5), p959–984.

Noor, N. M., Abdullah, A. and Hashim, M. (2018). *Remote Sensing UAV/Drones and its Applications for Urban Areas: A Review*. Vol. 169 of *IOP Conference Series: Earth and Environmental Science*. Kuala Lumpur, Malaysia. [online]. Available at: https://iopscience.iop.org/article/10.1088/1755-1315/169/1/012003/meta (Accessed: 12 June 2018).

Oghenekome, M. E. (2012). *Sedimentary Environments and Provenance of the Balfour Formation (Beaufort Group) in the Area between Bedford and Adelaide, Eastern Cape Province, South Africa*. Master's thesis. University of Fort Hare.

Pennisi, E. (2015). 'Africa's Soil Engineers: Termites'. *Science*, **347**(6222), p596–597.

Pomeroy, D. (1977). 'The Distribution and Abundance of Large Termite Mounds in Uganda'. *Journal of Applied Ecology*, **14**(2), p465–475.

Pribadi, T., Raffiudin, R. and Harahap, I. S. (2011). 'Termites Community as Environmental Bioindicators in Highlands: A Case Study in Eastern Slopes of Mount Slamet, Central Java'. *Biodiversitas Journal of Biological Diversity*, **12**(4), p235–240.

Protazio, J. (2008). *Spatial Pattern Analysis Applied to Plant Ecology*. PhD thesis. University of Bremen.

R Core Team (2017). *R: A Language and Environment for Statistical Computing*.

Rehu, M. (2012). *Scoping Study of the Impacts of Fracking on Indigenous Reservations in Alberta using the Mauri Model Decision Making Framework*. Nga Pae O Te Maramatanga, Auckland. [online]. Available at: http://www.maramatanga.co.nz/sites/default/files/12-IN-07(Accessed: 3 September 2019).

Ripley, B. D. (1977). ‘Modelling Spatial Patterns’. *Journal of the Royal Statistical Society: Series B (Methodological)*, **39**(2), p172–192.

Ruwaimana, M., Satyanarayana, B., Otero, V., Muslim, A. M., Syafiq, M., Ibrahim, S., Raymaekers, D., Koedam, N. and Dahdouh-Guebas, F. (2018). ‘The Advantages of Using Drones Over Space-Borne Imagery in the Mapping of Mangrove Forests’. *PloS One*, **13**(7), p1–22.

Siddig, A. A., Ellison, A. M., Ochs, A., Villar-Leeman, C. and Lau, M. K. (2016). ‘How do Ecologists Select and use Indicator Species to Monitor Ecological Change? Insights from 14 years of Publication in Ecological Indicators’. *Ecological Indicators*, **60**(1), p223–230.

Smith, T. E. (2016). *Notebook on Spatial Data Analysis*. Lecture Note. [online]. Available at:https://www.seas.upenn.edu/ ese502/notebook (Accessed on 14 March 2018).

Ssekamatte, D. and Okello, S. M. (2016). ‘Using Baseline Studies as a Basis for Monitoring and Evaluation: A Review of the Literature’. *Uganda Management Institute*, **11**(1), p31–42.

Stein, A., Bastiaanssen, W. G., De Bruin, S., Cracknell, A., Curran, P., Fabbri, A., Gorte, B., Van Groenigen, J., Van Der Meer, F. and Saldana, A. (1998). ‘Integrating Spatial Statistics and Remote Sensing’. *International Journal of Remote Sensing*, **19**(9), p1793–1814.

Tankard, A., Welsink, H., Aukes, P., Newton, R. and Stettler, E. (2009). ‘Tectonic Evolution of the Cape and Karoo Basins of South Africa’. *Marine and Petroleum Geology*, **26**(8), p1379–1412.

Tarnita, C. E., Bonachela, J. A., Sheffer, E., Guyton, J. A., Coverdale, T. C., Long, R. A. and Pringle, R. M. (2017). ‘A Theoretical Foundation for Multi-Scale Regular Vegetation Patterns’. *Nature*, **541**(7637), p398–401.

Theraulaz, G., Gautrais, J., Camazine, S. and Deneubourg, J.-L. (2003). 'The Formation of Spatial Patterns in Social Insects: From Simple Behaviours to Complex Structures'. *Philosophical Transactions of the Royal Society of London. Series A: Mathematical, Physical and Engineering Sciences*, **361**(1807), p1263–1282.

Tobler, W. R. (1970). 'A Computer Movie simulating Urban Growth in the Detroit Region'. *Economic Geography*, **46**(1), p234–240.

Todd, S. W., Hoffman, M. T., Henschel, J., Cardoso, A. W., Brooks, M. and Underhill, L. G. (2016). 'The Potential Impacts of Fracking on Biodiversity of the Karoo Basin, South Africa'. *Hydraulic Fracturing in the Karoo: Critical Legal and Environmental Perspectivesâ*, **14**(10), p278–301.

Van Wyk, A. E. and Smith, G. F. (2001). *Regions of Floristic Endemism in Southern Africa: A Review with Emphasis on Succulents*. Umdaus Press.

Vengosh, A., Warner, N., Jackson, R. and Darrah, T. (2013). 'The Effects of Shale Gas Exploration and Hydraulic Fracturing on the Quality of Water Resources in the United States'. *Procedia Earth and Planetary Science*, **7**, p863–866.

Vlieghe, K. E. (2016). *The Ecology of Namibian Fairy Circles and the Potential Role of Sand Termites (Psammotermes allocerus Silvestri) in their Origin*. PhD thesis. University of Cape Town.

Vlok, J., Euston-Brown, D. and Cowling, R. (2003). 'Acocks Valley Bushveld 50 Years on: New Perspectives on the Delimitation, Characterisation and Origin of Subtropical Thicket Vegetation'. *South African Journal of Botany*, **69**(1), p27–51.

Vranken, I., Adam, M., Mujinya, B. B., Munyemba, F. K., Baert, G., Van Ranst, E., Visser, M. and Bogaert, J. (2014). 'Termite Mounds Identification Through Aerial Photographic Interpretation in Lubumbashi: Methodology Evaluation'. *Tropical Conservation Science*, **7**(4), p733–746.

Warner, N. R., Darrah, T., Jackson, R., Millot, R., Kloppmann, W. and Vengosh, A. (2014). 'New Tracers Identify Hydraulic Fracturing Fluids and Accidental Releases from Oil and Gas Operations'. *Environmental Science & Technology*, **48**(21), p12552–12560.

Wiegand, T. and Moloney, K. A. (2013). *Handbook of Spatial Point-Pattern Analysis in Ecology*. Chapman and Hall/CRC.

Woodford, A., Botha, J., Chevallier, L., Hartnady, C., Johnson, M. and Meyer, R. (2001). *Hydrogeology of the Main Karoo Basin: Current Knowledge and Research Needs*. Water Research Commission. [online]. Available at: http://www.wrc.org.za/wp-content/uploads/mdocs/TT179-02.pdf (Accessed: 3 September 2017).

Woodford, A. and Chevallier, J. (2002). *The Influences of Dolerite Sill and Ring Complexes on the Occurrence of Groundwater in Karoo Fractured Aquifers: A Morpho-Tectonic Approach*. Water Research Commission. [online]. Available at: https://www.cabdirect.org/cabdirect/abstract/20033095661 (Acccessed: 7 February 2019).

Appendix A

Derivation Of Clark And Evan's Aggregation Index

Finding the Mean

$$E(r) = \int_0^\infty 2\pi\lambda e^{-\lambda\pi r^2} dr$$

$$= \int_0^\infty re^{-\lambda\pi r^2} 2\lambda\pi r dr \text{ with y=}\lambda\pi r^2\text{; r=}\frac{\sqrt{y}}{\sqrt{\lambda\pi}} \text{ ; } \frac{dy}{dr}\text{=}\lambda\pi\text{2r ; dy=}\lambda\pi\text{2rdr. Then}$$

$$\int_0^\infty \frac{\sqrt{y}}{\sqrt{\lambda\pi}} e^{-y} dy$$

$$= \frac{1}{\sqrt{\lambda}} \frac{1}{\sqrt{\pi}} \int_0^\infty y^{1\frac{1}{2}-1} e^{-y} dy.$$

Introducing the Gamma function $\Gamma(\frac{3}{2}) = \frac{1}{\sqrt{\pi}}$; $(n-1)\Gamma(n)$; $(\frac{3}{2}-1)(\Gamma(\frac{1}{2})) = \frac{1}{2}\sqrt{\pi}$

$$= \frac{1}{\sqrt{\lambda}} \frac{1}{\sqrt{\pi}} \Gamma(1\frac{1}{2})$$

$$= \frac{1}{\sqrt{\lambda}} \frac{1}{\sqrt{\pi}} (\frac{1}{2}) \sqrt{\pi}$$

$$E(r) = \frac{1}{2}\frac{1}{\sqrt{\lambda}} \tag{A.1}$$

Finding the Variance $Var(\bar{r}) = E\left[r^2\right] - \left[E\left[r\right]\right]^2$ we have

$$E\left[r^2\right] = \int_0^\infty 2\pi\lambda r^3 e^{-\lambda\pi r^2} dr$$

$$= \int_0^\infty r^2 e^{-\lambda\pi r^2} 2\lambda\pi r dr$$

$$= \int_0^\infty \frac{y}{\lambda\pi} e^{-y} dy$$

$$= \frac{1}{\lambda\pi}\Gamma\left(2\right)$$

$$Var(\bar{r}) = \frac{1}{\lambda\pi} - \frac{1}{4}\frac{1}{\lambda} = \frac{4-\pi}{4\lambda\pi} \tag{A.2}$$

Taylor Series Expansion of the Exponential Function $e^n = \sum_0^\infty \frac{x^n}{n!}$

$$e^x = \sum_{i=0}^\infty \frac{x^i}{i!} = \frac{x^0}{0!} + \frac{x^1}{1!} + \frac{x^2}{2!} + \frac{x^3}{3!} + ... + \frac{x^i}{i!}.\text{ We have } e^{-\lambda\pi(r_1^2 - r^2)}$$

assume $r_1 \to r$. Then

$$e^{-\lambda\pi\left(r_1^2 - r^2\right)} = \sum_{i=0}^\infty \frac{-\lambda\pi\left(r_1^2 - r^2\right)^i}{i!} = \frac{(-\lambda\pi(r_1^2 - r^2))^0}{0!} + \frac{(-\lambda\pi(r_1^2 - r^2))^1}{1!} + dr$$

dr is a very small distance

$$= 1 - \lambda\pi\left(r_1^2 - r^2\right)$$

$$p(r) = e^{-\lambda\pi r^2}(1 - e^{-\lambda\pi(r_1^2 - r^2)})$$

$$= e^{-\lambda\pi r^2}(1 - (1 - \lambda\pi\left(r_1^2 - r^2\right)) \tag{A.3}$$

Appendix B

Summary Tables

Five Number Summary	Plot A1	Plot A2	Plot B1	Plot C1	Plot C2	Plot D1	Plot D2
Minimum	1.00	1.00	1.00	1.00	1.00	1.20	1.00
Lower Quartile	2.00	1.80	1.70	1.50	1.50	2.10	1.70
Median	2.70	2.50	2.20	1.90	1.80	2.90	2.50
Mean	2.74	2.52	2.28	2.09	2.03	2.86	2.54
Upper Quartile	3.35	3.10	2.70	2.40	2.50	3.45	3.20
Maximum	5.00	4.70	4.80	5.10	4.50	5.00	5.90
std	0.89	0.80	0.79	0.80	0.71	0.95	1.07

Table B.1: Termite mound basal circumference for all sites.

.

Five Number Summary	Plot A1	Plot A2	Plot B1	Plot C1	Plot C2	Plot D1	Plot D2
Minimum	0.00	0.00	0.00	0.00	0.00	0.00	0.00
Lower Quartile	0.20	0.00	0.00	0.00	0.00	0.25	0.20
Median	0.30	0.20	0.00	0.20	0.23	0.30	0.30
Mean	0.26	0.18	0.15	0.18	0.22	0.31	0.31
Upper Quartile	0.35	0.30	0.28	0.30	0.36	0.40	0.45
Maximum	0.70	0.55	1.00	0.90	0.80	0.85	0.70
std	0.17	0.17	0.20	0.18	0.20	0.18	0.18

Table B.2: Termite mound heights for all sites.

.

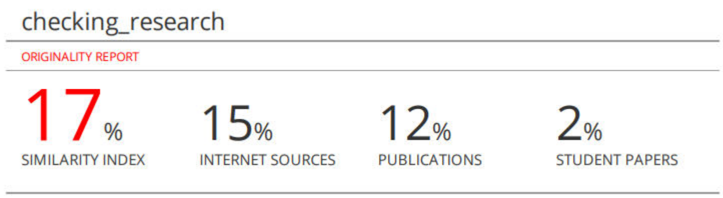
checking_research

ORIGINALITY REPORT

17%	15%	12%	2%
SIMILARITY INDEX	INTERNET SOURCES	PUBLICATIONS	STUDENT PAPERS

Figure B.1: Plagarism-Report.